THE
PHYSICAL REVIEW
A Journal of Experimental and Theoretical Physics
VOL. 44, NO. 8 OCTOBER 15, 1933 SECOND SERIES

X-Ray Satellites of High Atomic Number Elements

F. K. RICHTMYER* AND SIDNEY KAUFMAN, *Cornell University*
(Received August 2, 1933)

The x-ray lines $L\alpha_1$ and $L\alpha_2$ have been examined for accompanying satellites in the atomic number range from Ta(73) to U(92). $L\alpha$ is found to have two satellites, herein called $L\alpha^{12}$ and $L\alpha^2$. The former (longer wave-length) extends from Au(79) to U(92); the latter from Os(76) to Bi(83). Even over the short range of atomic numbers over which they occur, these two satellites change rapidly as to relative intensity and appearance. They do not seem to be connected with the prominent group of satellites of $L\alpha$ which occur in the region $36<Z<54$. $L\beta_2$ is found to have two satellites, $L\beta_2'$ and $L\beta_2''$. $L\beta_2''$ extends from Ta(73) to U(92). $L\beta_2'$ begins several atomic numbers below Ta(73) and extends to U(92). The satellite structure accompanying $L\beta_2$ in this high atomic number range is somewhat similar to that found in the range $40<Z<54$. But the absence of any satellites of $L\beta_2$ in the range $54<Z<70$ suggests that these high atomic number satellites may be new lines.

ONE of the most significant characteristics of x-ray satellites is the fact their atomic number range is not at all coincident with that of the parent lines with which the satellites are respectively associated. For example, although $L\alpha$ is first observed at Va(23), the satellites of $L\alpha$ are not found until Ni(28)[1] or Cu(29)[2] is reached. For higher atomic numbers the satellites become more prominent, reaching a maximum of intensity, relative to the parent line for elements in the neighborhood of Rh(45). Beyond Rh(45) the satellite structure becomes less prominent. At Sn(50) only a broad, unresolved band remains.[3] This band is very faint at Te(52). No trace of satellite structure accompanying $L\alpha$ is observable for Ba(56).

Similarly it has been shown[4] that the prominent satellites of $L\beta_2$ are not observed for the elements immediately above I(53).

There have been reported in the literature,[5] however, numerous satellites of L lines in the spectra of the elements of higher atomic number, particularly from Ta(73) to U(92). Since there has been no systematic and searching study of satellites in this atomic number range, the present work was undertaken primarily to ascertain whether these high-atomic-number satellites are in fact, as has been assumed,[5] identical with the satellites found associated with elements of lower atomic number; or whether they are to be regarded as new lines.

The spectrometer used was of the Siegbahn-Thoraeus high-vacuum type,[6] the distance be-

* The senior author wishes to express his best thanks to the Heckscher Research Council of Cornell University for a grant in aid of this investigation.

[1] A. Karlsson, Ark. Math. Astr. o. Fys. (Upsala) **22**, 1930.

[2] J. H. Van der Tuuk, *Dissertation*, Groningen, 1928.

[3] F. K. Richtmyer, J. Franklin Inst. **208**, 325 (1929).

[4] R. D. Richtmyer, Phys. Rev. **38**, 1802 (1931).

[5] These data are most readily found in tables in Siegbahn's *Spektroskopie der Röntgenstrahlen*, second edition, (1931), Siegbahn uses the term "spark lines" instead of "satellites."

[6] J. Opt. Soc. Am. and Rev. Sci. Inst. **13**, 235 (1926).

tween the entrance slit and the photographic plate being 54.9 cm for some of the plates; and 211.4 cm for others. The higher resolution attainable at the greater distance, with suitable slit widths, is an important factor in studying the satellite structure.

Satellites of $L\alpha$

In the atomic number range $29<Z<50$, $L\alpha$ has five (in some elements more) satellites, which, beginning with In(49), decrease rapidly in intensity and are not observed above Xe(54). Contrary to the observations of Coster[7] and Dauvillier[8] no trace of satellites accompanying $L\alpha$ has been found by the senior author for Ba(56), although spectrum plates have been made and examined with great care. If satellites do accompany Ba $L\alpha$, they must be exceedingly faint. From La(57) to Yb(70) inclusive, *no observer has reported satellites of* $L\alpha$. Dauvillier[9] reports one satellite ($L\alpha_3$, Siegbahn's notation) for Lu(71), although no such line was found by Wennerlöf[10] or by Coster.[7] Two observers, namely Wennerlöf[10] and Auger and Dauvillier[11] report a satellite ($L\alpha_3$, Siegbahn) for Ta(73), in disagreement with Idei,[12] whose work appears to have been most carefully done. Of the 14 observers quoted by Siegbahn as having measured $L\alpha_{1,2}$ of W(74) only Rogers[13] reports a satellite for $L\alpha$. The present authors have made many plates of Ta(73) and of W(74) under a variety of different conditions, and have failed to find the slightest trace of a satellite of $L\alpha$ for either element. One concludes, therefore, either that no satellites exist for $L\alpha$ between Cs(55) and W(74) inclusive, or, if there is a satellite in this atomic number range, it is so very faint as to have escaped detection by most of the observers.

For atomic numbers higher than W(74) there is ample evidence that $L\alpha$ is accompanied by one (or more) satellites, except possibly in the case of Rh(75), for which Beuthe[14] alone reports $L\alpha_3$.

In the present work, in addition to the observations on Ta(73) and W(74) mentioned above, we have studied the satellite structure accompanying $L\alpha$ for the elements Os(76), Ir(77), Pt(78), Au(79), Tl(81), Pb(82), Bi(83), Th(90) and U(92). Two satellites were found which we shall call $L\alpha^{iz}$ and $L\alpha^{z}$.† $L\alpha^{z}$ is found in the atomic number range Os(76)[14] to Pb(83); $L\alpha^{iz}$ in the range of Au(79) to U(82), although we failed to find definite evidence of this line for Tl(81), since on our plates the $L\beta_9$ line of W(74), appearing because of our use of a tungsten filament in the x-ray tube, comes at exactly the same wave-length as would $L\alpha^{iz}$ of Tl(81). Data regarding these two satellites are given in Table I.

Table I. *Satellites of* $L\alpha$ *for the range Os(76) to U(93).*

	$L\alpha^{iz}$				$L\alpha^{z}$			
Element	λ(X.U.)*	$\frac{\Delta\lambda}{(\alpha_1-\alpha^{iz})}$	$\frac{\Delta\nu}{R}$	$\left(\frac{\Delta\nu}{R}\right)^{\frac{1}{2}}$	λ	$\frac{\Delta\lambda}{(\alpha_1-\alpha^{z})}$	$\frac{\Delta\nu}{R}$	$\left(\frac{\Delta\nu}{R}\right)^{\frac{1}{2}}$
Os 76					1383.07	5.52	2.62	1.62
Ir 77					1343.17	5.30	2.66	1.63
Pt 78					1305.13	5.20	2.77	1.66
Au 79	1270.54	3.23	1.82	1.35	1268.63	5.14	2.89	1.70
Tl 81	**				1200.00	4.93	3.10	1.76
Pb 82	1169.29	3.26	2.16	1.47	1167.85	4.73	3.13	1.77
Bi 83	1138.14	3.36	2.35	1.53	1136.95	4.55	3.18	1.78
Th 90	950.80	3.25	3.26	1.81				
U 92	905.35	3.39	3.72	1.93				

* Siegbahn's values of λ for $L\alpha_1$ for each element are taken as standard.

** Obscured by $L\beta_9$ of W(74).

The values of $(\Delta\nu/R)^{\frac{1}{2}}$ are shown graphically in Fig. 1 as a function of atomic number for these satellites, $L\alpha^{iz}$ and $L\alpha^{z}$. The circles represent the data of the present authors. The crosses are from the observations of Idei.[12] For comparison, there are plotted on the same graph the (six) satellites of $L\alpha$ in the atomic number range $36<Z<50$, from the measurements of Richtmyer and Richtmyer.[15]

If one relies solely upon the graphical relations shown in Fig. 1, one might conclude that the

[7] Coster, Phil. Mag. **43**, 1070; **44**, 545 (1922).
[8] Dauvillier, C. R. **174**, 1347 (1922).
[9] Dauvillier, J. d. Physique et le Radium **3**, 230 (1922).
[10] Wennerlöf, Ark. Math. Astr. o. Fys. **22**, No. 8 (1930).
[11] Auger and Dauvillier, C. R. **176**, 1297 (1923).
[12] Idei, Tohoku Imp. Univ., Sci. Rep. **19**, 651 (1930).
[13] Rogers, Proc. Camb. Phil. Soc. **21**, 430 (1923).
[14] Beuthe, Zeits. f. Physik **46**, 873 (1928).

† Idei (reference 12) recognizes the existence of these two lines, although he did not find both of them for any one element. He designates them $L\alpha'$ and $L\alpha''$, respectively. Since it is obvious from Fig. 1 that these lines are *not* to be identified with the satellites $L\alpha'$ and $L\alpha''$ which occur in the atomic number range Rb(37)–Te(52), we have adopted the symbols $L\alpha^{iz}$ and $L\alpha^{z}$ to avoid confusion. Siegbahn (reference 5) does not distinguish between these two lines and calls them $L\alpha_3$.

[15] Richtmyer and Richtmyer, Phys. Rev. **34**, 574 (1929).

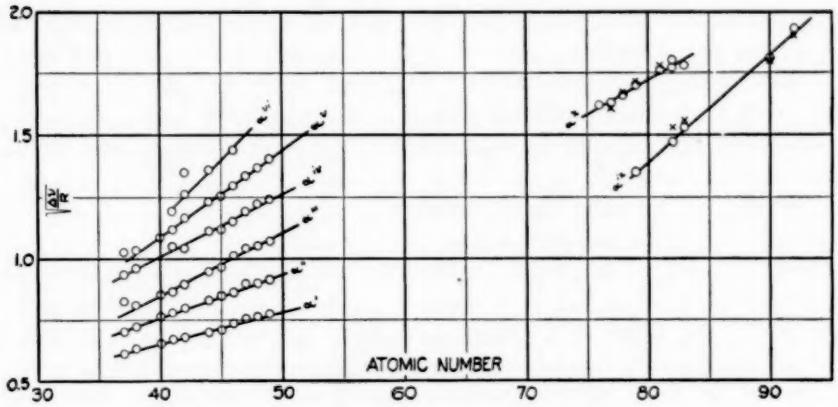

FIG. 1. $(\Delta\nu/R)^{\frac{1}{2}}$ as a function of atomic number for satellites of $L\alpha$. ($\Delta\nu \equiv$ difference in frequency between satellite and parent line.) The crosses are from the measurements of Idei.[12] The circles, for elements 76–92, are from data by present authors; for elements 37–50, from data by Richtmyer and Richtmyer.[15]

satellite designated $L\alpha^x$ is to be identified with $L\alpha''$ and $L\alpha'''$, perhaps unresolved for these high atomic number elements, which latter are the most intense satellites of the lower atomic number range.

There are, however, weighty arguments against this conclusion. First of all, there is no evidence that additional satellites accompany $L\alpha^{ix}$ and $L\alpha^x$, similar to $L\alpha^{iv}$ and $L\alpha^v$ which are associated with $L\alpha''$ and $L\alpha'''$ in the lower range. The intensities of $L\alpha^{iv}$ and $L\alpha^v$ are such that, if present with $L\alpha^x$, they should be readily detected. Second, the combination $L\alpha^{ix}$ and $L\alpha^x$ presents a structure very different from $L\alpha' - L\alpha^{vi}$, as may be seen from Fig. 1. Third, and most important, $L\alpha^x$ appears very abruptly at Os(76), and can therefore hardly be regarded as an extension of $L\alpha''+'''$, which, as above noted, are not found above I(53).

Of greater importance than the wave-length and atomic number range of $L\alpha^{ix}$ and $L\alpha^x$, is the rapid change in character of these lines as one advances up the atomic number scale above Os(76). At Os(76) $L\alpha^x$ is a sharp, fairly prominent line, well separated from $L\alpha_1$. At Ir(77) the satellite is still sharp, but the "valley" between it and the parent line is less pronounced. At Pt(78) this "valley" has become almost as intense as the satellite itself, which now appears almost like a sharp, prominent edge to a narrow band. At Au(79) there is unmistakable evidence of the presence of *two* lines, the new line, $L\alpha^{ix}$, appearing in what was formerly the valley between $L\alpha^x$ and $L\alpha_1$. Very likely the "filling up" of this valley in Ir(77) and Pt(78) foreshadows the appearance of $L\alpha^{ix}$. For Tl(81), Pb(82) and Bi(83) there is clear evidence of the presence of both $L\alpha^{ix}$ and $L\alpha^x$, although, as above noted, $L\alpha^{ix}$ for Tl(81) is probably covered up by $L\beta_9$ of W(74). For Th(90) and U(92) our plates are not as intense as they should be for best observation, but unmistakably there is only one satellite present, namely $L\alpha^{ix}$.

One concludes tentatively, therefore, that $L\alpha^{ix}$ and $L\alpha^x$ are *new* satellites, having a different origin from the group of satellites $L\alpha' - L\alpha^{vi}$. Furthermore, the rapid change in the character of these two satellites with atomic number after passing Os(76) suggests that their origin is in some way connected with the changes which take place in the O_{IV} and the several P electron shells in the region of Os(76) to U(92), *there being over this atomic number range no change in the L and M shells in which* $L\alpha_{1,2}$ *originates.*

It is not easy to reconcile these data with the Wentzel-Druyvesteyn theory, according to which satellites have their origin in atoms which are doubly ionized as to their *inner* electron shells. W(74) differs from Os(76) *only* as regards the number of electrons in the O_{IV} shell: W(74) has no electrons in this shell while Os(76) has two. Yet in Os(76) there is a prominent satellite while in W(74) there is none.

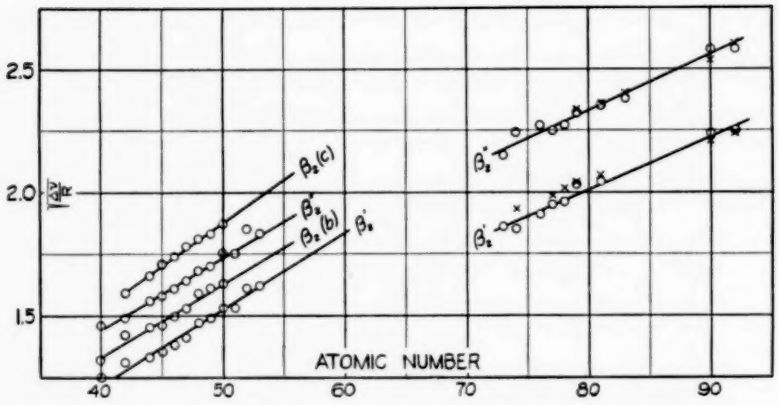

FIG. 2. $(\Delta\nu/R)^{\frac{1}{2}}$ as a function of atomic number for satellites of $L\beta_2$. The crosses are from the measurements of Idei.[12] The circles, for elements 73–92, are from data by present authors; for elements 40–54, from data by Richtmyer and Richtmyer.[15]

SATELLITES FOR $L\beta_2$

In the atomic number range $40<Z<54$, $L\beta_2$ has four satellites, well separated from the parent line. Two of these, $L\beta_2'$ and $L\beta_2''$ are quite sharp and, for satellites, are relatively intense. Associated with these two lines is a short continuous spectrum extending toward shorter wave-lengths from $L\beta_2'$ well past $L\beta_2''$. Midway between $L\beta_2'$ and $L\beta_2''$ is a faint, diffuse satellite[15] called $L\beta_2$(c); beyond $L\beta_2''$ is a fourth line, similarly faint and diffuse, called[15] $L\beta_2$(d). This type of structure persists substantially unchanged, except as to intensity relative to parent line, over the above atomic number range.

These satellites disappear, abruptly, at I(53), as has been shown by R. D. Richtmyer,[4] who pointed out that the lines designated by Coster[16] as satellites, in the spectrum of Ba(56) are, in reality, diagram lines ($L\beta_7$ and $L\beta_{10}$ respectively). *There are no other satellites of $L\beta_2$ reported in the literature for elements above Ba(56) until Er(68) is reached.* For this element Coster[17] reports a single satellite, $L\beta_2'$. This one line is reported by various observers for the elements Yb(70) to Ir(77). For the remaining elements two satellites $L\beta_2'$ and $L\beta_2''$ are reported.

Our own measurements begin at Ta(73) and include all elements readily available up to U(92). For each element studied, two satellites, $L\beta_2'$ and $L\beta_2''$ have been found,† as is shown in Table II.

$(\Delta\nu/R)^{\frac{1}{2}}$ as a function of Z is shown in Fig. 2, in which, for comparison there is also shown the four satellites of $L\beta_2$ in the lower atomic number range. The circles are the observations of the present authors. The crosses are from the work of Idei.[12]

TABLE II. *Satellites of $L\beta_2$ for the range Ta(73) to U(92).*

	$L\beta_2'$				$L\beta_2''$			
Element	λ(X.U.)*	$\Delta\lambda$ $(\beta_2-\beta_2')$	$\frac{\Delta\nu}{R}$	$\left(\frac{\Delta\nu}{R}\right)^{\frac{1}{2}}$	λ(X.U.)	$\Delta\lambda$ $(\beta_2-\beta_2'')$	$\frac{\Delta\nu}{R}$	$\left(\frac{\Delta\nu}{R}\right)^{\frac{1}{2}}$
Ta(73)	1275.68	6.22	3.46	1.86	1273.57	8.33	4.62	2.15
W(74)	1236.21	5.82	3.43	1.85	1233.53	8.50	5.02	2.24
Os(76)	1163.38	5.46	3.65	1.91	1161.13	7.71	5.15	2.27
Ir(77)	1127.61	5.36	3.80	1.95	1125.85	7.12	5.07	2.25
Pt(78)	1094.64	5.10	3.86	1.96	1092.93	6.81	5.15	2.27
Au(79)	1062.86	5.15	4.12	2.03	1061.28	6.73	5.39	2.32
Tl(81)	1003.58	4.64	4.17	2.04	1002.07	6.15	5.53	2.35
Pb(82)	976.09				974.50			
Bi(83)	(masked by $L\beta_1$)				947.62	5.62	5.67	2.38
Th(90)	788.47	3.45	5.02	2.24	787.36	4.56	6.66	2.58
U(92)	749.92	3.15	5.07	2.25	748.93	4.14	6.66	2.58

* Siegbahn's values for $L\beta_2$ for each element taken as standard.

As in the case of the satellites of $L\alpha_1$, the wave-length data, either in tabular or graphical form, do not tell the whole story. There is no doubt concerning the absence of both β_2' and β_2'' over a considerable range of atomic numbers in the rare earth region. There is agreement in the literature that β_2' is the first to reappear. It seems to increase in intensity until Os(76) is reached,

[16] Coster, Phil. Mag. **44**, 545 (1922).

[17] Coster, Phil. Mag. **43**, 1070 (1922).

† To save confusion in terminology Siegbahn's designation of these high atomic number satellites of $L\beta_2$, namely $L\beta_2'$ and $L\beta_2''$, has been retained, although it is by no means certain that these lines are to be identified with those similarly designated in the lower atomic number range.

beyond which its intensity seems to be constant. Our plates show clearly that, although β_2'' is unmistakably present at Ta(73) it is much weaker than β_2', and it grows in intensity less rapidly than does β_2'. Not until Tl(81) or Pb(82) is reached do the two lines have the same intensity, which equality is maintained up to U(92).

The behavior of these two satellites in the high-atomic number range is thus, as was found to be the case with the satellites of $L\alpha$, quite different from that observed in the lower range in which the two lines maintained the same intensity relative to each other throughout.

A further point of difference is that while $L\beta_2'$ and $L\beta_2''$ are equally sharp for the range $40<Z<54$, $L\beta_2''$ is noticeably "fuzzy" for the elements Ta(73) to Pt(78).

Again, as in the case of $L\alpha$, there is no change in the electron configurations in the shells which give rise to $L\beta_2$ over the atomic number range for which the satellites are observed.

The following two conclusions therefore, seem to be justified by the data above reported: First, the high atomic number satellites of $L\alpha$ and $L\beta_2$ are not to be identified with the satellites which accompany these lines at the lower atomic number range. Second, the peculiar behavior of these satellites in passing from element to element in this high atomic number region, seems to indicate a close connection of some kind between the satellites and the peripheral electron structures of the atom.

Since it is the purpose of this paper to present experimental results, no further comments will be made concerning the bearing of these data on current theories of the origin of satellites, beyond the obvious remark that any acceptable theory must be in agreement with the observations herein reported!

Soft X-Rays from (100) and (111) Faces of Copper Single Crystals

MORGAN L. WILLIAMS, *Brown University*

(Received July 13, 1933)

Between 90 and 220 volts 14 critical potentials were found for both the (111) and the (100) faces. Each break is the same within 1.5 volts for the two targets. Agreement with published results for polycrystalline copper is fair, although there are fewer discontinuities than for the ordinary metal, as in other experiments with single crystals. The critical potentials may be grouped to show level differences, attributed by Richardson to structure electrons in the crystal lattice. Comparison with other results for metals of similar structure casts doubt on this theory. Kronig's theoretical interpretation of fine structure in x-ray absorption presents a possible explanation of soft x-ray critical potentials. Assuming 4 to 7 volts inner potential, 10 of the 14 observed critical potentials agree with Kronig's calculated energy discontinuities and only one calculated discontinuity was not observed. A strong break at 104 volts, not predicted by this theory, is within 2 volts of Kurth's value for the N series convergence frequency. Similar good agreement exists between Thomas' critical potentials for polycrystalline iron and nickel and the energy discontinuities calculated from Kronig's theory. From these results it appears that the theory of forbidden energy zones may account for soft x-ray critical potentials.

INTRODUCTION

SOFT x-ray emission measurements by critical potential methods show many discontinuities not explained by the simple Bohr theory. Andrewes, Davies and Horton[1] suggested that some of these critical potentials might be due to the arrangement of atoms at the target surface, since the M electrons are not very deeply seated within the atoms of lighter elements. This suggestion was supported by Farnsworth's[2] observation that the position and shape of many of the discontinuities in secondary electron emission curves depend on the surface arrangement of atoms in the target or the orientation of single crystal targets. Using an imperfect natural graphite crystal, Richardson and Andrewes[3] found a decided reduction in the number of discontinuities, compared with those previously found for carbon targets. Richardson and Rao[4] reported similar results for the (100) face of a nickel single crystal. Using the same (100) face of nickel Rao[5] found the changes in slope of secondary electron curves to be in good agreement with the positions of the soft x-ray discontinuities. With a (111) face of a nickel crystal, Rupp[6] found electron diffraction maxima and soft x-ray breaks to agree as either the primary voltage or the angle of incidence was varied. He concluded that some, at least, of the soft x-ray critical potentials are connected with properties of the crystal grating.

The object of the present investigation was to determine whether there is a real difference in the soft x-ray critical potentials for different faces of the same metal crystal.

DESCRIPTION OF APPARATUS

Fig. 1 shows the electrical connections and a cross section of the experimental tube which is of Pyrex in the form of a cross consisting of a main tube G, 7 cm in diameter, with side arms A–A of 3 cm diameter placed near the top of the main tube. Targets T_1 and T_2, mounted on a pair of quartz rods R, may be moved by magnets acting on M–M. The targets were both cut from the same single crystal made in this laboratory.[7] The faces were prepared as described by Farnsworth.[8] Ammonium persulphate solution was used for final etching of the (100) target. The

[1] Andrewes, Davies and Horton, Proc. Roy. Soc. **A117**, 649 (1928).

[2] Farnsworth, Phys. Rev. **25**, 41 (1925); **31**, 419 (1928).

[3] Richardson and Andrewes, Proc. Roy. Soc. **A128**, 1 (1930).

[4] Richardson and Rao, Proc. Roy. Soc. **A128**, 57 (1930).

[5] Rao, Proc. Roy. Soc. **A128**, 57 (1930).

[6] Rupp, Naturwiss. **18**, 880 (1930).

[7] Farnsworth, Phys. Rev. **40**, 690 (1932).

[8] Farnsworth, Phys. Rev. **34**, 679 (1929).

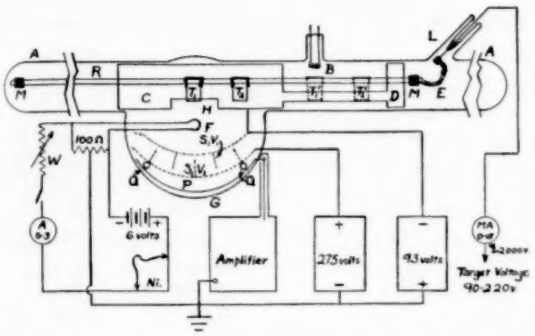

FIG. 1. Experimental tube and electrical connections.

(111) target was etched electrolytically in slightly acid copper sulphate solution. Low current density of about 3 m.a. per cm² produced best development of the (111) face. Final dimensions of the targets were about 8.0×7.5 mm face and 10.5 mm height. A cylindrical nickel shield C, 24 mm in diameter, surrounded the targets and with collar D supported the rods carrying them. An opening H, 18×19 mm, permitted exposure of only one target at a time to the filament F. Both targets were connected to the tungsten seal L by a tungsten spring E. A filament B of 8 mil tungsten was placed so that the targets could be withdrawn to position T_1' and heated by electron bombardment of their molybdenum supports which fitted into grooves cut in the targets. The x-ray filament F of oxide coated nickel, placed 7 mm below the target face, was usually operated at 2.2 amperes, so that the drop across the emitting portion was less than 0.5 volt. A large-capacity storage battery supplied the heating current, which was controlled by a tapped oil immersed chromel resistance W and clips sliding on nickel wires for fine adjustment. The ion trap consisted of two sets of screens and vanes S_1V_1 and S_2V_2, of 1/16-inch mesh nickel screening, insulated by Pyrex tubes. The potentials, −9.2 volts for the top screen S_1V_1 and cylinder C, and +275 volts for the lower screen S_2V_2, were supplied by dry cells shielded in sheet iron boxes. The photoelectric plate P of sheet nickel rested on the bottom of the main tube G and was insulated from the screens by 3 mm rods Q of clear fused quartz. The insulation resistance of P was higher than 10^{10} ohms. The photoelectric current was measured by a one-tube balanced amplifier of the type described by Soller,[9] slightly modified, having a sensitivity of 7.33 $\times 10^{-15}$ amp./mm with grid resistance 3.74×10^{9} ohms (pencil mark on amber). Part of the plate resistance R_1 (Soller's figure) was made variable, so the plate current could be balanced out for any grid input in the operating range. The effect was the same as in Compton and Thomas' method[10] of balancing out part of the electrometer current, allowing use of the full sensitivity to measure changes of photoelectric current over a small range of target voltages. The variable resistance used in this compensating circuit was a 400 ohm Centralab potentiometer. Large B batteries supplied the x-ray target voltage which could be adjusted to any value by taps and potentiometers. It was measured by a special high-resistance Weston voltmeter, which could be read accurately to less than 0.1 volt on the 300 volt range. The thermionic current I_t, of the order 0.5 m.a., was measured to 1 part in 5000 by a null circuit using a galvanometer to indicate balance of a standard cell against the potential drop in a resistance carrying I_t. Balance was secured and I_t held constant by changing the filament current. The experimental tube was shielded with Aquadag, and all wires entering the room were fully shielded.

The vacuum system, consisting of two mercury vapor pumps in series, backed by a Hyvac pump, was connected to the experimental tube through two traps immersed in carbon dioxide snow and acetone. Liquid air was used until experiments on contact potential difference in this laboratory had shown that results were the same with either carbon dioxide or liquid air. Pressure was measured by a General Electric FP62 ionization gauge placed near the x-ray chamber. The experimental tube and trap nearest to it were outgassed by baking for 3 periods totalling 50 hours at 430 to 480°C. Between bakings the filaments were flashed and the targets heated several hours at red heat. After this outgassing process, pressures while bombarding the targets did not rise above 10^{-6} mm of mercury. Pressures while taking readings, 2 to 5 hours after heating the targets, were 1 to 2×10^{-7} mm.

[9] Soller, Rev. Sci. Inst. **3**, 416 (1932).
[10] Compton and Thomas, Phys. Rev. **28**, 601 (1926).

Experimental Procedure

Before each run, the target was heated 2 to 10 hours. As outgassing progressed, the target temperature was gradually increased but evaporation was prevented until the last stages. At the conclusion of bombardment the target was immediately moved to the x-ray position and the target voltage adjusted at the highest value to be used in the run. As soon as the thermionic current I_t could be held at the desired value, the amplifier was adjusted by means of the variable resistance in the plate compensating circuit, so that its reading I_p' would be near the higher end of the scale. With the target voltage and I_t constant, readings of I_p' were taken at intervals until it ceased to change. During this time, 2 to 5 hours, I_p' decreased, rapidly at first, then more slowly. This is attributed to changing photoelectric characteristics of the nickel plate as it was outgassed by action of the soft x-rays. Nakaya[11] observed similar effects on outgassing a photoelectric plate by bombardment.

When I_p' had reached a steady state, readings were taken from which the soft x-ray critical potential curves were plotted. The amplifier sensitivity was adjusted by an Ayrton shunt on the galvanometer so that I_p' would cover nearly the whole scale for the range of voltages to be used in the run. While the target voltage was decreased by steps of 1.0 or 2.0 volts and I_t was kept constant, I_p' was read for each voltage. All runs were taken in the order of decreasing voltage, since I_t reached equilibrium more quickly than in the reverse order. Check runs taken with increasing target voltage showed breaks in the same positions. At the conclusion of each run the constancy of the amplifier was checked by repeating readings at certain voltages. A slight change in target voltage, too small to be observed on the voltmeter, could be detected by its effect on I_p'. Since I_t was held constant to 1 part in 5000, the limiting factor in the sensitivity of the apparatus was the accuracy of measuring the voltage, less than 0.1 volt. The oxide coated filament used at low temperature and the small potential drop along the emitting part of the filament make the speeds of the electrons more uniform than in most soft x-ray experiments to date.

[11] Nakaya, Proc. Roy. Soc. **A124**, 616 (1929).

Results

Fig. 2 shows a typical soft x-ray critical potential curve. Since I_t was held constant during each run, the amplifier reading I_p' is proportional to I_p/I_t minus a constant and is plotted directly against the voltage. The intensity or certainty of the break is estimated from the change in slope of the curves. Intensity (1) signifies the least change of slope which can be detected or a break dependent on the positions of only a few points and (3) indicates the most pronounced breaks.

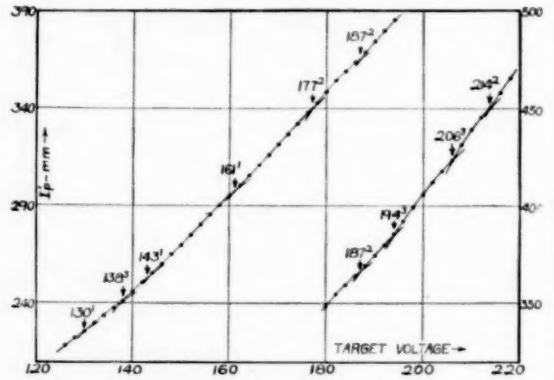

Fig. 2. Typical critical potential curve. Run No. 240, (100) target. The uncorrected voltage of each break is shown above the curve, followed by a superscript denoting the intensity or certainty of the break.

The uncorrected voltages of all breaks found in 20 runs with the (111) target, in the range 90–220 volts, are tabulated in Table I. Table II shows the critical potentials found in 18 runs with the (100) target. Readings were started 1.5 to 8 hours after heating the targets. The pressure while taking readings varied from 1.1 to 2.2×10^{-7} mm in different runs, although it was nearly constant during each run. No significant changes in either intensity or position of the breaks can be attributed to these variations of pressure or to the amount of outgassing or time since outgassing the target. Runs taken during the earlier stages of outgassing were so irregular, from other causes, that no conclusions can be drawn from them. In an attempt to determine whether changed surface conditions on the target cause changes in the soft

TABLE I. *Critical potentials for (111) target (uncorrected).*

Groups including nearly all of the breaks are indicated at the heads of the columns. Breaks falling less than two volts outside of these groups are included in the column, *in italics*. They are included in the averages and the same weight is given to each value regardless of intensity. Breaks not obviously belonging to any group are written between the columns. A break missing in any run is indicated by an x where it should appear and is considered as zero intensity when computing the mean value. Superscripts denote intensity of the breaks. Numbers 243–257 are the final series of readings taken under most carefully controlled conditions. The remaining 6 runs which were taken before certain improvements in apparatus were made and were noted as exceptionally steady at time of reading, are seen to agree with the final series. Target was heated a total of 157.5 hours for run 243 and 243 hours for the last run 257. For the earlier runs given the total heating was from 20 to 74 hours.

Run No.	93–94	97–99	107–108	116–118	122–124	129–132	136–137	144–146	159–160	177–178	185–186	192–194	202–204	213–214
243							136^2	144^2	*158*^{2}	178	186^2	192	204^2	214^2
244	93^3	98^2	108^3	116^2	122^2	130^2								
246										177^2	*184*	193^2	204^2	214^2
247							136^2	146^3	159^2	178	186			
248						132	x	146^2	160^3	176^2				
249		98^2	108^3	118^2	124^2	132^1	136	145^2	159^2					
250	93^3	*100*	108^2	x	122^2									
251	93^2	97^2	108^3	*115* / *119*^{2}	*125*	129^2	136^2							
252							137	144^2	160^2	178	186^2	194	203^2	214^2
									? 172					
253	94^2	99	108^2	x	122^2	129^2								
254									160^3	177	186^2	194^2	203^2	214
255	93^2	97^2	107^2	117^2	x	130^2	x	144^2	*162*^{2}					
256				118^3	122	130	137^2	146^2	160^2	178	186^2	192^2		
257										177	186^2	194^2		
										?				
189							137^3	144^2	159^2	168 x	186^2	194^2	204	x
196	93^2	99^2	108^3	116	x	130								
211	93^2	97^2	108^3	116^2	124	*133*	137							
212	93^2	*100*^{3}	108^3	116^2	123	129	136							
216										178^2	185	192^2	*201*^{2} / *207*	213^2
217	*95*^{2}	99	107^2	117^2	x	131	137	145^2	160^2	x	185^2			
Mean voltage	93.3	98.4	107.8	116.8	123.0	130.5	136.5	144.9	159.7	177.4	185.6	193.1	203.7	213.8
Mean int.	2.2	1.8	2.6	1.5	1.1	1.5	1.3	2.1	2.3	1.1	1.5	1.5	1.9	1.5

x-ray characteristics, before runs 256 and 257 the (111) target was heated to a higher temperature than before, until a considerable amount of copper evaporated. No definite changes were observed in these runs.

The construction of the x-ray tube did not permit an experimental determination of the contact potential difference between target and filament. Farnsworth has found that for a copper target and an oxide coated filament the correction is negative and of the order 3 volts. Adding 1 volt for drop in the null resistances, we find 4 volts, to be subtracted from the voltmeter readings, as the most probable correction for the soft x-ray critical potentials.

DISCUSSION

The average critical potentials for the (111) and (100) faces of copper single crystals from Tables I and II are shown in the first two columns of Table III. Here the most probable correction of -4.0 volts is applied. It is evident that the same critical potentials appear for both targets. In the region 90–220 volts, 14 breaks are found and, in all cases, the voltage of the break agrees within 1.5 volts for the two targets.

Critical potentials for polycrystalline copper targets published by Compton and Thomas[10] and by Richardson and Rao[12] are shown, respectively, in columns 3 and 4. In both cases the corrected

[12] Richardson and Rao, Proc. Roy. Soc. **A128**, 16 (1930).

TABLE II. *Critical potentials for (100) target (uncorrected).*

Notation is the same as for Table I. Numbers 233–241 are the final series with total heating of target between 220 and 250 hours. Others were obtained in earlier runs under best conditions after 100 hours of heating.

Run No.	92–93	98–99	108–109	116–118	122–123	130–131	137–138	144–146	159–160	176–178	186–188	193–196	204–206	212–214
	Final series of readings													
233									160^3	176	187^2	194^3	206^2	214^2
234										178^2	188^3	*x*	206	212^2
235										178^3	187^2	195^2	206^2	212^2
236						130	138^3	145^2	159^2	176^2				
237		98^2	108^3	116	122^2	130^2	138	144^2	160^2	176^2				
238	93^2	98^2	109^3	118^2	123^2	131^3	138							
		? 104												
239	92^2	98^3	109^2	118	122^2	130^2								
240						130	138^3	*143*	*161*	177^2	187^2	194^3	206^3	214^2
241	93^2	$\left\{\begin{matrix} 96^2 \\ 100^2 \end{matrix}\right\}$	109^3	*115*	*121*	$\left\{\begin{matrix} 129^2 \\ 133 \end{matrix}\right\}$	138							
	Earlier runs													
203					*124*	130	137	144^3	160^2	178	187	*x*	204	212^2
206	92	$\left\{\begin{matrix} 96^2 \\ 100^2 \end{matrix}\right\}$	108^2	118^2	123	131	*136*							
207								144^3	159	178^2	186^2	193^2	204	213
208							138^2	144^3	160^2	177^2	187^3	193^2	204^2	214^2
221							138^3	146^2	160^2	176^2	186^2	195^2	206^2	214^2
222		99^2	108^2	116	123^2	130^2	138^2	146^2	159^2					
223	93^2	99^2	108^3	116^2	123^3	130								
227	92^2	98^2	108^3	116	122^2	*132*	138^2	145^2	159	176				
228		98^2	*107*^{2}	116^2	122^2	130^3								
Mean voltage	92.5	98.2	108.2	116.6	122.5	130.4	137.7	144.6	159.7	176.9	186.9	194.0	205.2	213.1
Mean int.	1.8	2.3	2.6	1.4	1.9	1.7	1.8	2.2	1.9	1.8	2.1	2.2	1.7	1.9

voltages are given. Both groups of experimenters found more breaks for polycrystalline copper than were found by the author with single crystal targets. This is in agreement with the results of others[3, 4] using single crystals. Agreement between the author's results and published results for polycrystalline copper is only fair since, on considering the small separation of the breaks found for the ordinary metal in this voltage range, it is evident that a considerable number of points might accidentally agree within two volts. However, it may be said that agreement of the critical potentials found for the single crystals with certain of the critical potentials for the polycrystalline metal is as good as is usually found in soft x-ray measurements of different experimenters.

All of the 14 breaks observed in this experiment may be separated into 3 groups and arranged in a table showing horizontal and vertical differences of the order of magnitude predicted by an approximate calculation based on Richardson's theory of structure electrons.[13] Some doubt is cast upon this apparent correlation by comparison of results of other observers for metals of similar crystal structure. For example, nickel has the same crystal structure as copper and the atomic numbers and lattice constants of these metals differ only slightly, hence correction terms neglected in the approximate calculation should be of the same order of magnitude. If we use the true lattice constants in the development of Richardson's formula and substitute the atomic number for z (neglecting screening effects) the calculated level spacings for copper and nickel are very nearly the same; but Richardson's[13] tabulation of Rao's[5] critical potentials of secondary electron emission from a nickel single crystal shows level spacing considerably larger than that found for the soft x-ray

[13] Richardson, Proc. Roy. Soc. **A128**, 63 (1930).

TABLE III. *Comparison of critical potentials for copper.*

1 (111) Face Corrected Author		2 (100) Face Corrected Author		3 P.C.Cu C. & T.[9]		4 P.C.Cu R. & R.[12]		5 Absorption Kronig[14]	
Volts	Int.	Volts	Int.	Volts	Int.	Volts	Int.	Volts	r
89.3	2.2	88.5	1.8	86.7	1.2			93	6
				92.2	1.6				
94.4	1.8	94.2	2.3	94.5	0.9			101	24
				98.8	1.6			104	15
103.8	2.6	104.2	2.6	104.5	2.0			—	—
				108.2	1.8	107.3	1.0		
112.8	1.5	112.6	1.4	111.0	1.4	111.0	0.7	116	12
				115.2	1.8				
119.0	1.1	118.5	1.9	117.8	1.5	117.8	0.6	124	12
								127	12
126.5	1.5	126.4	1.7	127.1	1.4	128.0	1.5	—	—
132.5	1.3	133.7	1.8	132.9	0.9	133.5	1.8	139	4
140.9	2.1	140.6	2.2	140.6	1.5	139.5	0.8	148	24
				148.4	1.4	148.3	0.9	150	12
155.7	2.3	155.7	1.9	157.1	1.4	157.4	0.9	162	24
				164.6	1.6				
				168.3	1.1	166.3	1.1	170*	36
173.4	1.1	172.9	1.8					—	—
				178.6	1.5	178.4	0.7		
181.6	1.5	182.9	2.1					—	—
189.1	1.5	190.0	2.2	188.8	1.7	188.0	0.6	194	12
								197	24
199.7	1.9	201.2	1.7	—	—	197.1	1.3	208	18
				204.8	1.4	205.3	0.6		
209.8	1.5	209.1	1.9					217	28
				216.8	1.4	217.1	0.5		

critical potentials of copper in the present experiment.

It thus seems necessary to seek other possible explanations of the soft x-ray discontinuities. One such possibility, suggested to the author by Dr. Farnsworth, is presented by Kronig's[14] recent interpretation of fine structure of x-ray absorption spectra by means of the quantum mechanics of electrons in crystal lattices. This theory is based on the idea introduced by Bloch that influence of the crystal lattice can be replaced by a periodic potential field having the same period as the lattice. The theory shows that not every value of velocity is possible for electrons moving through a crystal lattice but rather that an energy spectrum exists, consisting of alternating zones of permitted and forbidden energies. Kronig has calculated, from the wave equation, the perturbed energy of an electron travelling in a crystal lattice. It is shown that there are discontinuities in the energy of the perturbed electron when its momentum parameters are related in a certain way to parameters α, β, γ, which may be considered as defining planes in the crystal lattice. Although these discontinuities or forbidden energy zones depend on direction of propagation of the electron, Kronig has shown that there are still finite variations in the absorption coefficient corresponding to each discontinuity, after integration over all directions of propagation. In terms of the parameters, the energies of these discontinuities are $W_{\min}=(\alpha^2+\beta^2+\gamma^2)h^2/8ma^2$, where h is Planck's constant, m the electron mass, and a the distance between potential barriers equal to the lattice constant of the absorbing substance. Using values of α, β, γ determined by the sequence of planes in the metal lattice, Kronig calculated the energies, in electron volts, of these discontinuities for copper. Results of these calculations are shown in the fifth column of Table III. Here r represents the abundance of the

[14] Kronig, Zeits. f. Physik **75**, 191 (1932).

discontinuity planes considering permutations and changes of sign of the parameters.

In 4 cases, pairs of Kronig's calculated values are separated by 3 volts or less. If we group these pairs as indicated by the brackets in Table III, it can be seen that 10 of the 14 critical potentials found by the author fall 4 to 7 volts below a calculated value or group. This uses all but one of the calculated values—the one at 170 volts marked with a star. This calculated discontinuity is due to the (553) and (731) planes of the crystal, planes in which atomic density is very small. The four observed critical potentials which do not correspond to a calculated value are 104, 126.4, 173.2, and 182.2 volts. All of these were found by other observers with polycrystalline copper targets, so it is improbable that they might be due to impurities. The break at 104 volts is very strong, in fact, for both targets the intensity is the highest of all the breaks observed. Kurth,[15] gives 116A, or 106 volts, as the convergence frequency of the N series for copper, which checks closely with this observed strong break.

Similar correlation can be shown between Kronig's table of energy values for iron, which has different crystal structure, and soft x-ray breaks observed by Thomas[9] for the polycrystalline metal. Strikingly good agreement is found on comparing Thomas' critical potentials for nickel with the energy discontinuities, which may be calculated from Kronig's table for copper by correcting for the difference in lattice constants. Thomas found one break not predicted by the theory and the calculations show two discontinuities close together which were not reported by Thomas. All except 2 of the 12 breaks reported by Thomas fall within 4 volts below a calculated value. It was noted above that critical potentials for copper found in the present experiment also fall below the calculated values by 4 to 7 volts. This might be explained by an inner potential of the metal which causes acceleration of electrons on entering the target. Farnsworth[7] found that the experimental voltage for electron diffraction beams from a copper crystal falls below the theoretical voltage, so that an inner potential ϕ of the order 25 volts is required. Since it appears that the full value of ϕ is not effective unless the velocity of incident electrons exceeds a certain value, Farnsworth suggests that ϕ depends on depth of penetration of the surface layer. The fact that a smaller inner potential is required to correlate soft x-ray data is in accord with this suggestion, since the high absorption coefficient for soft x-rays requires that they be generated near the surface of the target.

The observed agreement between soft x-ray critical potentials and Kronig's calculated absorption discontinuities may be explained as follows: The absorption discontinuities are calculated for forbidden zones of energy of electrons moving through the crystal lattice. Electrons having energies falling within these forbidden zones cannot enter the target so they are reflected, either diffusely or as diffraction beams. Consequently, electrons having these energies are not available for production of x-rays and a minimum in the soft x-ray curves results. These minima in the continuous radiation, superimposed on the general upward trend as voltage is increased, appear as discontinuities in the critical potential curves and account for the breaks not predicted by the Bohr theory. Thus many of the observed soft x-ray critical potentials are not due to true characteristic radiation of the atoms, but are characteristic rather of the lattice structure of the target.

The observed agreement between the breaks found for the two different crystal faces remains to be considered. Since Kronig's values are obtained by integrating over all directions of motion of electrons in the lattice, it appears at first sight that some of the discontinuities might not appear when bombarding electrons fall within 15 to 20° of normal incidence on a single crystal target, as in the present experiment. Obviously one would expect different breaks to be missing for different orientations of the targets. Failure to observe this difference may be accounted for by random changes of direction of the incident electrons on first striking the targets. In Kikuchi's[16] experiments on diffraction of high-speed electrons from mica, certain lines in the photographs are explained as due to electrons scattered on first entering the crystal and

[15] Kurth, Phys. Rev. **18**, 461 (1921).

[16] Kikuchi, Japanese J. Phys. **5**, 83 (1928).

subsequently reflected from crystal planes at the Bragg angle. This requires an amount of scattering, on first striking the target, sufficient to account for the agreement of the soft x-ray breaks for the two targets. It is known from diffraction experiments with low-speed electrons that only a small fraction of incident electrons is returned as diffraction beams and consequently a considerable number must also be scattered diffusely.

In conclusion, the author wishes to express his sincere thanks to Dr. H. E. Farnsworth, for his many helpful suggestions and criticisms during the course of this research.

Decay of Luminescence and Light Absorption in Phosphorescent Materials

D. H. KABAKJIAN, *University of Pennsylvania*

(Received May 1, 1933)

Effect of continuous irradiation with α, β and γ-rays on the light absorption coefficient of certain phosphorescent materials. With continuous irradiation the light absorption coefficient of each sample reaches a characteristic saturation value which is a function of the intensity of the radiation and the temperature at which the irradiation takes place, but is independent of the variations in the light emission of the material and also of the total amount of energy absorbed by it. The experimental curves of the rise and decay of phosphorescence and of the changes in light absorption coefficient of these materials cannot be explained by the generally accepted theories of these phenomena.

THEORIES of luminescence produced in certain materials by absorption of various forms of radiation can be classified in two groups: (1) the "excitation" theory which considers the emission of light as due to displacement of electrons and their subsequent return to normal energy levels without any permanent change in the material; and (2) the "destruction" theory which considers the emission of light as resulting from a chemical change and therefore gradual disappearance of luminescent centers in the material. The second theory was adopted to explain the decay of luminescence, in some cases, as a result of continuous irradiation.[1] In the case of scintillations produced by alpha-particles in phosphorescent zinc sulfide Rutherford's destruction theory seems to be generally accepted.[2] The theory postulates that each active center upon being hit by an alpha-particle is destroyed and emits a flash of light. Hence the brightness of the material, when bombarded by a constant source of alpha-particles, decays exponentially with time. This law of decay, however, is not verified experimentally.

In studying the decay of self-luminous zinc sulfide paints, extending over a period of ten years, Walsh came to the conclusion that the discrepancy between the destruction theory and his experimental curves could be explained if the change in the light absorption coefficient of the material was taken into consideration. By making certain assumptions as to the nature of light absorption in an irradiated material he succeeded in deriving a theoretical formula which agrees with his curves within the limits of experimental error, thereby apparently confirming the original destruction theory of Rutherford.[3]

According to this modified theory the destruction of active centers which results in the emission of light, also results in increasing the light absorption coefficient of the material. This assumes a close relationship between the two phenomena, since both result from the destruction of the same active centers, the contribution of the non-active centers to this change being considered as negligible. Also, in correcting for the absorption of the glass containers, Walsh assumes the change in absorption coefficient of glass to follow a simple exponential curve of the type $\tau = \tau_0 e^{-pt}$, where τ is the transmission factor, p a constant depending upon the intensity of the radiation, and t the time.

In a previous paper[4] attention has been drawn to the inadequacy of this modified destruction theory to explain luminescence phenomena in a number of materials, including zinc sulfide, and doubt was expressed as to the validity of the assumptions on which the theory is based. It will be shown further that the luminescence of these materials is of a complex nature and a simple ex-

[1] *Bulletin of Research Council*, No. 30, pp. 7–27, 1923.

[2] E. Rutherford, Proc. Roy. Soc. **A85**, 561 (1909–10); J. Charitan and C. A. Lea, Proc. Roy. Soc. **A122**, 335 (1929).

[3] J. T. Walsh, Proc. Phys. Soc. London **38**, 318 (1926–27).

[4] D. H. Kabakjian, Phys. Rev. **37**, 1120 (1931).

ponential decay curve cannot be expected except as an approximation.

The coloration of transparent substances resulting from irradiation has been extensively studied but there is no general agreement as to the nature of the phenomenon. In some luminescent substances this coloration is quite intense and would certainly affect the brightness of the samples. The variation of brightness due to this cause alone has never been studied to my knowledge. Therefore it was considered desirable to make an experimental study of this effect and of any relationship that might exist between the brightness decay and progressive changes in the absorption coefficient of a number of substances.

Materials and Methods of Procedure

Several types of glass, some of known composition, furnished by Corning Glass Company, were used for the absorption measurements. Data given in this paper refer to an ordinary microscope slide glass and to one containing 15 percent BaO, 25 percent K_2O, and 60 percent SiO_2 (Corning Glass No. 6). No luminescence measurements were made on these. Both luminescence and absorption measurements were made on crystals of fluorite, calcite, and anhydrous calcium sulfate activated with manganese. The latter was prepared by crystallizing calcium sulfate from a solution in concentrated sulfuric acid. These were cut into more or less transparent plates. Similar measurements were also made on thin films of crystalline powders of willemite and zinc sulfide. The powder was mixed with a dilute solution of Canada balsam and deposited on very thin glass or mica. The thickness of the ZnS films varied from 0.03 to 0.05 mm. Changes in absorption of very thin glass and a small thickness of balsam irradiated with α-rays was found to be negligible.

These materials were exposed to radiation of known intensity and changes in their brightness as well as in their absorption coefficients were made at various intervals of time.

The sources of radiation consisted of films of crystalline radium sulfate applied with a varnish on gold plates. The varnish was thin enough to absorb only a small part of the α-rays. Although there was a slight loss of emanation from the surface, after equilibrium had been reached with the occluded emanation and the short-life products of radium these plates could be considered as constant sources of α, β and γ-rays. The radium contents mentioned in this paper refer to γ-ray determinations of radium C in the plates. For purely α-ray sources, polonium deposits on silver plates were used. A correction for the decay of polonium was made in the computations, by using 136 days as the half-life period of polonium.

Absorption measurements were made with an ordinary Lummer-Brodhun photometer. The transmission of each plate before irradiation and after measured intervals of irradiation were determined, and the absorption coefficient computed from the known thickness of the plates. In the case of powder films, these measurements do not give the absorption coefficient of the material of which the film is made but of the film itself. This was considered sufficient for the present purpose.

Luminosity measurements were made with a special type of photometer somewhat similar to the one described by Meacock and Lambert[5] for the measurement of luminous paints, with, however, a Lummer-Brodhun cube for comparison of brightness. The photometer was calibrated with a Nutting polarization photometer. This calibration introduces an additional experimental error in the absolute values of the brightness of the samples. It does not affect, however, the relative values of brightness with which I was concerned. The experimental error in these measurements was about 5 percent.

Results

Variation of absorption coefficient

Fig. 1 shows the effect of irradiating with different amounts of radium, ordinary microscope slide glass; Fig. 2, glass containing 15 percent BaO, 25 percent K_2O, and 60 percent SiO_2. It may be seen that in both cases the coefficient of absorption, μ, in cm^{-1}, defined by the relation $I/I_0 = e^{-\mu x}$ (where I/I_0 is the fraction of the light transmitted and x the thickness of the medium in cm), increases with time and approaches a saturation value. It is also quite evident that this

[5] H. F. Meacock and G. E. V. Lambert, J. Sci. Inst. **8**, 214 (1913).

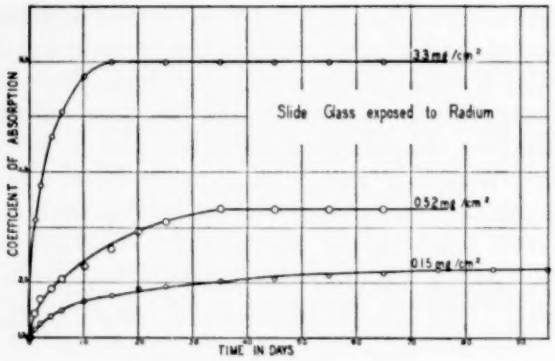

FIG. 1. Change in the coefficient of absorption for samples of ordinary microscope slide glass exposed to 3.3, 0.52, and 0.15 mg/cm² of radium.

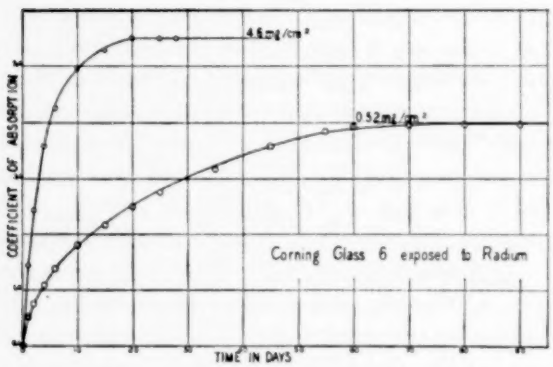

FIG. 2. Change in coefficient of absorption for samples of glass containing 60 percent SiO_2, 25 percent K_2O, and 15 percent BaO when exposed to 4.6 and 0.52 mg/cm² of radium.

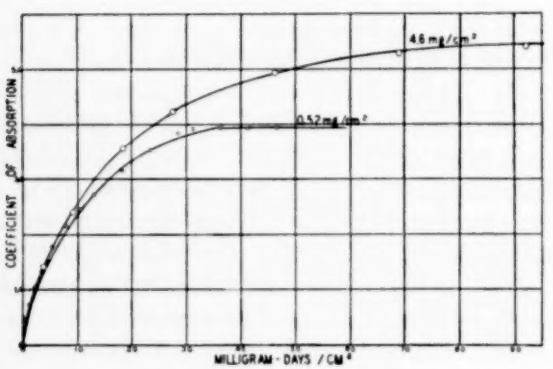

FIG. 3. Same samples as in Fig. 3. Coefficient of absorption plotted against the energy absorbed, the energy being expressed in milligram-days per square centimeter.

saturation value is a function of the intensity of the radiation rather than of the amount of energy absorbed by the material. In Fig. 3 the variation of μ is plotted against the energy absorbed in milligram-days/cm² for one of these samples.

Variation of absorption coefficient of strongly luminescent materials was quite similar to that observed in glass, with different constants characteristic of each material. There was always an initial rapid rise with an approach to a saturation value. An absorption curve for zinc sulfide is shown in Fig. 7.

The effect of temperature

The maximum value of μ in irradiated glass is fairly constant at ordinary room temperature. If, however, the temperature is raised the value of μ decreases reaching different constant values for different temperatures, until at a critical temperature the effect of irradiation completely disappears. Irradiating glass at this temperature does not produce any coloration. Fig. 4*A* shows

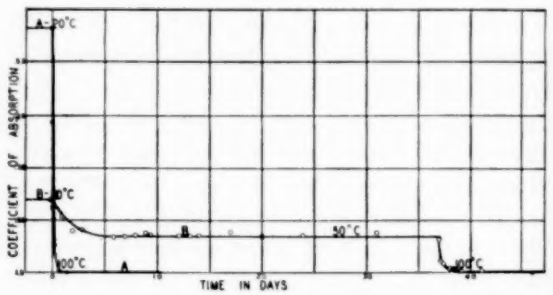

FIG. 4. Effect of temperature on the coloration for two samples of ordinary microscope slide glass. Both were irradiated at 20°C. Before irradiation μ was 1.5. Temperature of sample *A* was raised to 100°C and kept constant; that of sample *B* was first 50°C and later 100°C.

the recovery at 100°C and *B* the recovery first at 50°C and later at 100°C of the transmission of glass which had been irradiated at 20°C. It is seen that both glasses have completely recovered their original transmission. No attempt was made to determine the critical temperature at which complete recovery takes place. Qualitative observations indicate, however, that the critical temperature for recovery is different for different materials and for glasses of different composition.

Brightness decay and light absorption

Simultaneous determinations of change in brightness and in absorption coefficient on the same samples show that these two phenomena are not directly related to each other. In Fig. 5 is

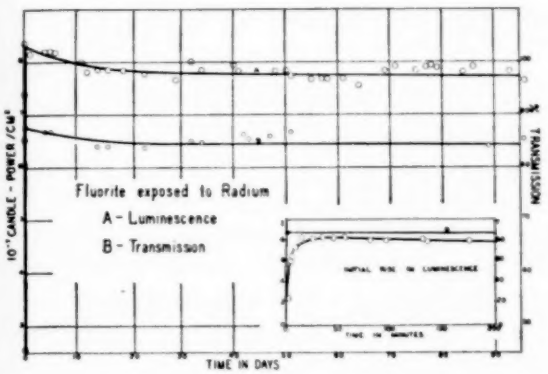

FIG. 5. Luminescence and transmission of a sample of fluorite 0.09 cm thick exposed to 11.7 mg/cm² of radium.

shown the change in luminescence and in transmission for a clear plate of fluorite exposed to radium. There is a very large initial rise in brightness with no corresponding change in the transmission. Fig. 6 shows the rise of brightness in calcite followed by a gradual decay. There was no measurable change in transmission in this case.

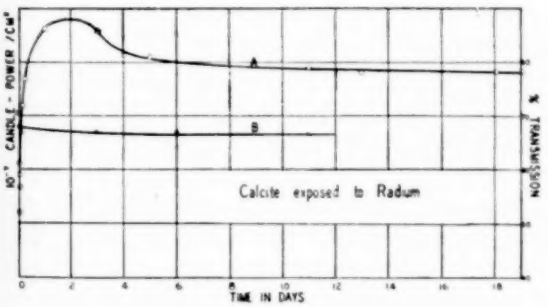

FIG. 6. Luminescence and transmission for a sample of calcite exposed to 11.7 mg/cm² of radium.

Because of the photosensitivity of zinc sulfide, brightness and absorption measurements could not be made on the same plate, as in the case of fluorite and calcite. They were made on two similar plates prepared from the same material and irradiated with approximately equal quantities of polonium. In Fig. 7, curve *A* represents the

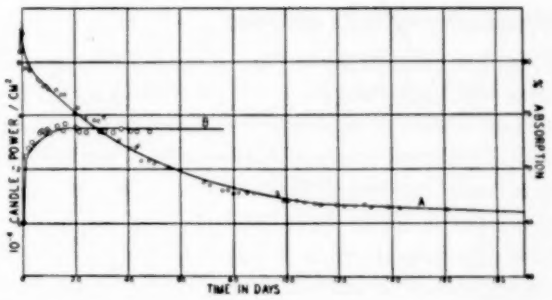

FIG. 7. Luminescence and absorption for a crystalline deposit of ZnS 0.005 cm thick, exposed to polonium.

rise and decay of brightness in zinc sulfide and curve *B* the increase in its absorption. It is seen that the absorption has reached a saturation value in about 8 days while the decay of luminescence continues over 100 days. Therefore the relationship between the decay of brightness and light absorption assumed by Walsh for this material is not borne out by these observations.

It is possible to check the modified destruction theory in another way. From the curve *B*, Fig. 7, and the known thickness of the film of zinc sulfide the value of the absorption coefficient for each point on curve *A* can be determined. It is now possible to plot a luminous flux-time curve, eliminating the effect of absorption. Since the brightness I is given by the relation

$$I=(F/4\pi\mu)(1-e^{-\mu x}),$$

where F is the flux in lumens per cc, x the thickness, and μ the coefficient of absorption, then

$$F=4\pi\mu I/(1-e^{-\mu x}).$$

The variation of flux in time is represented in Fig. 8. This is not a simple exponential curve as required by the destruction theory.

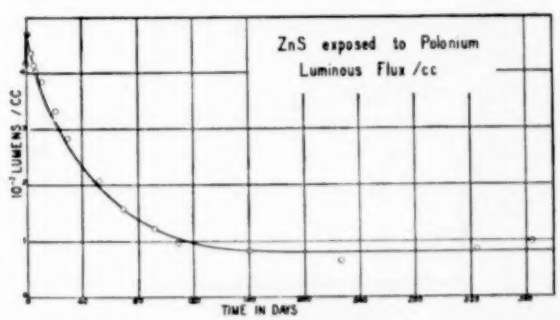

FIG. 8. Same material as Fig. 7. Luminous flux/cc.

Complexity of light emission

It has been observed by several investigators that the light emitted by phosphorescent materials consists of fluorescence and often more than one type of phosphorescence. This in itself precludes the possibility of observing a simple exponential decay curve of brightness. A quantitative determination of the relative importance of these factors in zinc sulfide is rather difficult. A more suitable substance for this purpose is the anhydrous calcium sulfate described above. Fairly transparent plates cut from crystals of this substance when irradiated with rays from radium show fluorescence and phosphorescence to about equal degrees.

A plate of this material was exposed to 4.6 mg/cm² of radium and its brightness measured at successive short intervals. After each measurement the radium was removed and the residual brightness measured immediately. The first set of measurements gives the combined fluorescence and phosphorescence while the second set gives the phosphorescence alone. The difference between the two readings gives the fluorescence. A small correction was necessary for the decay of phosphorescence between the removal of the radium and the measurement of the residual brightness, an interval of about 30 seconds.

In Fig. 9, curve *A* gives the luminescence of such a sample, *B* its phosphorescence, and *C*, which is obtained by subtracting the ordinates of *B* from those of *A*, its fluorescence. The luminescence curve, then, is a composite of a decaying

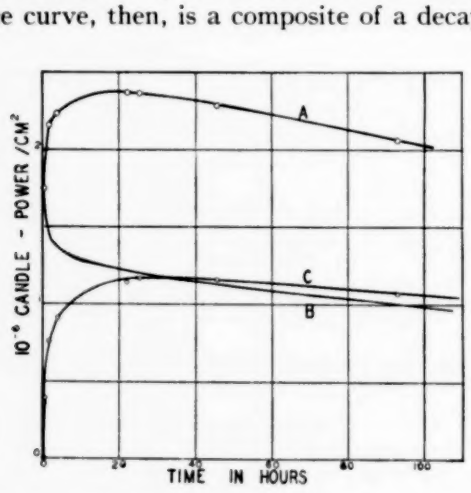

FIG. 9. Plate cut from a crystal of anhydrous calcium sulfate exposed to 4.6 mg/cm² of radium: *A*, luminescence; *B*, fluorescence; *C*, phosphorescence.

fluorescence and a rising phosphorescence curve, both modified by an increase in the absorption coefficient of the material. The luminescence curves shown in Figs. 5–8 are all of the same type with variations which must be attributed to the relative intensities of their fluorescence and phosphorescence factors.

DISCUSSION

Light emission

It has been shown that a simple destruction theory of light emission is inadequate to explain the brightness decay of the materials discussed in this paper even when the change in the absorption coefficient of the material is taken into consideration. Light emission in phosphorescent materials by α, β and γ-rays must therefore be considered as due to excitation. The nature of this excitation is not clear. The curves 5–8 show, however, that the process of light emission does not result in permanent changes such as coloration.

It has been shown in the previous paper[4] that if each active center cannot be excited more than once, the number of such centers necessary to account for the luminous energy obtainable from a given quantity of zinc sulfide is greater than the number of molecules in the material. The conclusion to be reached is that the emission of light does not destroy the luminescent centers. This conclusion is in agreement with the findings of Wolf and Riehl[6] that each luminescent center may be excited 1000 to 2000 times before being destroyed.

The curves 5–8 also show that coloration alone does not account for the decay of brightness as was previously suggested by the present writer. A chemical decomposition, not necessarily connected with the process of light emission might be assumed to account for the destruction of the luminescent centers. It has been shown that the coloration reaches a saturation value. Chemical decomposition produced by the rays may be considered a process of the same type and therefore reach sooner or later an equilibrium value. Since these two factors determine the brightness of a continuously irradiated material, its final bright-

[6] Wolf and Riehl, Ann. d. Physik **11**, 103–112 (1931).

ness would not necessarily be zero but would reach a constant value determined by the extent of its coloration and its degree of decomposition. This is in agreement with the experimental observations on a number of materials where complete extinction of brightness was never observed even when the time was made very large.[7]

Light absorption

Examination of absorption curves in Figs. 1–3 shows that no simple explanation such as destruction of molecules of glass or of a limited number of centers due to impurities dissolved in it, is adequate to explain the phenomenon. The first is eliminated by the fact that the curves are not simple exponentials, and the second by the failure of the samples to attain the same saturation value of absorption with different intensities of radiation.

If the coefficient of absorption is considered as proportional to the number N of absorbing centers, and the formation of these centers is similar to ionization and recombination of ions in air, then N would be given by the equation.

$$dN/dt = kR - \alpha N^2,$$

where R is the intensity of radiation and α is the recombination constant of the ions. The solution of this equation is

$$N = C(e^{2C\alpha t} - 1)/(e^{2C\alpha t} + 1).$$

C, the saturation value of the number of absorbing centers, is a function of the intensity of radiation. A theoretical curve from this equation does not agree very closely with the experimental curve. If a limited number of potential absorption centers be assumed to exist in the material, then

$$dN/dt = kR(m - N) - \alpha N^2,$$

where N can never be larger than m. The solution of this is of the form

$$N = C(e^{\beta t} - 1)/(e^{\beta t} + 1 - C/m)$$

where $\beta = [4\alpha kRm + (kR)^2]^{\frac{1}{2}}$. A theoretical curve obtained from this equation agrees well with the experimental curve of absorption. The constants m and C, however, as determined from the curve give a value for C which is larger than m and therefore inconsistent with the original assumption. It is also very difficult to explain on the ionization theory the permanency of coloration in glass at ordinary room temperatures.

Decay of phosphorescence

Similar difficulties are encountered in explaining by some such simple theory the decay of phosphorescence in luminescent materials after the removal of the exciting source. In Fig. 10 the continuous curve represents the decay of phosphorescence in a calcium sulfate plate which had been previously irradiated with 4.6 mg/cm² of radium until maximum brightness was attained.

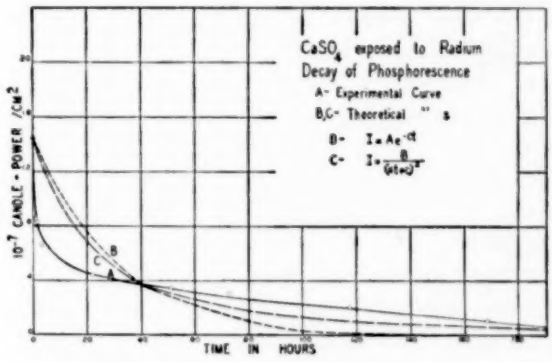

FIG. 10. Decay of phosphorescence for the same sample as in Fig. 9.

If the luminescence is due to excited electrons returning to their normal energy levels, as is usually assumed, the brightness should decay in accordance with the equation[8] $I = Ae^{-ct}$, where I is the brightness, t the time, and A and c are constants for a given sample. If, however, luminescence results from the recombination of ions, the brightness should decay in accordance with the equation[8] $I = B/(\alpha t + c)^2$, where B, α, and c are constants for the given sample. Curves corresponding to these two equations of decay are given in dotted lines in Fig. 10. Neither of these agrees even approximately with the experimental curve.

These experiments seem to indicate that in phosphorescent materials irradiated by α, β and γ-rays, light emission, coloration, and chem-

[7] J. A. Rodman, Phys. Rev. **23**, 4 (1925). Leon E. Smith, Phys. Rev. **28**, 3 (1926). G. S. Gessner, Phys. Rev. **36**, 2 (1930).

[8] H. S. Allen, *Photo-Electricity*, p. 222, 1925.

ical decomposition take place more or less independently of each other and are not easily explainable as simple monomolecular transformations. A number of simple exponentials with different constants might be found to fit each experimental curve. Further investigation, however, seems necessary to determine these and their physical significance.

In conclusion, the author wishes to express his indebtedness to Miss Sara H. Kehler who made the photometric measurements and to Dr. Horace C. Richards for assistance and criticism of the work, also to Corning Glass Company who furnished the glass specimens. This investigation was made possible by a special grant of the Faculty Research Committee of the University of Pennsylvania which is hereby gratefully acknowledged.

The Theory of Forced Double Refraction

K. F. HERZFELD AND R. H. LEE, *Johns Hopkins University, Baltimore*

(Received May 10, 1933)

An attempt is made to better understand the nature of the double refraction in crystals by calculating the forced double refraction induced in rocksalt and KCl crystals through elastic stress (photoelasticity). In a previous paper only the change in the Lorentz-Lorenz force had been taken into account. In this paper is also considered the "potential dip" which is due to the forced anisotropic arrangement of the ionic charges. The formulas are developed according to classical theory and to wave mechanics but they contain too many unknown constants to be checked against experiment.

INTRODUCTION

THE question how the anisotropy of non-cubic crystals results in double refraction is not yet solved. Ewald[1] who investigated the question first assumed that the anisotropy of the Lorentz-Lorenz force was alone responsible. This anisotropy results from the fact that in different directions from a particle the surroundings are different. He could give only rough estimates as insufficient data were known at the time. Bragg[2] and Hylleraas[3] calculated double refraction for carbonates, nitrates, alum, quartz, Hg_2Cl_2, Hg_2Br_2 and succeeded in getting approximately correct values. They took into account not only the anisotropy of the Lorentz-Lorenz force but also that of the charges of the surrounding atoms. They could adapt the values which they ascribed to the polarizability of the constituent ions to fit their results.

If an isotropic, transparent medium is subjected to pressure perpendicular to two parallel surfaces it becomes double refractive. If one chooses as such a medium sodium or potassium chloride one has a cubic crystal made artificially double refracting by changing the structure by a known amount and has to deal only with ions, the refractivity of which is known from the investigation of the undisturbed state. For this reason Herzfeld[4] calculated the double refraction resulting from the anisotropy of the Lorentz-Lorenz force (as had been done before in an unpublished thesis by Heine[5]) and compared it with experimental results of Pockels[6] and Maris.[7] No agreement was, however, reached. In a discussion with Professor Ewald and Dr. Hermann of Stuttgart it was pointed out that the success of Bragg and Hylleraas depended on the fact that these two investigators took into account what Ewald called the potential dip. In the case of an ionic lattice the field from the electrical (excess) charges of the surrounding ions forms a potential dip at the place of the ion which we have just considered, a dip which changes the restoring force on an electron subjected to the influence of an outside electric wave. Hence the anisotropy of arrangement due to the pressure might result in an anisotropy of the potential dip and, therefore, in an anisotropy of the restoring force and of the refractive index itself. These effects are calculated here for a sodium chloride type lattice under the action of pressure. It turned out that in the undisturbed lattice the potential dip is zero to the order considered here.

GENERAL THEORY OF FORCED DOUBLE REFRACTION

Following the notation of Herzfeld we consider a lattice of the rocksalt type compressed in the

[1] P. P. Ewald, *Thesis*, Munich, 1912; Ann. d. Physik **49**, 1 (1916).

[2] W. L. Bragg, Proc. Roy. Soc. **A105**, 370 (1924); **A106**, 346 (1924).

[3] E. Hylleraas, Zeits. f. Physik **36**, 859 (1926); **44**, 871 (1927).

[4] K. F. Herzfeld, J.O.S.A. **17**, 1 (1928).

[5] W. Heine, *Thesis*, Munich, 1922.

[6] F. Pockels, Ann. d. Physik **39**, 440 (1890).

[7] H. B. Maris, J.O.S.A. **15**, 194 (1927).

z direction. The outside electrical field might have either the z or the y direction. We call the electrical moment induced in a positive ion $p_{||+}$ and $p_{\perp+}$ respectively in the two cases. For the negative ions we have similarly $p_{||-}$ and $p_{\perp-}$. If we have N ions of each kind per cubic centimeter the total polarization is

$$P_{||}=Np_{||+}+Np_{||-}. \tag{1}$$

The connection with the refractive index is

$$(n_{||}{}^2-1)/n_{||}{}^2=4\pi P_{||}/D, \tag{2}$$

where D is the electric displacement. Furthermore the moment p of an ion is given by

$$p=(3r/4\pi)(D+E'), \tag{3}$$

where E' is the field at the place of the ion due to all the other ions and is, in the undisturbed lattice, given by

$$E'=-4\pi P+(4/3)\pi P, \tag{4}$$

where the second term on the right side of the equation is the Lorentz-Lorenz force. $3r/4\pi$ is the polarizibility of the ion and is given by

$$r=\sum_i f_i e^2/3\pi m(\nu_i{}^2-\nu^2). \tag{5}$$

When pressure is applied, the lattice is compressed in the z direction so that the lattice distance becomes $a_0(1+\delta_{||})$ in the z direction and $a_0(1+\delta_\perp)$ in the x and y directions. That modifies the factor $(4/3)\pi$ in (4) as well as r in (3).

Assume that in the parallel case the Lorentz-Lorenz force on a positive ion gives

$$E'_{||+}=-\tfrac{2}{3}4\pi N(p_{||+}+p_{||-})+4\pi N(\alpha_{||}p_{||+}+\beta_{||}p_{||-})\delta, \tag{6}$$

where

$$\delta=\delta_{||}-\delta_\perp.$$

The coefficients of $p_{||+}$ and $p_{||-}$ are different because the positive ion considered is not arranged geometrically in the same way in respect to other positive ions as in respect to negative ions; but for $E'_{||-}$, the force on negative ions, p_+ and p_- are exchanged.

Calculation of Lorentz-Lorenz Force

E' is due to the action of all other ions, each polarized in the z direction by a homogeneous field, on the ion considered, which we locate at the origin. The potential of a dipole is $-p(\partial/\partial z)(1/r)$. Accordingly the resultant potential at the origin is

$$V_1=-p_+(\partial/\partial z)\sum_+(1/r)-p_-(\partial/\partial z)\sum_-(1/r), \tag{7}$$

where the summations have to be extended, respectively, over all positive and negative ions, excluding the one at the origin. It follows that

$$E'=-(\partial V_1/\partial z)=+(\partial^2/\partial z^2)[p_+\sum_+(1/r)+p_-\sum_-(1/r)]. \tag{8}$$

From this, Herzfeld has calculated

$$\alpha_{||}=-0.585,\quad \alpha_\perp=-0.081,$$
$$\beta_{||}=1.248,\quad \beta_\perp=-2.255. \tag{9}$$

Calculation of the Potential Dip

The potential due to the excess charges is

$$V_2=e\sum_+(1/r)-e\sum_-(1/r). \tag{10}$$

The electric field E' is $-e\partial V_2/\partial z$ and is zero at the origin, because of the symmetry of the arrangement. The restoring force on an electron k in the z direction is defined by

$$(-e)E_z=-kz=(-e)[E(z=0)+z\partial E/\partial z], \tag{11}$$

where z is the small deviation of the electron from the origin. Therefore

$$\frac{k}{e}=-\frac{\partial^2 V_2}{\partial z^2}=-\left[e\frac{\partial^2}{\partial z^2}\sum_+\frac{1}{r}-e\frac{\partial^2}{\partial z^2}\sum_-\frac{1}{r}\right]. \tag{12}$$

Comparing with (8), one sees that no new coefficients are needed but that

$$k_+/e=-4\pi Ne[\alpha-\beta]\delta. \tag{12'}$$

There, k and $\alpha-\beta$ take simultaneously either the index $\|$ or the index $\perp$. That applies to positive ions. For negative ions the ions of like sign (i.e., contributing the coefficient α) have the opposite charge, k_- has the opposite sign.

For an undistorted rocksalt lattice the charges contribute nothing to the restoring force.

The task of calculating the influence of the additional restoring force on r is different according to the classical and the quantum theory.

Classical Theory

The restoring force on one electron without the potential dip, is

$$k^0 = 4\pi^2 m \nu_j^{02}. \tag{13}$$

The restoring force in the distorted lattice is then

$$k^0 + k = 4\pi^2 m(\nu_j^{02} + \Delta\nu_j^2). \tag{13'}$$

The corresponding addition to each term of (5) is

$$-\frac{f_j e^2}{3\pi m(\nu_j^2 - \nu^2)} \frac{\Delta\nu_j^2}{\nu_j^2 - \nu^2} = \pm \frac{f_j e^2}{3\pi m(\nu_j^2 - \nu^2)} \frac{e^2}{4\pi^2 m} 4\pi \frac{N\delta(\alpha - \beta)}{\nu_j^2 - \nu^2} = \pm \frac{f_j e^2}{3\pi m(\nu_j - \nu^2)} \frac{e^2 N\delta(\alpha - \beta)}{\pi m(\nu_j^2 - \nu^2)}, \tag{14}$$

where the sign is the sign of the charge of the ion.

According to Herzfeld and Wolf, it is possible to represent the mol refraction of rocksalt and sylvin by three terms

$$[(n^2-1)/(n^2+2)] = (e^2N/3\pi m)([f_1/(\nu_1^2 - \nu^2)] + [f_2/(\nu_2^2 - \nu^2)] + [f_3/(\nu_3^2 - \nu^2)]). \tag{5'}$$

Of these, the third was attributed to the positive ion, the first two to the negative. If we change the numbering of the terms and call them (including the common factor outside the bracket) P_1, P_2, P_+ designate the second term in (5') by P_1 (which is by far the largest and is due to the negative ion), the first term P_2 and the last P_+ we can, upon introducing the values α and β from (9), write for $n_{||}' - n_\perp'$, the difference due to the potential dip,

$$\frac{(n_{||}' - n_\perp')2n}{(n^2+2)^2} = -\frac{4.007}{f_1} P_1^2 \left[1 + \frac{P_2}{P_1} \frac{\nu_1^2 - \nu^2}{\nu_2^2 - \nu_2} - \frac{P_+}{P_1} \frac{\nu_1^2 - \nu^2}{\nu_+^2 - \nu^2}\right]\delta, \tag{15}$$

since

$$(n^2-1)/(n^2+2) = P_1 + P_2 + P_+ = P_1[1 + (P_2/P_1) + (P_+/P_1)].$$

Division of Eq. (15) by $(n^2-1)^2/(n^2+2)^2$ and multiplication by $(n^2-1)^2/2n$ gives us finally

$$n_{||}' - n_\perp' = -\frac{(n^2-1)^2}{2n} \frac{4.007}{f_1} \left\{ \frac{\left(1 + \frac{P_2}{P_1} \frac{\nu_1^2 - \nu^2}{\nu_2^2 - \nu^2} - \frac{P_+}{P_1} \frac{\nu_1^2 - \nu^2}{\nu_+^2 - \nu^2}\right)}{\left(1 + \frac{P_2}{P_1} + \frac{P_+}{P_1}\right)^2} \right\} \delta. \tag{16}$$

It should be noted that in deriving Eqs. (6), (15) and (16) no account was taken of the change in N, the number of molecules per cubic centimeter. To do so would have introduced a term in δ^2. For both kinds of crystal $|\delta|$ is of the order of magnitude of 10^{-6}. Hence δ^2 is negligible compared with δ.

Calculations and Tables

Numerical calculation of Eq. (16) has been made for three wave-lengths by using the formulae of Herzfeld and Wolf. The value of δ was obtained from the paper by Herzfeld as were the terms calculated by him from Eq. (6) which we have added to our result to obtain the complete difference $(n_{||} - n_\perp)$. The experimental values for this difference were also taken from the same paper.

Two tables are included, the first for sodium chloride, the second for potassium chloride. Column I gives the wave-length for which the calculations were made; column II gives the numerical values of the terms calculated by Herzfeld; column III gives those calculated here from Eq. (16) multiplied by 10^7; column IV gives the sum of II and III, namely $(n_{||} - n_\perp)10^7$; column V gives the corresponding experimental results; lastly, column VI gives the ratio of V to IV.

TABLE I. *Sodium chloride. Negative pressure of 1 kg per square centimeter.*

I	II	III	IV	V	VI
λ	Last two terms of Eq. (6) $\times 10^7$	Eq. (16) $\times 10^7$	$(n_{\|\|}-n_\perp)10^7$ Calc.	$(n_{\|\|}-n_\perp)10^7$ Obs.	Obs./Calc.
4358	1.382	−12.388	−11.006	2.197	−0.20
5461	1.185	−11.419	−10.234	2.059	−0.20
5790	1.152	−11.245	−10.093	1.922	−0.19

TABLE II. *Potassium chloride. Negative pressure of 1 kg per square centimeter.*

I	II	III	IV	V	VI
λ	Last two terms of Eq. (6) $\times 10^7$	Eq. (16) $\times 10^7$	$(n_{\|\|}-n_\perp)10^7$ Calc.	$(n_{\|\|}-n_\perp)10^7$ Obs.	Obs./Calc.
4358	−12.98	−10.43	−23.40	−2.973	0.13
5461	−12.67	− 9.70	−22.37	−2.900	0.13
5790	−12.56	− 9.57	−22.13	−2.895	0.13

There is no agreement between experiment and theory except the order of magnitude. Experiments made in this physical laboratory recently by Mr. A. Smith and calculations by Joseph E. Mayer[8] seem to indicate that the results which Herzfeld and Wolf got for the position of the main absorption by evaluating the dispersion formula are wrong. As long as no better values are known, it is impossible to say how far this accounts for the failure of the calculations shown in the tables.

QUANTUM THEORY

Consider an ion in the undisturbed crystal. The Schrödinger equation of a dispersion electron is

$$(h^2/8\pi^2 m)\Delta\psi+(V-E)\psi_0=0.$$

We now add the perturbation function due to the potential dip,

$$\begin{aligned} V' &= \mp(4\pi N/2)e^2\delta[(\alpha_{\|}-\beta_{\|})z^2+(\alpha_\perp-\beta_\perp)(x^2+y^2)] \\ &= \mp 2\pi N e^2\delta[(\alpha_{\|}-\beta_{\|}-\alpha_\perp+\beta_\perp)r^2\cos^2\vartheta+(\alpha_\perp-\beta_\perp)r^2] \\ &= \pm 2\pi N e^2\delta[4{,}007 r^2\cos^2\vartheta-2{,}174 r^2]. \end{aligned} \tag{17}$$

In the last line the sign is the sign of the ion. This perturbation function has cylindrical symmetry and accordingly the appropriate undisturbed wave functions are the ones that occur in the Stark effect.

The unexcited state has, of course, spherical symmetry and is, therefore, not degenerate. Call the undisturbed wave function ψ_0, then the ground state is not split up.

We assume that the unperturbed wave function can be written

$$\psi_j=\left(\frac{(2l+1)(l-m)!}{4\pi(l+m)!}\right)^{\frac{1}{2}}P_l^m(\cos\vartheta)e^{+im\varphi}F(j,l) \tag{18}$$

where $F(j, l)$ depends on r only and is so normalized that

$$\int |F(j,l)|^2 r^2 dr=1. \tag{18'}$$

The perturbation matrix is given by

$$V(j,l,m;k,l',m')=\int\bar{\psi}_j V'\psi_k d\tau. \tag{19}$$

From the form of V' (17) it follows that (19) is different from 0 only if $m'=m$; $l'=l$ or $l'=l\pm 2$. Furthermore, the transition probabilities in (5), $f(i, l, m; j, l', m')$ are different from zero only if

[8] Joseph E. Mayer, J. Chem. Phys. **1**, 270 (1933).

$l'=l\pm1$ and either $m'=m$ (for light polarized parallel to z) or $m'=m\pm1$ for light polarized normal to z. Each member of the mol-refraction formula (5) will be changed by

$$\Delta\frac{f(0;j)}{\nu_j^2-\nu^2}=\frac{f(0;j)}{\nu_j^2-\nu^2}\left(-\frac{\nu_j^2+\nu^2}{\nu_j^2-\nu^2}\frac{\Delta\nu_j}{\nu_j}+\frac{\Delta|p(0;j)|^2}{|p(0;j)|^2}\right), \tag{20}$$

where we have put

$$f(0;j)\sim\nu_j|p(0;j)|^2; \tag{21}$$

we have the same selection rule for the electric moment p as we stated before for f.

It is true that there will also appear formerly "forbidden" lines, but their amplitude is of the first order in V', their intensity therefore quadratic.

Now the application of the general theory of perturbations[9] together with the properties of V' and the selection rules leads to the following formula:

$$\Delta|p(0;j,1,m)|^2=2p(0;j,1,m)\sum_k\left\{\frac{V(0;k,0,0)}{W_0-W_k}p(k,0,0;j,1,m)-\frac{V(k,1,m;j,1,m)}{W_k-W_j}p(0;k,1,m)\right.$$
$$\left.+\frac{V(0;k,2,0)}{W_0-W_{k,2}}p(k,2,0;j,1,m)\right\}. \tag{22}$$

Here we have made use of the fact that the p's can be chosen real.[10] From (22) we get therefore:[11]

$$h\Delta\sum_j\frac{f(0;j)}{\nu_j^2-\nu^2}=-\sum\frac{\nu_j^2+\nu^2}{(\nu_j^2-\nu^2)^2}[V(j,1,m;j,1,m)-V(0;0)]p^2(0;j,1,m)$$
$$+2\sum_j{\sum_k}'\frac{W_j-W_0}{\nu_j^2-\nu^2}\left\{\frac{V(0;k,0,0)}{W_0-W_k}p(0;j,1,m)p(k,0,0;j,1,m)\right.$$
$$\left.-\frac{V(k,1,m;j,1,m)}{W_k-W_j}p(0;j,1,m)p(0;k,1,m)+\frac{V(0;k,2,0)}{W_0-W_{k,2}}p(0;j,1,m)p(k,2,0;j,1,m)\right\}$$
$$=-\sum_j\sum_k\frac{\nu_j\nu_k+\nu^2}{(\nu_j^2-\nu^2)(\nu_k^2-\nu^2)}V(k,1,m;j,1,m)p(0;j,1,m)p(0;k,1,m)$$
$$+V(0;0)\sum_j\frac{\nu_j^2+\nu^2}{(\nu_j^2-\nu^2)^2}p^2(0;j,1,m)$$
$$-2\sum_j{\sum_k}'\frac{\nu_j}{\nu_k}\frac{1}{\nu_j^2-\nu^2}V(0;k,0,0)p(0;j,1,m)p(k,0,0;j,1,m)$$
$$-2\sum_j\sum_k\frac{\nu_j}{\nu_k}\frac{1}{\nu_j^2-\nu^2}V(0;k,2,0)p(0;j,1,m)p(k,2,0;j,1,m). \tag{23}$$

Define now

$$\bar{r^2}(j,l,m;k,l',m)=\int F(j,l,m)r^2F(k,l',m)r^2dr,\qquad A=\mp2\pi Ne^2\delta.$$

[9] See, for example, M. Born and P. Jordan, *Elementare Quanten Mechanik*, p. 198, Eq. (22), Berlin, 1930.

[10] J. H. Van Vleck, *Electric and Magnetic Susceptibilities*, p. 273, Oxford, 1932.

[11] The prime on the double sum means $j\neq k$.

We have then

$$V(k,1,0;j,1,0)=A\ \ 0{,}231\quad \bar{r}^2(k,1;j,1),$$
$$V(k,1,\pm1;j,1,\pm1)=-A\ \ 1{,}373\quad \bar{r}^2(k,1;j,1), \tag{24}$$
$$V(0;k,2,0)=A(2/15)5^{\frac{1}{2}}\cdot 4{,}007\quad \bar{r}^2(0;k,2).$$

We have for light polarized in the z direction, $m=0$; for light polarized in the x-direction, $m=\pm1$ and, as each of these corresponds to circularly polarized light

$$p_x^2=\tfrac{1}{2}\{p^2(0;j,1,+1)+p^2(0;j,1,-1)\}=p^2(0;j,1,+1)=p^2(0;j,1,0)=p_z^2, \tag{25}$$

the latter because of the "law of spectroscopic stability."

Therefore, if we form for (23) the difference between light polarized parallel and at right angles to z (designating this difference with Δ'), the second and third terms drop out.

Furthermore, we have[12]

$$p^2(k,2,0;j,1,0)=2/5\ p_z^2(k,2;j,1),$$
$$p_x^2(k,2,0;j,1)=\tfrac{1}{2}\{p^2(k,2,0;j,1,+1)+p^2(k,2,0;j,1,-1)\}=1/10\ p_z^2(k,2;j,1). \tag{26}$$

$p(k,2,0;j,1,+1)$ and $p(0;j,1,+1)$ have opposite signs because the increase of m by 1 is in the former case accompanied by a decrease, in the latter by an increase in l. The corresponding is true for $m=-1$. On the other hand $p(k,2,0;j,1,0)$ has the same sign as $p(0;j,1,0)$, because no change in m occurs.

The final formula for the difference in refractive index due to the potential dip, apart from the Lorentz-Lorenz force, is:

$$\Delta' n=\frac{(n^2-1)(n^2+2)}{6n}\frac{4\pi Ne^2\delta}{5h}\,4{,}007\left\{\sum_j \frac{f(0;j,1)}{\nu_j^2-\nu^2}\right\}^{-1}\sum_j\sum_k a_{jk}\left\{\left(\frac{f(0;j,1)}{\nu_j}\frac{f(0;k,1)}{\nu_k}\right)^{\frac{1}{2}}\right.$$
$$\left.\frac{\nu^2+\nu_j\nu_k}{(\nu_j^2-\nu^2)(\nu_k^2-\nu^2)}\bar{r}^2(j,1;k,1)+\left(\frac{2\nu_j f(0;j,1)f(j,1;k,2)}{\nu^2(0;k,2)\nu(j,1;k,2)}\right)^{\frac{1}{2}}\frac{1}{\nu_j^2-\nu^2}\bar{r}^2(0;k,2)\right\}. \tag{27}$$

Here a_{jk} is $+1$ if the absorption lines j and k both belong to the negative ion
is -1 if the absorption lines j and k both belong to the positive ion
is zero if the absorption lines j and k belong to different ions.

While the first sum includes $j=k$, this is excluded in the second sum. Comparing with the classical expression (16), one sees

$$\frac{\Delta' qu}{\Delta' kl}\sim\frac{n^2+2}{3(n^2-1)}\,f_1\frac{1}{\nu_1}\frac{4\pi Ne^2}{5h}\bar{r}^2(1;1)=0{,}84\,\frac{n^2+2}{n^2-1}\frac{Ne^2\bar{r}^2(1;1)}{h\nu_1}f_1.$$

As $N=1/2r_0^3$, where r_0 is the distance between two adjacent ions

$$\frac{\Delta' qu}{\Delta' kl}\sim 0{,}42\,\frac{n^2+1}{n^2-1}\frac{e^2}{r_0}\frac{\bar{r}^2(1;1)}{r_0^2}\frac{1}{h\nu_1}f_1.$$

Now $h\nu_1$ is somewhat larger than the lattice energy $1.74\ e^2/r_0$, therefore this expression is probably <1, although of this order of magnitude.

One sees from Tables I and II, that (27) should be about $-1/10$ of column III for rocksalt, -1 of column III for KCl to give the experimental values. Whether that is possible cannot be determined

[12] Born and Jordan, reference 9, p. 160.

until more is known about the absorption spectrum and the atomic states in crystals, so that the different expressions can be calculated. The difference between the classical and quantum results is primarily due to the use of a more general dynamical model in the latter. When the matrix amplitudes involved in (27) are specialized to the harmonic oscillator, the quantum formula is the same as the classical one.

We wish to thank Professor Dieke and Dr. M. Goeppert-Mayer for helpful discussion and advice, and particularly Mr. Serber and Professor J. H. Van Vleck of the University of Wisconsin for important corrections.

Magnetic Rotation Spectrum of the Red Bands of Sodium

W. R. FREDRICKSON AND CARL R. STANNARD, *Syracuse University*

(Received June 30, 1933)

The magnetic rotation spectrum of the red bands of sodium shows a large number of doublets. A doublet is interpreted as made up of an R-branch and a P-branch line having a common upper K' rotational level. The K' values for the doublets are calculated and it is found that the rotational levels in the various initial vibrational states from 0–12 which give rise to magnetic rotation doublets are 53, 45, 33, 14, 60, 52, 43, 31, 16, 58, 51, 40, 28 respectively. That just these levels give rise to magnetic rotation lines suggests that these levels are perturbed. Since a $^3\Pi$ state is predicted to lie below the upper $^1\Sigma$ state we have perhaps here evidence of a perturbation between a $^1\Sigma$ and a $^3\Pi$ state. To account for the magnetic rotation doublets it has been necessary to revise the vibrational numbering, increasing the initial state numbering by three.

SOME twenty-five years ago R. W. Wood[1] and his collaborators reported the magnetic rotation spectrum of the blue-green and red bands of sodium. The experimental procedure was to pass light through two nicols between which was placed a tube of absorbing vapor, the latter being arranged between the poles of an electromagnet in such a way that light passed through the tube in a direction parallel to the magnetic field. When the nicols were set for extinction, the magnetic rotation spectrum was produced upon the excitation of the magnetic field.

F. W. Loomis[2] has shown that in the blue-green system most of the magnetic rotation lines correspond to the first lines in the R-branch and from this fact he has been able to make a very accurate vibrational analysis of this system. The blue-green bands are due to a $^1\Pi-{}^1\Sigma$ electronic transition and Loomis and Nusbaum[3] have shown that the same electronic transition in other molecules shows the same magnetic rotation effect. Serber,[4] in a theoretical discussion of the problem, concludes that the magnetic rotation effect is associated with the Zeeman effect in such a way that lines showing large Zeeman splitting should also show large magnetic rotation. The magnetic rotation lines in the $^1\Pi-{}^1\Sigma$ bands agree with this conclusion.

The red sodium bands, however, are due to a $^1\Sigma-{}^1\Sigma$ transition and should therefore show no Zeeman or magnetic rotation effects. Yet one finds that the red bands show more magnetic rotation lines than the blue-green and that the rotation in the red system must be greater since the lines can be obtained with weaker magnetic fields. The red rotation lines also differ from the blue-green in that they show no relation to the band origins.

Experimental Results and Interpretation

The magnetic rotation spectrum was obtained by the same method as used by Wood with the exception that a long solenoid was substituted for the electromagnet. The entire spectral region from the D lines to λ8000A was photographed with a one meter grating in a Rowland mounting and the region from the D lines to λ7400A was photographed in the first order of a twenty-one foot grating in a similar mounting. Some two hundred lines were measured on the low dispersion plates while over eight hundred were measured on the high dispersion plates. The great increase in the number of lines on the latter is mainly due to fact that what appears as a single broad line at low dispersion shows up as a group of lines at high dispersion.

Fig. 1A shows the spectrum at high dispersion. The spectrum falls into two distinct sections.

[1] R. W. Wood, Phil. Mag. **10**, 408 (1905); **12**, 499 (1906); Wood and Hackett, Astrophys. J. **30**, 339 (1909).

[2] F. W. Loomis, Phys. Rev. **31**, 323 (1928).

[3] Loomis and Nusbaum, Phys. Rev. **38**, 1447 (1931); **39**, 89 (1932).

[4] Serber, Phys. Rev. **41**, 489 (1932).

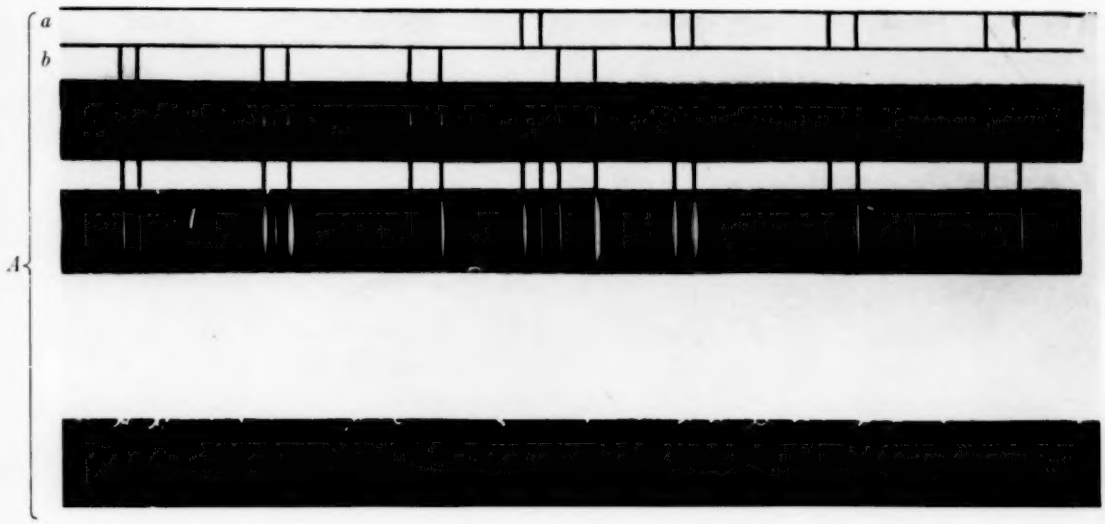

FIG. 1A. High dispersion magnetic rotation spectrum of sodium.

The first, typified by the middle strip, extends from the D lines to about 6800A and shows a large number of doublets. The second, designated by the bottom strip, shows groups of lines forming doublets. The top strip covers exactly the same region as the middle but the temperature of the absorbing vapor in this case is considerably less than for the middle strip. This top strip shows only two series of doublets, a and b, which increase in doublet separation as the series progresses to the red. Most of the high-wave number components of doublet show negative rotation (see Table I) while the other component shows positive rotation which, according to Serber,[4] should correspond to an R and P branch line, respectively.

The immediate interpretation of a doublet was that it consisted of an R and P line having a common upper K' level. Two interpretations of a series seemed possible. The first being that a series arises from transitions (in absorption) to a common upper vibrational state from lower vibrational states (i.e., doublets similar to those observed in fluorescence series). If such were the case the doublet spacing should decrease slowly as the series progressed to the red while it was observed that the spacing rapidly increased. The second interpretation was that since these doublets, shown on the top strip, appeared when the vapor was relatively cold they must all be due to transitions from low final vibrational states to various upper levels.

This latter interpretation could be tested in the following way: The doublet separation is $R(K''-1)-P(K''+1)$ and therefore can be equated to the expression for the final state combination. Thus,

$$\text{doublet separation} = \Delta_2 F'' = (4K''+2)B'' + (8K''^3+12K''^2+12K''+4)D''.$$

Using the B's and D's obtained from the rotational analysis of the blue-green[5] and red[6] bands, we could calculate the value of K'' which is numerically the value of K' of the upper level

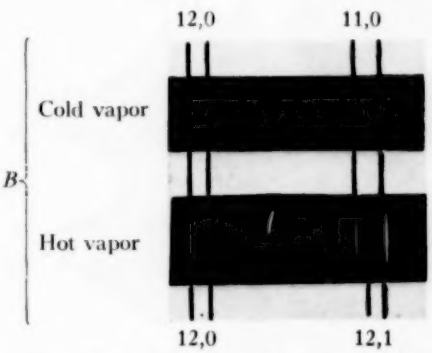

FIG. 1B. Part of Fig. 1A showing that the 12,1 band appears only on the hot vapor plate.

[5] Loomis and Wood, Phys. Rev. **32**, 223 (1928).
[6] Fredrickson, Phys. Rev. **34**, 207 (1929).

which is common to both members of a doublet. Then taking the P-branch component of a doublet together with the value of the B's and D's and increasing the K value by one since for the P-branch $K''=(K'+1)$, the origin of the band to which the doublet belonged could be calculated from the expression[7]

$$\nu_P=\nu_0-(B'+B'')K''+(B'-B''+D'-D'')K''^2 -2(D'+D'')K''^3+(D'-D'')K''^4.$$

Since it is known that the R-branch turns at very low K values, the head of the band should be very close to the origin and thus the calculated origins should agree with the heads of the bands as measured in absorption.

In Table I are listed the nine doublets observed in the top strip of Fig. 1. The first column gives the wave numbers of the lines, the second the rotation observed by Wood, the third the doublet separation, the fourth the calculated upper K' level, the fifth the calculated origin of the band, and the sixth the observed absorption band. The agreement between the fifth and sixth columns is good,—only one doublet (No. 7) showing any disagreement. As seen from the last two columns, what appeared on the photographic plate as two separate series is really only one progression arising from a common vibrational state $v''=0$.

TABLE I. *Magnetic rotation doublets appearing on top strip of Fig. 1.* The sign of the rotation is taken from Wood and Hackett's paper, Astrophys. J. **30**, 339 (1909).

	Doublets	Rot.	Separation	K'	ν_0 (calc.)	ν_H (absorption)	Vibrational assignments old	new
1	14973.5		36.2	60	15121.3	15121.5	1,0	4,0
	14937.3	+						
2	15125.1	−	31.9	52	15236.7	15236.8	2,0	5,0
	15093.2	+						
3	15273.3	−	26.5	43	15348.8	15349.3	3,0	6,0
	15246.8	+						
4	15423.9	−	19.5	31	15461.1	15461.7	4,0	7,0
	15404.4	+						
5	15566.1	−	10.3	16	15574.1	15574.4	5,0	8,0
	15555.8	+						
6	15537.2	−	35.0	58	15684.9	15684.0	6,0	9,0
	15502.2	+						
7	15685.4	−	31.3	51	15798.6	15794.8	7,0	10,0
	15654.1	+						
8	15823.8	−	24.7	40	15902.8	15904.0	8,0	11,0
	15809.1	+						
9	15981.1	−	17.5	28	16013.0	16012.3	9,0	12,0
	15963.6	−						

[7] Mulliken, Rev. Mod. Phys. **2**, 69 (1930).

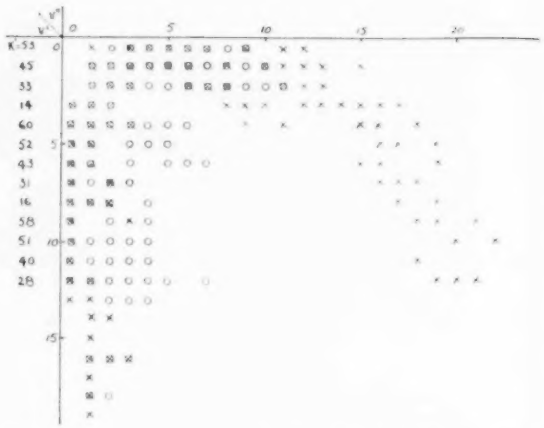

FIG. 2. Square array of vibrational analysis. Circles represent the magnetic rotation data, crosses the absorption data.

If this interpretation is correct, bands with final vibrational states other than zero should likewise show similar doublets. For example, if the rotational level $K=28$ in the upper vibrational state $v'=12$ gives rise to a doublet in the 12,0 band, it should also give rise to almost identical doublets in the (12,1) (12,2), etc., bands. There is evidence that these doublets do appear as indicated in Fig 1B. Here the 12,1 band appears quite clearly on the hot vapor plate while it can scarcely be detected on the cold vapor plate. The bands with v'' other than zero which have been identified are shown schematically in Fig. 2. Not many doublets are assigned to these bands but this failure of the bands to make their appearance is really what might be expected since the vibrational distribution follows a wide Condon parabola and, as seen from Fig. 2, one likewise finds only a few absorption bands.

In extending the interpretation to the region to the red of λ6800A one has difficulty because the lines appear in groups. By plotting the groups to a large scale it was observed that the lines in the various groups were somewhat similarly spaced. Taking a line representing a so-called center of gravity of a group, one obtains doublets whose doublet separation is practically constant and whose spacing between the successive doublets indicates that they belong to low v'' values. Following the procedure for the doublets mentioned above, the origins were cal-

TABLE II. *Magnetic rotation doublets and absorption band heads in the region beyond 6800A.*

v'	v''	Doublets	Separation	K'	ν_0 (calc.)	ν_H (absorption)	ν_H (calc.)	v'	v''	Doublets	Separation	K'	ν_0 (calc.)	ν_H (absorption)	ν_H (calc.)
0	1					14499.1	14501.2								
0	2	14241.5 14210.3	31.2	53	14342.8	———	14344.9	1	7	13638.6 13610.3	28.3	45	13701.5		13703.2
0	3	14088.6 14057.1	31.5	53	14187.0	14190.6	14190.1	1	8	13489.2 13461.3	27.9	45	13550.4	13556.2	13556.0
0	4	13938.8 13906.7	32.1	53	14034.2	14038.0	14036.8	2	1	14696.1 14675.7	20.4	33	14735.0	14734.7	14734.2
0	5	13789.7 13757.9	31.8	53	13882.9	13886.8	13885.1	2	2	14539.8 14519.6	20.2	33	14577.6	14575.9	14577.9
0	6	13642.2 13610.6	31.6	53	13732.6	13731.8	13734.8	2	3	14387.0 14366.3	20.7	33	14423.3	14421.2	14423.1
0	7	13496.2 13464.8	31.7	53	13584.3	13581.6	13586.2	2	4	14235.0 14214.8	20.2	33	14270.8	———	14269.8
0	8	13351.6 13320.0	31.6	53	13433.0	———	13439.0	2	5	14085.3 14065.3	20.0	33	14120.6	———	14118.1
0	9	13182.9 13211.0	31.9	53	13296.0	13292.4	13293.6	2	6	13933.6 13913.8	19.8	33	13968.0	13967.4	13967.8
1	1	14545.6 14517.6	28.0	45	14619.6	14618.0	14618.2	2	7	13786.2 13766.4	19.8	33	13819.6	13818.2	13819.2
1	2	14387.0 14359.1	27.9	45	14459.3	14461.6	14461.9	2	8	13636.6 13617.1	19.5	33	13669.2	13665.0	13672.2
1	3	14235.0 14207.0	28.0	45	14306.0	14308.7	14307.1	2	9	13492.5 13472.2	20.3	33	13523.3	———	13526.6
1	4	14085.2 14057.1	28.1	45	14153.5	14154.5	14153.8	3	0	15003.3 14994.4	8.9	14	15008.6	15006.7	15008.0
1	5	13933.6 13905.7	27.9	45	14000.4	14003.0	14002.1	3	1	14845.4 14836.2	9.2	14	14850.1	14850.4	14850.2
1	6	13781.6 13754.3	27.3	45	13847.0	13848.3	13851.8	3	2	14688.6 14679.1	9.4	14	14692.8	14691.9	14693.9

TABLE III. *Additional band heads from absorption plates.*

v'	v''	ν (obs.)	ν (calc.)	v'	v''	ν (obs.)	ν (calc.)	v'	v''	ν (obs.)	ν (calc.)
0	11	13008.3	13007.4	3	16	12670.3	12669.9	6	19	12619.4	12619.8
0	12	12864.7	12866.8	3	17	12534.3	12537.7	7	16	13123.2	13123.5
1	13	12846.2	12844.8	4	9	13760.0	13757.1	7	17	12993.1	12991.3
1	14	12706.4	12707.5	4	11	13473.2	13470.9	7	18	12861.6	12860.8
2	11	13239.1	13240.4	4	15	12918.5	12918.3	8	17	13101.5	13102.8
2	12	13098.6	13099.8	4	16	12783.5	12784.4	8	19	12842.3	12843.6
2	13	12960.2	12960.8	4	18	12522.3	12521.8	9	18	13087.5	13083.1
3	8	13787.6	13788.2	5	11	13585.1	13584.7	9	19	12960.2	12954.4
3	9	13641.5	13641.6	5	12	13442.6	13444.1	9	21	12706.4	12702.3
3	10	13499.4	13498.8	5	16	12899.3	12898.2	10	20	12942.3	12937.5
3	12	13214.2	13285.8	5	17	12764.8	12766.0	10	22	12693.7	12689.0
3	13	13076.2	13076.8	5	19	12507.2	12506.7	12	20	13156.1	13155.2
3	14	12942.3	12939.5	6	15	13145.4	13145.2	13	21	13140.8	13137.8
3	15	12802.9	12803.8	6	16	13008.3	13011.3	13	22	13017.2	13014.5

culated. These origins, however, corresponded to nothing in the known absorption vibrational analysis but agreed quite well with what the absorption heads would be if we increased the numbering of the initial state vibrational levels by three. These doublets are listed in a manner similar to the preceding table in Table II,—the vibrational assignments in the first two columns being the new assignments required to account for the magnetic rotation doublets.

Vibrational Analysis

The suggested change in the vibrational assignments demanded a reinspection of the absorption bands. A change in the vibrational numbering was not altogether unexpected for it had been shown by Loomis[8] that the formula for the final state vibrational levels, which he was able to determine very accurately from the magnetic rotation data, of the blue-green bands, failed to represent the red bands in their reported position.[9]

The region beyond λ6800A was therefore rephotographed. The new measurements are listed in the next to the last column in Table II and in Table III. The band heads agree quite well with Loomis' formula for the final state and the entire system can be represented by the formula

$$\nu = 14{,}680.4 + 117.6(v'+\tfrac{1}{2}) - 0.38(v'+\tfrac{1}{2})^2 - 159.23(v''+\tfrac{1}{2}) + 0.726(v''+\tfrac{1}{2})^2 + 0.0027(v''+\tfrac{1}{2})^3;$$

the last three terms are the recent values given by Loomis and Nusbaum[10] for the final state of the green bands. The last column in Table II represents the wave numbers of the bands as calculated from the above formula. The last three columns should agree in value and it is observed that the agreement is fairly good.

Conclusion

In Fig. 2 we have the usual square array for representing vibrational data. The circles represent the bands in which the origins could be calculated from the magnetic rotation doublets and the crosses represent the measured absorption heads. The magnetic rotation doublets have not been recorded beyond λ7400A because beyond that region we have only low dispersion plates and the magnetic rotation lines on these plates are very broad,—each line undoubtedly made up of many lines belonging to a number of bands.

At the left in Fig. 2 are listed the K' values of the various rotational levels of the various upper vibrational states which give rise to magnetic rotation doublets. It is interesting to see how the numbering seems to repeat itself at every fifth vibrational state.

That just these levels should be the ones which give rise to magnetic rotation doublets is strong evidence that these levels are perturbed. We have previously mentioned that the red bands, being a $^1\Sigma - {}^1\Sigma$ system, should show no magnetic rotation because there exists in neither state a magnetic moment along the internuclear axis. It has been considered possible, however, that the molecule may develop a magnetic moment at high rotational quantum numbers[11] because of the uncoupling of the orbital angular momentum, but if such were the case we would expect all high levels to cause rotation. The presence of only an isolated doublet in a band practically limits the interpretation to that of perturbation between the upper $^1\Sigma$ state and some state which has a magnetic moment.

We may speculate as to what that perturbing state might be. A $^3\Pi$ state is predicted to lie below the upper $^1\Sigma$ state[12] and recently Van Vleck[13] has shown that perturbations between such states are possible. If the $^3\Pi_1$ or $^3\Pi_2$ are the perturbing levels we could account for the magnetic rotation by the presence of the magnetic moment in these states. If the perturbing level is $^3\Pi_0$ we would expect no magnetic rotation unless the state had developed a magnetic moment at high rotation due to the uncoupling

[8] Loomis, Phys. Rev. **31**, 328 (1928).
[9] Fredrickson and Watson, Phys. Rev. **30**, 431 (1927).
[10] Loomis and Nusbaum, Phys. Rev. **40**, 383 (1932).
[11] Jevons, *Report on Band Spectra of Diatomic Molecules*, p. 260.
[12] Mulliken, Rev. Mod. Phys. **4**, 16 (1932).
[13] Van Vleck, presented at the Washington Meeting of the Am. Phys. Soc., April, 1933. Phys. Rev. **43**, 1047A (1933).

of the angular and spin momenta as in case b or in Paschen-Back effect. It is found that the observed doublets do have large K' values which is in agreement with the preceding requirement.

The fact that the K' value seems to repeat itself at every fifth state suggests that the perturbing state closely parallels the $^1\Sigma$ state and has very nearly the same r_e and ω_e values.

The authors wish to thank Dr. W. W. Watson for his helpful discussions and also the Rumford Fund Committee for a grant which made possible the construction of the solenoid.

The Spectrum of Sulphur Dioxide

TUNG-CHING CHOW,* *Palmer Physical Laboratory, Princeton University*

(Received August 2, 1933)

A study has been made of the emission and absorption spectrum of sulphur dioxide with special emphasis on the region from 2000 to 2600A. It was found possible to run a discharge in flowing SO_2 with comparatively little dissociation. The work on absorption was supplementary to that on emission and carried out at the same moderate dispersion. A large proportion of both the emission and absorption bands found fit into a scheme of vibrational levels. The upper levels indicate a frequency of about 375 cm^{-1} or an integral multiple of that value. The lower levels confirm the 1150 and 520 frequencies previously observed but leave the third frequency in doubt. The $x_r\omega_e$ for both the 1150 and 520 frequencies are small, of the order of one cm^{-1} for the latter as determined from a progression of sixteen bands.

TWO years ago a systematic study of emission spectra of polyatomic gases was begun in this laboratory by Smyth's[1] work on carbon dioxide. The present author undertook a similar study of sulphur dioxide but found it desirable to extend his original plan to include the investigation of the absorption spectrum as well as the emission spectrum.

There was already a good deal of information available about the spectrum of sulphur dioxide. The absorption spectrum had been first studied in the region between λ3882 and λ2200 by Miss Lowater.[2] Henri[3] later reported three systems of absorption bands; one weak system from 3900A to 3400, one moderately strong system from 3370 to 2450 and one very strong system from 2350 to 2000 and beyond. There was no evidence that these systems corresponded to three electronic transitions except the fact that the three portions were greatly different in absorbing power. Watson and Parker[4] measured the bands in the region from λ3880 to 2630. They picked out bands (about 20 percent of the total) from this region and arranged them into progressions, using the fundamental frequencies 1369 (ν_3), 1164 (ν_1) and 610 (ν_2) cm^{-1} for the lower state and 341, 387 and 290 for the excited state. In view of the new interpretation of the infrared spectrum the 610 cm^{-1} frequency is probably incorrect. Nor do the frequencies of the upper state seem probable.

The study of the emission spectrum was also started by Lowater.[2] Later studies made by Johnson and Cameron,[5] by Henri and Wolff,[6] by Martin[7] and by Bair[8] show two different spectra. The one most easily obtained and most extensively studied is definitely attributable to SO. Another set of bands, degraded toward the violet were found by Johnson and Cameron, and by Bair. These are apparently from SO_2 and in fact can be very simply correlated with some of Watson and Parker's absorption bands as was pointed out by Chow and Smyth.[9] Other bands were found by Bair scattered over the region between 2200 and 3200A and for the most part degraded toward the red.

In the present work measurements of the SO_2 bands, particularly those of shorter wave-length, have been repeated and extended both in emission and absorption. An attempt has then been made to arrange the observed wave-numbers in a rational scheme of vibrational levels.

* Now at Peking University, Peiping, China.

[1] H. D. Smyth, Phys. Rev. **38**, 2000 (1931) and the literature given there.

[2] F. Lowater, Astrophys. J. **23**, 324, 338 (1906); **31**, 311 (1910).

[3] V. Henri, Nature **125**, 275 (1930).

[4] W. W. Watson and Allan E. Parker, Phys. Rev. **37**, 1484 (1931).

[5] R. C. Johnson and W. H. B. Cameron, Proc. Roy. Soc. **A106**, 195 (1924).

[6] V. Henri and F. Wolff, J. de Physique et le Radium **10**, 81 (1921).

[7] Emmett V. Martin, Phys. Rev. **41**, 167 (1932).

[8] Bair, Astrophys. J. **52**, 301 (1920).

[9] T. C. Chow and H. D. Smyth, Phys. Rev. **38**, 838 (L) (1931).

Experimental

The first thing attempted was the reproduction of the emission bands observed by Johnson and Cameron between 3105 and 2866A. This was unsuccessful but a great number of bands was observed below 2300 and attention was directed to them.

For studying polyatomic spectra the first essential is a constant flow of gas. In the present experiment, sulphur dioxide was let into the discharge tube from the reservoir through an artificial leak and was drawn out by condensing it in a liquid-air cooled trap on the other side of the discharge tube. A three-stage Gaede diffusion pump was also operating to take care of the oxygen resulting from dissociation in the discharge tube. The amount of dissociation and loss of SO_2 resulting from passage through the discharge was found to be less than 4 percent. The sulphur dioxide was from an ordinary tank of SO_2 but was distilled under vacuum several times before use and was stored over P_2O_5.

After trying a number of types of discharge it was concluded that a weak glow discharge in a tube, such as is shown in Fig. 1, was most suitable. This was run at a pressure of about 0.5 mm with a voltage of 920–1100 and a current of 3 to 5 m.a. When such a discharge was running properly there was no sulphur deposit detectable on any part of the walls of the tube after a run of twenty hours. It was the positive column that was photographed. This filled the whole narrow glass tube with a bluish violet color. The quartz window was put as near as possible to the source to avoid reabsorption.

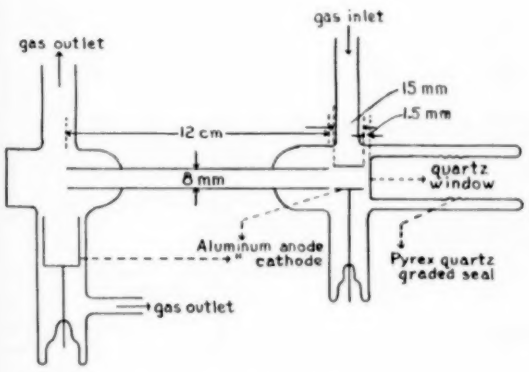

Fig. 1. Discharge tube.

The source proved too weak to give satisfactory plates with a Hilger E 1 spectrograph and consequently all our measurements are from plates taken with the medium size quartz Hilger, E 315. The spectra on these plates can be generally described as consisting of the SO bands (4000–2500A) studied by Henri and Wolff[6] and by Martin,[7] and a set of bands of entirely different character in the region 2600–2040A (38,000–49,000 cm^{-1}). Fortunately the main parts of the two sets do not overlap. The measurements of band heads and of some of the maxima of the bands (where the heads were not sharp) are assembled in the table below. The discussion of these bands will be given later.

The Absorption Spectrum

In this short wave-length region the only absorption measurements available were by Garret[10] and were not sufficiently accurate to compare with our emission data. Therefore a study of the absorption spectrum was made. The continuous spectrum of a hydrogen discharge was sent through an absorption cell 23.5 cm long filled with SO_2 at a pressure of from 0.08 to 10 mm. This was at room temperature. Some plates were also taken at 240°C with a 7.8 cm quartz tube in an electric furnace as an absorption cell. The band heads observed are listed in Table I. A more thorough study of the absorption spectrum by using a bigger instrument was not carried out mainly because it was known that two other investigators were working on this problem. However, the plates obtained were very useful for comparison with those showing emission. In each case various checks led to the conclusion that the accuracy of the measurements is about 5 cm^{-1} or better.

Before attempting an analysis of the emission bands it is necessary to establish their origin. They might conceivably arise from SO_2, SO, SO^+, O_2, O_2^+, S_2 or S_2^+. Each of these possibilities has been considered in detail and all but the first discarded as unlikely. The strongest evidence for the assignment of the bands to SO_2 is the absence of fine structure (at the dispersion used) and the many coincidences between the emission and absorption wave numbers. It is believed safe to

[10] Scott Garret, Phil. Mag. **31**, 505 (1906).

TABLE I. *Emission and absorption bands in sulphur dioxide.*

Absorption	Transition	Emission	Transition
50302	A_6		
50248	C_5		
49910	B_5		
49550	A_5		
49477	C_4		
49133	B_4		
48781	A_4	48789	A_4
48724	C_3		
48375	B_3	48387	B_3?
		48269	b_1A_4
48355	b_3B_5		
48121			
48083			
48005	A_3	48009	A_3
48000	b_3A_5		
47965	C_2		
47922	b_3C_4		
47889	α_1A_5		
		47776	
47742		47747	b_2A_4
47707	α_2B_5		
47636	a_1A_4	47631	B_2?, a_1A_4
47623	B_2		
47576	a_1C_3, b_3B_4	47586	b_3B_4
47548			
		47489	b_1A_3, b_4A_5
47391			
		47345	α_2A_5
47246	A_2, a_2A_5		
47232	a_1B_3	47230	A_2?, a_1B_3, b_5A_4
47223	C_1, a_1B_3, b_2A_4		
47198			
		47110	b_1B_2, α_1A_4
47074			
47052	α_1C_3		
		47031	
		46968	b_2A_3, b_5A_5
46874	B_1	46871	B_1
46865	a_1A_2	46851	a_1A_3, a_3A_6
46829	a_2B_4		
46818	a_1C_2, b_3B_3		
46704	α_1B_3	46710	b_4A_4, α_1B_3
46697			
		46632	δ_1B_4
		46588	b_2B_2, α_2A_4
46570			
46482	C_0, a_2A_4		
46472	a_1B_2	46474	a_1B_2, a_2A_4, b_6A_5
46464			
46444	b_3A_3		
		46425	
46348		46350	b_1B_1
		46330	b_7B_5
		46277	δ_1A_4
		46259	
46217			
		46190	b_2A_2?
46118	B_0		
46104	a_1A_2	46105	a_1A_2, a_3A_5
46084		46094	
46077	a_1C_1, a_2B_3, b_3B_2	46074	a_2B_3, b_3B_2
		46060	
		45968	b_7A_5
45923			
		45888	
45859			
		45833	b_2B_1
		45817	b_8B_5
45757	A_0, α_2C_2	45757	A_0
45725	a_1B_1	45717	a_1B_1, a_4A_6
45706	a_2A_3		
45686	b_3A_2		
45672	a_2C_2, b_3C_1	45665	
		45588	b_1B_0, α_1A_2
45572		45560	b_4B_2
		45500	δ_1A_3
		45455	b_2A_1, b_5A_5
		45414	α_2B_2
45393			
		45367	
45351	a_1A_1	45350	a_1A_1
45333	a_1C_0, a_2B_2		
		45314	b_3B_1, b_9B_5
		45199	α_1B_1
		45188	
		45119	δ_1B_2
		45069	b_2B_0
		45051	b_5B_2
45030	α_2A_2		
44987			
44978	a_1B_0	44977	a_1B_0
		44953	a_2A_2, b_9A_5
		44833	α_1A_1
		44798	b_4B_1
44674		44672	α_2B_1
44663	α_2B_1		
44603	a_1A_0		
44570	a_2B_1, b_3B_0	44573	a_2B_1, b_3B_0
		44543	b_6B_2, a_4B_4
		44457	$b_{10}A_5$
		44437	b_4A_1
		44362	δ_1B_1
		44340	
44305		44310	$b_{11}B_5$
44293	α_2A_1	44285	α_2A_1
44236			
		44199	a_2A_1, b_3A_0
		44121	
44100			
44085			
		44057	b_4B_0
		44039	b_7B_2
43929		43925	b_5A_1
43918	α_2B_0		
		43824	
		43807	a_2B_0?, a_3A_2, $b_{12}B_5$
43714			
		43683	b_4A_0, γ_1B_2
		43657	
43550	α_2A_0		
43538			
		43453	a_2A_0, $b_{11}A_5$
43407		43406	b_6A_1, a_4A_3
43340			
43329			
		43310	$b_{13}B_5$, γ_2A_2
43145		43140	
43137			
		43054	a_3A_1
		43034	b_6B_0
43018			
42966			
42954			
		42938	γ_1B_1
		42895	b_7A_1?
		42847	
42759			
		42681	
		42658	a_3B_0, a_4A_2
		42634	
42589			
42575			

TABLE I. (*Continued.*)

Emission	Transition	Emission	Transition	Emission	Transition	Emission	Transition
42531	b_7B_0	41600		40735		39412	$b_{14}A_1$
42525	$b_{10}B_2$	41573		40644		39372	
42513		41544		40598		39351	
42366	γ_2B_2	41530	b_9B_0, $b_{12}B_2$	40534		39335	
42306	a_3A_0, $b_{15}B_5$	41422		40522	$b_{11}B_0$, $b_{14}B_2$	39224*	
42271	a_4B_1	41398	$b_{10}A_1$	40482		39137*	
42251		41380		40372		39087	
42171	γ_1B_0	41346		40330	$b_{13}B_5$	39074	
42156		41313	$b_{17}B_5$	40278		39061	
42103		41231		40139		38977	γ_4B_1
42079		41108		40100		38956	
41994	γ_2A_2	41089		40008	$b_{12}B_0$	38919	
41923		41038	$b_{13}B_2$, γ_3B_2	39973		38907	$b_{15}A_1$
41902	b_9A_1	41022	$b_{16}B_0$	39930		38847	
41855		40939		39855*		38723*	
41817	$b_{16}B_5$	40888		39825		38611*	
41802		40859	γ_2B_0	39755		38534	
41723		40841		39730		38232	
41701		40822	$b_{18}B_5$	39541	$b_{16}B_2$	38213	
41661		40767		39522	$b_{13}B_0$		
41621	γ_2B_1	40743		39472			

*SO band.

conclude that the bands under consideration arise from the sulphur dioxide molecule both in emission and absorption.

The wave numbers given in Table I are in most cases the violet edge of bands degrading toward the red. In the cases of a few very diffuse bands the measurements are of intensity maxima. The first column gives the wave numbers measured in absorption, the third those in emission. The second and fourth columns give the suggested transitions in terms of the levels of the upper and lower states shown in Fig. 3. These transitions are recorded only where the agreement between observed and calculated values is better than 10 cm^{-1}. Nor are transitions recorded where the agreement is good but the absence of other bands in the progression indicates that it is accidental. The levels used are discussed below.

ANALYSIS OF ABSORPTION DATA

The most striking features of the absorption spectrum are seen more clearly in the densitometer records of the plates than in the plates themselves. Such a record is reproduced in Fig. 2. The most natural assumption seems to be that the strong bands or groups of bands standing out so clearly on the short wave-length side of the spectrum correspond to transitions from the normal state of the molecule to various vibrational states of an excited electronic level. There are nine or ten of these groups with separations of about 370 cm^{-1}. Closer inspection shows that

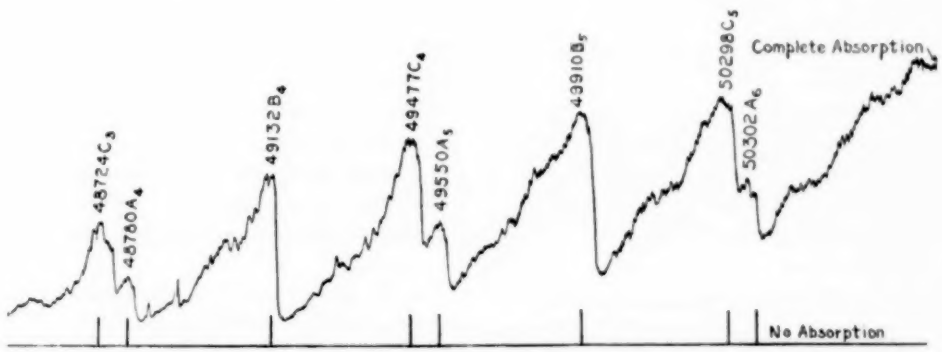

FIG. 2. Densitometer record of part of plate showing absorption spectrum of SO_2 at a temperature of 240°C, pressure of 1.5 mm and path length of 7.8 cm.

these groups do not constitute a simple v' progression as both their structures and separations vary in a complicated way. Various level schemes give a fairly satisfactory correlation of the band heads but none has been found that seems so much better than the others as to be established with certainty as the correct one. In any case the various level schemes devised have certain features in common. For the upper levels the vibrational frequencies used are of the order of 375 cm^{-1} or integral multiples of that number. The separation of successive levels seems to increase for the first two or three and then to decrease again. This effect can be seen clearly in the upper level scheme of Fig. 3 which is the most satisfactory on the whole. On this scheme one vibration frequency is about 750 to 770 cm^{-1}

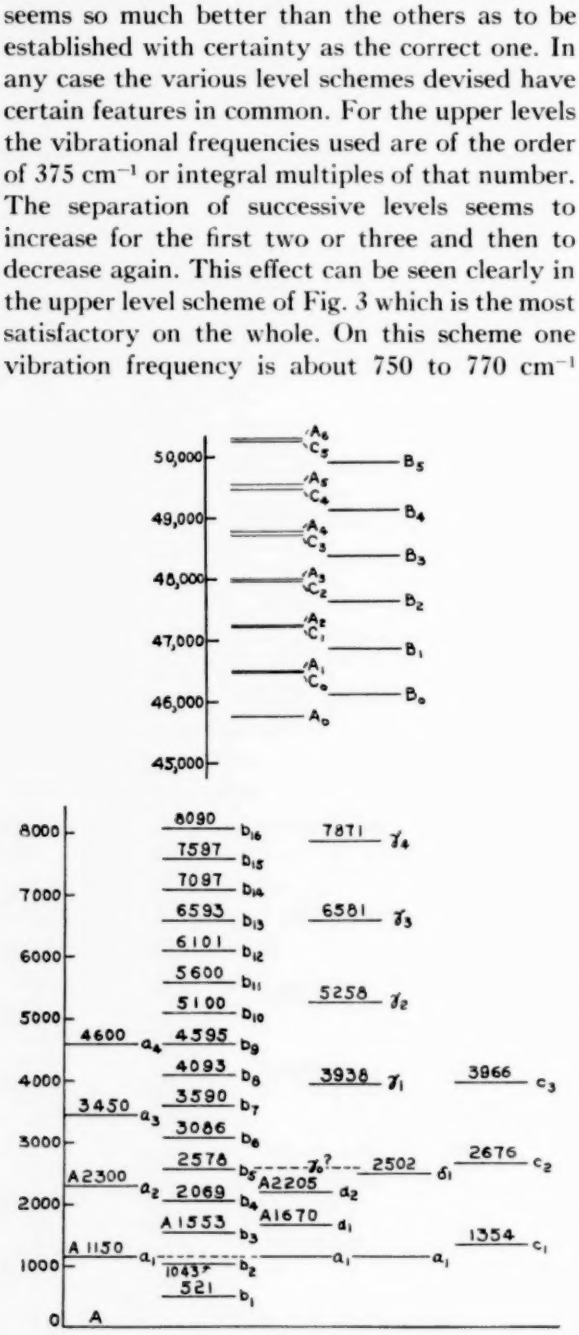

FIG. 3. Vibrational levels in SO_2. In upper electronic state C levels were not used in analyzing emission spectrum. In lower (normal) electronic state only levels marked A were used in analyzing absorption spectrum.

with the others uncertain, though the constant differences $B_n - A_{n-1} = 1129$ suggest this as another. An interesting point is the regular increase of the A_nC_{n-1} separation, the successive values being 23, 40, 57, 73 and 54 cm^{-1} giving a second difference of 17 cm^{-1} if the last value be omitted. However the C levels are necessary for only a few bands and most of their combinations with the lower levels are definitely missing or coincide with other bands. They are perhaps not real.

A single lower level and the triple system of upper levels given in Fig. 3 explain the principle features of the strong absorption shown in the densitometer record. But if this record is examined more carefully or the table of measured wave-lengths consulted it is clear that there are many bands that do not fit into such a scheme. Probably there are many more vibration levels in the upper state than have been used but it is also probable that other levels than that of zero vibration in the normal state contribute to the absorption. From the Raman[11] and infrared[12,13] spectra we know that the vibration frequencies of the normal state are $\nu_1 = 1150$, $\nu_2 = 525$ and $\nu_3 = 1360$ (or 1340?). An examination of the measurements shows 1150 cm^{-1} differences frequent but 525 and 1360 differences only occasional. Levels corresponding to $v_1'' = 1$ and 2 at 1150 and 2300 are well established and combination levels at 1674 for $v_1'' = 1$, $v_2'' = 1$ and at 2210 for $v_1'' = 1$, $v_2'' = 2$ seem probable. A level at 1555 $v_2'' = 3$ also gives several bands and is included in spite of the absence of $v_2'' = 1$ and 2.

The intensities of the bands from the higher vibrational states are lower than those from the initial state as they should be, but there is no consistent variation with temperature between the plates taken at room temperature and 240°. However these experiments were not sufficiently extensive to be of much value.

The predominance of vibrations involving ν_1 in the lower state remains unexplained, particularly as ν_2 and perhaps ν_3 states were observed in emission. It suggests the possibility that the observed 1150 differences should be attributed to

[11] C. R. Bailey and A. B. D. Cassie, Proc. Roy. Soc. London, **A137**, 622 (1932); C. R. Bailey, A. B. D. Cassie and W. R. Angus, Proc. Roy. Soc. London, **A130**, 142 (1930).

[12] K. W. F. Kohlrausch, *The Smekel-Raman Effect*, p. 172.

[13] Dadieu and Kohlrausch, Phys. Zeits. **33**, 165 (1932).

the upper state, the 1128 difference already observed there being the interval between the second and third levels of this particular vibration.

Analysis of Emission Data

Taking the same upper levels and lower frequencies used for absorption it is possible to put some 70 percent of the emission bands into a level scheme. As is to be expected many new levels appear in the lower state. These are shown in Fig. 3. The most striking features are long v_2'' progressions. In one case there are transitions from the B_2 upper level to 17 v_2'' levels having successive differences between 520 and 493 cm^{-1}. Other v_2'' progressions are interpreted as transitions from B_0, A_1, A_5 and B_5 to the same set of lower levels.

The $v_1''=1$, 2 levels appear as in absorption. A level at $v_1''=3$ gives a number of bands but most of them correspond to other transitions also. The $v_1''=4$ level falls on the $v_2''=9$ level.

A search was made for v_3'' progressions and the levels c_1, c_2, c_3, were established tentatively as $v_3''=1$, 2, 3. The same differences among bands of lower wave number led to the γ_1, γ_2, γ_3 levels interpreted as $v_2''=5$, $v_3''=1$, 2, 3. However, all but one of the bands given by the c levels have other interpretations so that no c transitions are recorded in the table. This is not the case with the γ levels but their interpretation is very dubious.

Turning to other combinations, transitions to the α_1, α_2, i.e., $v_1''=1$, $v_2''=1$, 2 levels of absorption are also present in emission. An additional level $\delta_1=2502$ is quite well established and is apparently $\nu_1+\nu_3$.

It may be of interest to note that the second differences in both the v_1'' and v_2'' progressions are very small. A similar result has been observed in CO_2.

Fluorescence

Just as the number of lower levels involved is restricted in an absorption spectrum the number of upper levels observed is restricted in a fluorescence spectrum. Mr. Lotmar in Göttingen has kindly communicated to us his preliminary results on fluorescence in SO_2. They seem to be reconcilable with the level scheme suggested above but not an emphatic confirmation of it. A detailed discussion must await publication of Lotmar's work.[14]

The Electronic States of SO_2

In the early part of this paper the possibility was mentioned that there was more than one electronic transition involved in these spectra. The present work deals mainly with the shortest wave-length portion of the spectrum. Absorption here is stronger than that at longer wave-length and is separated from it by a gap. Furthermore no emission bands were found on our plates above 2600A. It seems probable that there are two excited states, one having a ν_e of about 46,000 and the other having a ν_e of about that used by Watson and Parker, i.e., 31,500 cm^{-1}. The publication of the data on fluorescence may throw further light on the question.

The ultimate purpose of the experiments described in this paper was to throw light on the structure of SO_2 molecule in normal and excited states, its normal vibrations, translation probabilities, etc. But the results seem hardly to justify a discussion of these questions as yet. It is hoped, however, that they may be of assistance to others working in this field.

In conclusion the writer wishes to express his deep gratitude to Professor H. D. Smyth who directed this work and helped to prepare this article. He also wants to thank Professor R. Ladenburg and Professor A. G. Shenstone for their help.

---

[14] *Note added in proof:* Lotmar's paper appeared in the Zeits. f. Physik **83**, 765 (1933) and is discussed in a letter by Smyth in this issue of the Physical Review.

On the Inversion of Doublets in Alkali-Like Spectra

MELBA PHILLIPS, *University of California*

(Received June 29, 1933)

Many of the doublets in the spectra of alkalies and alkali-like ions are inverted or anomalously narrow. This "tendency to inversion" may be explained by the polarizability of the core, which may be formulated as the repulsion by the excited core configuration states of the levels of the optical doublet. A study is made of the energies and wave functions of these states for the spectra Na I to S VI, on two coupling schemes which allow approximate computations to be made. On the assumption of *LS* coupling the separations of the excited core doublets turn out to be of the order of magnitude of the $2p$ x-ray doublet; half the excited core doublets are inverted and half of them normal. The two sets of doublets repel the levels of the optical doublet unequally, and, in the series of spectra considered, the differential repulsion is of the right sign to give an inverting tendency of the same order, though somewhat less, than the observed inversion. The same problem is then treated by another approximation, by assuming the $2p$ x-ray doublet energy large compared to the electrostatic interaction energy of the $3p$ and $3d$ electrons. The results with both models are proportional to the spin orbit interaction energy of the "hole" in the $2p$ shell. The condition that the effects studied should tend to invert and not to broaden the optical doublets, and the further conditions that they should produce an actual inversion are considered. In most cases these questions may be answered from a consideration of the quantum numbers associated with the states capable of perturbing the doublet, and the ratio of optical and x-ray doublet separations. In this way we can understand the observed incidence, both of the tendency toward inversion and of the inversion itself.

THE ordinary spin doublet formula may be derived from a consideration of the interaction of the magnetic moment of the electron and the magnetic field, $\mathbf{H}=1/c[\mathbf{E}\times\mathbf{v}]$, produced by its velocity relative to the nucleus. For a Coulomb field the energy of this interaction is given by

$$W_s{}^l=\frac{Rhc\alpha^2Z^4}{n^3l(l+\frac{1}{2})(l+1)}\,\frac{j(j+1)-l(l+1)-s(s+1)}{2}.$$

The doublet separation in wave numbers is

$$\Delta\nu=R\alpha^2Z^4/n^3l(l+1)$$

with the level of greater j value lying higher. This formula is applied to the spectra of alkalies and alkali-like ions, with an effective nuclear charge substituted for Z to take account of the screening by the core electrons. The formula often fails, however, and the occurrence of inverted or anomalously narrow doublets is frequent in alkali spectra.[1] Thus the $5f$ doublet of Cs I is inverted, with $\Delta\nu=-0.16$; the $4f$ doublet has not been resolved. The d and f doublets of Rb I are believed to be inverted.[2] We quote in Table I the $3d$ separations in frequency numbers for stripped atoms from magnesium through sulphur, as observed by Bowen and Millikan.[3] The theoretical separations are calculated of the assumption of perfect screening, with

$$Z_{\text{eff}}=(Z-10).$$

TABLE I. *3d and 4d separations. The observed values are from Bowen and Millikan.*

	3d		4d	
	observed	from theory	observed	from theory
Mg II	−0.91	0.576		0.243
Al III	−1.70	2.92	−1.28	1.23
Si IV	1.57	9.2	0.08	3.9
P V	6.32	22.5	4.41	9.5
S VI	37.75	46.6		19.7

For an electron moving in a central static field the doublet separation is

$$W=(h/4\pi mc)^2e\overline{E_r/r}$$

where E_r is the radial component of the electric intensity, and the bar denotes an average over the stationary state of the electron. Now for a neutral atom, and for all r, E_r is positive; this follows from Gauss' theorem, since the charge

[1] Bacher and Goudsmit, *Atomic Energy States*, 1932.

[2] Ramb, Ann. d. Physik **10**, 311 (1931).

[3] Bowen and Millikan, Phys. Rev. **25**, 301 (1925).

within any spherical surface is necessarily positive. Thus the model of an electron moving in any central static field necessarily gives a normal doublet, with the level of greater j lying higher.

Two distinct quantum mechanical aspects of the core are neglected in the one electron model. The first of these arises from the circumstance that the interaction of the valence electron and the electrons of the core is not completely represented by the field of the mean charge distribution of the core electrons; the application of the exclusion principle to the formulations of these interactions introduces, as is well known,[4] terms which correspond to the interchange of core and valence electrons. These terms give contributions to the energy of the two states of the optical doublet which are in general unequal. Their effect has recently been investigated by Johnson and Breit,[5] but is apparently too small to account for the observed inversions.

The second, which seems to us to give greater promise of an explanation, involves a consideration of the excited states of the core. This aspect may be stated in various ways: as a polarization of the core, expressed by transitions of the inner electrons to excited states; as an admixture of wave functions for the excited states in that for the true stationary state described approximately by the definite configuration of closed shells and the quantum numbers of the valence electron; or as a repulsion of the levels of the ordinary optical spectrum by those of the excited core configurations. These are three statements of the same effect, but one quite different from that mentioned in the preceding paragraph.

Strictly a level is said to be "perturbed" by another of the same parity (oddness or evenness of $\Sigma|l|$) and the same angular momentum, which lies close to it so that the nondiagonal element of the energy referring to the two states, in general small, is no longer negligible compared with the unperturbed energy difference. An example of a perturbation of this sort which anomalously inverts the doublets of certain terms is known in the spectrum of copper, in the configuration $(3d)^{10}\,(np)$. Shenstone and Russell[6] have shown that the perturbing levels in this case are the inverted doublets of $(3d)^9\,(4s)\,(np)$, and have given on this basis a complete explanation of the inversions observed. A similar explanation has been suggested at various times for the inverted doublets of alkalies.[7] This case cannot really be an example of spectroscopic perturbation: the excited core states lie far from the optical ones, and the interaction energy is at best only a small fraction of this energy difference. The separations of states of the excited core configurations, however, are relatively enormous, arising partly from a deep lying unpaired spin, and in some of the states the j values will be inverted, analogous to those of x-ray doublets. It might be expected, then, that the existence of these higher states can totally alter the doublets of the optical terms, and that their arrangement may be such as to give a net inverting effect.

The atomic wave function for a true stationary state of an atom may be built up as a sum of wave functions for the approximately stationary states of definite configuration, and equal parity and angular momentum. In general nearly the whole of the true wave function is given by the term arising from one specific configuration, and this configuration is used (in addition to the quantum numbers $m_l m_s$) to index the state; the coefficients in the sum of wave functions referring to other configurations are small unless the conditions for a genuine perturbation are fulfilled. Thus we may write

$$\psi_i = \psi_{i_0} + \sum_j [V_{ij}/(E_i - E_j)]\psi_{j_0},$$

where ψ_{i_0} is the approximate function for a state of definite configuration i and V_{ij} is the matrix element of the electrostatic interaction energy corresponding to a transition between the configurations i and j. The two terms i and j repel each other by an amount

$$\Delta E = |V_{ij}|^2/|E_i - E_j|.$$

Suppose that ψ_{j_0} represents a doublet of the same orbital angular momentum L as the optical doublet, and neglect the normal doublet splitting in comparison with that of the excited one, ϵ.

[4] Fock, Zeits. f. Physik **81**, 195 (1933).
[5] Johnson and Breit, Phys. Rev. **44**, 77 (1933).
[6] Shenstone and Russell, Phys. Rev. **39**, 415 (1932).
[7] H. E. White, Phys. Rev. **40**, 316 (1932); R. F. Bacher, Phys. Rev. **43**, 269 (1933).

$$(E_i-E_j)_{L+\frac{1}{2}}=E_0, \quad (E_i-E_j)_{L-\frac{1}{2}}=E_0+\epsilon,$$
$$|V_{ij}|_{L-\frac{1}{2}}=|V_{ij}|_{L+\frac{1}{2}}-v.$$

The shift in doublet separation is given, to first order in ϵ and v, by

$$\delta E=\Delta E_{L+1/2}-\Delta E_{L-1/2}=|V_{ij}|^2\epsilon/E_0^2+2V_{ij}v/E_0.$$

For definiteness we shall use this theory in an attempt to explain the data given in Table I, and in particular the inversion of the $3d$ doublet ($j=3/2$, $5/2$) of Mg II, observed to have a separation of -0.9ν instead of 0.56ν as predicted by the spin theory. The normal Mg II atom consists of a single valence electron outside a completed $2p$ shell, so that a full description of the $3d$ configuration is $(1s)^2\,(2s)^2\,(2p)^6\,(3d)$. We shall consider only transitions of the p electrons, and need not include $(1s)^2\,(2s)^2$ in designating the configurations. The lowest even levels with $j=3/2$, $5/2$ arising from core excitation are in $(2p)^5\,(3s)\,(3p)$, but this involves a double jump from $(2p)^6\,(3d)$, so that a much more considerable contribution may be expected from $(2p^5)\,(3p)\,(3d)$. Higher terms, with transitions of one of the $2p$ electrons to $4p$, $5p$, etc., will have similar but smaller effects. Unfortunately these states cannot be observed experimentally; the energy required to excite a core electron is much greater than the ionization potential of the valence electron, so that auto-ionization occurs.

The number of possible combinations of the individual l and s vectors of an almost closed shell is equal to that for the missing electrons. Thus in the elements of Table I the number of levels arising from $(2p)^5\,(3p)\,(3d)$ is the same as that which would arise from $(2p)\,(3p)\,(3d)$, and we are justified, insofar as multiplicities are concerned, in treating the atom as a three electron atom, $2p$ representing a "hole" in the $2p$ shell. Two different coupling schemes for the excited core will be considered as limiting cases, although, since the electrostatic interactions and the $2p$ spin orbit interactions are of the same order of magnitude, the actual atom will be of some intermediate type. Calculations will be made first on the assumption of LS coupling, then according to a scheme in which the valence and excited electrons are coupled LS and then to the quantized j of the $2p$ hole. In the latter case the levels fall into two groups, corresponding to the two members of the inverted x-ray doublet. It will be seen that the repulsion of both components of the optical doublet is the same if only the direct integrals of V_{ij} are considered, i.e., those which would appear even if the wave functions were not antisymmetrized. If exchange terms are included, however, there is a net effect, proportional on both models to the spin orbit interaction energy of the $2p$ hole.

Effect of LS Coupled Excited Core States

Since the electrostatic energy commutes with L and S it has no matrix elements connected with transitions in which L and S change. Thus the whole effect of the excited core states, if LS coupled, comes from the ^2D's of the excited configuration. An enumeration of these relevant states may be made from the vector model. First couple the $3p$, $3d$ electrons to form singlet and triplet P, D and F terms. One ^2D ($L=2$) arises from each singlet and triplet of the two electron configuration, making six in all. There are no equivalent electrons and all states are allowed.

Table II. *Diagonal elements of* $\xi_1(l_1\cdot s_1)+\xi_2(l_2\cdot s_2)$.

Parent term	$\xi_1(l_1\cdot s_1)+\xi_2(l_2\cdot s_2)$ $J=s/2$	$J=3/2$	Separation
^1P	$\frac{1}{2}\xi_1$	$-\frac{3}{4}\xi_1$	$\frac{5}{4}\xi_1$
^1D	$\frac{1}{6}\xi_1$	$-\frac{1}{4}\xi_1$	$\frac{5}{12}\xi_1$
^1F	$-\frac{1}{3}\xi_1$	$\frac{1}{2}\xi_1$	$-\frac{5}{6}\xi_1$
^3P	$-\frac{1}{2}\xi_1+\xi_P$	$\frac{3}{4}\xi_1-\frac{1}{2}\xi_P$	$-\frac{5}{4}\xi_1+\frac{5}{2}\xi_P$
^3D	$-\frac{1}{6}\xi_1+\frac{5}{3}\xi_D$	$\frac{1}{4}\xi_1-\frac{5}{2}\xi_D$	$-\frac{5}{12}\xi_1+\frac{5}{6}\xi_D$
^3F	$\frac{1}{3}\xi_1+\frac{8}{3}\xi_F$	$-\frac{1}{2}\xi_1-4\xi_F$	$\frac{5}{6}\xi_1+\frac{20}{3}\xi_F$

The separations ϵ of the individual doublets are given by the matrix of the spin orbit interaction energy. This matrix is not diagonal in the LS scheme but we may assume the diagonal elements large and calculate them for the ^2D's formed by the addition of $2p$ to ^1PDF, ^3PDF. A method for obtaining the spin orbit interactions in LS coupling directly from the matrix equations has been given by Johnson.[8] Table II contains the diagonal elements of $\xi_1(l_1\cdot s_1)+\xi_2(l_2\cdot s_2)$, where

$$\xi_1=R\alpha^2Z^4_{\text{eff}}/n^3l(l+\tfrac{1}{2})(l+1)$$

[8] M. H. Johnson, Phys. Rev. **38**, 1628 (1931).

for $2p$, and ξ_2 is the corresponding parameter associated with the ionic multiplet. It may be assumed that these parameters for the ionic multiplets are negligibly small compared with ξ_1. As has been pointed out by Shortley[9] the spin orbit parameter of a missing electron in an otherwise closed shell is negative. Those doublets arising from ^1P, ^1D, ^3F are thus seen to be inverted, while the other three are normal. The orientation of the doublets with P and F parent terms could have been predicted from the vector model.

The linear combinations of determinantal eigenfunctions to represent the various D doublets were obtained by using angular momentum operators, a method given by Gray and Wills.[10] The valence and excited electrons are first combined, then coupled with $2p$, so that correlations with the individual doublets shown by the vector model may be made. No constant factor arises in the V_{ij} because of the presence of six electrons in the p shell. Specifying the quantum numbers of $3p$ (of which there are six possibilities) in the excited core wave functions automatically selects terms in the antisymmetrized function for the ordinary ^2D which combine. There are 3! nonvanishing terms for each pair of determinantal functions in the three electron case, and this factor is cancelled by the normalizing factor $1/(3!)^{\frac{1}{2}}$. If the problem is done explicitly in all seven electrons the 7! terms in V_{ij} are taken care of by the $1/(7!)^{\frac{1}{2}}$ of the antisymmetric permutations. The coefficients of the first direct and interchange radial integrals of V_{ij}, the matrix element of e^2/r_{12}, where 1 and 2 refer to $3d$ and the electron making the transition $2p \rightarrow np$, then, are found by multiplying the coefficients of determinantal functions which combine with the optical doublet by the proper angular integrals (tables of which may be constructed from Slater's b's) and summing. This result is independent of the m of the $j=5/2$, of course, and is the same for both members of the doublet. Because of the antisymmetry in spin of the singlet the sign between the direct and exchange integrals is different according to whether the parent term of state j is a singlet or a triplet. To this order, then:

$$V_{ij}(^1P) = \left(\frac{3}{10}\right)^{\frac{1}{2}}\left(F_0 + \frac{1}{15}G\right)$$

$$V_{ij}(^3P) = \frac{3}{10^{\frac{1}{2}}}\left(F_0 - \frac{1}{15}G\right)$$

$$V_{ij}(^1D) = \frac{1}{2^{\frac{1}{2}}}\left(F_0 - \frac{1}{5}G\right)$$

$$V_{ij}(^3D) = \left(\frac{3}{2}\right)^{\frac{1}{2}}\left(F_0 + \frac{1}{5}G\right)$$

$$V_{ij}(^1F) = \left(\frac{7}{10}\right)^{\frac{1}{2}}\left(F_0 + \frac{2}{5}G\right)$$

$$V_{ij}(^3F) = \left(\frac{21}{10}\right)^{\frac{1}{2}}\left(F_0 - \frac{2}{5}G\right).$$

The shift of optical doublet separation may be calculated from the formula $\delta E = |V_{ij}|^2\epsilon/E_0^2$, substituting the values of the separations from Table II. The terms in F_0^2 cancel, but the further terms in V_{ij}^2 give a net result. Since the exchange integral G_1 is much smaller than the direct integral F_0 we shall here record only the first nonvanishing terms (Table III). Whether this result means inversion depends on the relative sign of F_0 and G_1, on their magnitudes, and the energy differences of the levels, but before making an application to an actual case we shall investigate the other coupling scheme outlined above.

TABLE III.

$$\delta E(^1P) = \tfrac{1}{20}(F_0G/E_0^2)\xi_1, \qquad \delta E(^3D) = -\tfrac{1}{4}(F_0G/E_0^2)\xi_1,$$
$$\delta E(^3P) = \tfrac{3}{20}(F_0G/E_0^2)\xi_1, \qquad \delta E(^1F) = -\tfrac{7}{15}(F_0G/E_0^2)\xi_1,$$
$$\delta E(^1D) = -\tfrac{1}{12}(F_0G/E_0^2)\xi_1, \qquad \delta E(^3F) = -\tfrac{7}{5}(F_0G/E_0^2)\xi_1,$$
$$\Sigma\delta E = -2(F_0G/E_0^2)\xi_1.$$

EFFECT OF jJ COUPLED EXCITED CORE STATES

In this scheme the quantized j of $2p$ is coupled to the ionic multiplets of the outer two electron configuration. Since the total orbital angular momentum of the three electrons is no longer quantized there will be matrix elements V_{ij} between the optical ^2D and all the $J=3/2$, $5/2$ states of the excited core, of which there are altogether thirty-six. The appropriate angular

[9] Shortley, Phys. Rev. **40**, 185 (1932)
[10] Gray and Wills, Phys. Rev. **38**, 248 (1931).

momentum operators were used to obtain the three electron eigenfunctions. Products of coefficients of combining terms of the excited core and optical state wave functions were multiplied by the appropriate angular integrals and summed, for each of the relevant excited core levels. The contributions to the energy of the mutual repulsion are proportional to the squares of these sums. Since the levels from a single multiplet coupled to a particular j of $2p$ lie very close together, the inverting effect of such a set of levels is proportional to $\Sigma(|V_{ij}|^2_{5/2}-|V_{ij}|^2_{3/2})$. The results are given in terms of the first direct and interchange integrals.

$$j_{2p}=3/2: \quad \Sigma(|V_{ij}|^2_{5/2}-|V_{ij}|^2_{3/2})=-\tfrac{2}{3}F_0G_1,$$

$$j_{2p}=1/2: \quad \Sigma(|V_{ij}|^2_{3/2}-|V_{ij}|^2_{3/2})=\tfrac{2}{3}F_0G_1.$$

The coupling scheme here assumed implies that all states associated with a definite j of $2p$ are grouped together, and their spread of energies is neglected. The two sets of levels act in opposite ways on the optical doublet separation, but they are separated by ϵ, the width of the $2p$ x-ray doublet. The sum of their effects is

$$\Sigma\delta E=\tfrac{2}{3}F_0G_1(-1/E_0+1/(E_0+\epsilon)),$$

since the $2p_{3/2}$ group lies nearer the optical doublet.

$$\Sigma\delta E=-\tfrac{2}{3}\epsilon(F_0G_1/E_0^2).$$

Now, since

$$\epsilon=\tfrac{1}{2}(2l+1)\xi_1=(3/2)\xi_1,$$

$$\Sigma\delta E=-(F_0G_1/E_0^2)\xi_1.$$

The net effect in this case is due entirely to the difference in the sign between F_0 and G_1 for excited core levels with singlet and triplet parent terms, and is equal to that portion of the LS result which arises from the same cause. Because of the different enumeration and character of the states no extra contribution from the triplets occurs here. Owing to the quantization of the j of the $2p$ "hole" instead of the total orbital angular momentum the electrostatic interaction energy associated with the transition $2p\rightarrow np$ must be calculated separately for the $J=3/2, 5/2$ states arising from each component of a triplet, and the individual elements squared before summing. Thus the weighting of terms from triplet parents, which appears in LS coupling, is lost, and the whole effect comes from the difference in symmetry between singlets and triplets.

Application of Theory to Mg II. Evaluation of Integrals

F_0 and G_1 are the first two radial integrals of

$$V_{ij}=\int\int\psi_i(e^2/r_{12})\psi_j d\tau_1 d\tau_2,$$

when $1/r_{12}$ is expanded in spherical harmonics. In the evaluation of these integrals for a particular case, Mg II, hydrogen like one electron functions were used, with screening constants derived by interpolation from those given by Pauling and Sherman.[11] For the configuration whose energy lies closest to the optical state, $(2p)\ (3p)\ (3d)$, the values of Z_{eff} were 7 for $2p$, 3.7 for $3p$ and 2 for $3d$. The results were found to be surprisingly stable under a reasonable variation of screening constants.

$$F_0=e^2\int\int R_1(2p)R_1(3p)R_2^2(3d)(1/r_7)r_1^2r_2^2dr_1dr_2$$

$$\backsimeq 1.73 \text{ volts}$$

where R is the radial factor of the one electron eigenfunction.

$$G_1=e^2\int\int R_1(3p)R_1(3d)R_2(2p)R_2(3d)(r_2/r_7^2)$$

$$\times r_1^2r_2^2dr_1dr_2\backsimeq -0.43 \text{ volt electron.}$$

The radial wave function corresponding to spins parallel and antiparallel to the orbital angular momentum are not identical. This difference is appreciable only for the $2p$ electron, since only there are the energies for the two spin orientations considerably separated. Thus V_{ij} for levels associated with $2p_{3/2}$ and $2p_{1/2}$ are different. $|V_{ij}|_{3/2}-|V_{ij}|_{1/2}=v$ is small but since it is associated with only one set of the perturbing levels $V_{ij0}v$ is weighted by a factor E_0/ϵ in comparison with $|V_{ij0}|^2$.

To ascertain a correction for this difference we may write

[11] Linus Pauling and J. Sherman, Zeits. f. Krist. **81** (1932).

$$F_{0\ 3/2}-F_{0\ 1/2}=f, \quad G_{1\ 3/2}-G_{1\ 1/2}=g,$$

$$f=e^2\int_0^\infty\int_0^\infty R_2^2(3d)R_1(3p)\rho_1(2p)(1/r_7)r_1^2r_2^2dr_1dr_2,$$

where $\rho_1=R_1(2p)_{3/2}-R_1(2p)_{1/2}$. The relativistic radial wave functions for a Coulomb field have been given as series in r by Darwin[12]:

$$R(2p)_{3/2}=re^{-cr}\left(1-\frac{\alpha_1^2}{4}\ln 2cr+\frac{3}{8}\alpha_1^2\right),$$

$$R(2p)_{1/2}=re^{-cr}\left\{1-\frac{\alpha_1^2}{2}\ln 2cr-\frac{\alpha_1^2}{4}\left(-\frac{37}{8}-\frac{cr}{2}+\frac{3}{4cr}\right)\right\},$$

where α_1 is the fine structure constant times the nuclear charge. $c=Z_{eff}/na$.

$$\rho=re^{-cr}\frac{\alpha_1^2}{4}\left(\ln 2cr-\frac{25}{8}+\frac{2(cr)^2+3}{4cr}\right).$$

To apply this to our problem we must determine what effective nuclear charge to use in evaluating α_1. It is not possible to do this rigorously in any simple way; we have contented ourselves with elementary considerations which fix the possible limits of Z, and give us an estimate of the correction term. A mean for the parenthesis was estimated before integrating, and found to be approximately unity, so that the integral is merely $\alpha_1^2F_0/4$. Since both $3d$ and $3p$ weight the difference $R(2p)_{3/2}-R(2p)_{1/2}$ far out from the nucleus the corresponding parenthesis in g is of the same sign, and is of the same order of magnitude. The overlapping coefficients are just as before, and the ratio of the correction to the effect previously considered is

$$\frac{F_0g+G_1f}{2F_0G_1}\frac{\alpha_1^2}{4}\frac{E_0}{\epsilon}\backsimeq\frac{\alpha_1^2}{4}\frac{E_0}{\epsilon}.$$

The change in the optical ^2D splitting predicted by the theory depends on the data assumed and on the coupling. $\epsilon=2219\nu$, the separation of ^2P in Mg IV. The energy difference between the excited core and optical states is that of the transition $2p\rightarrow 3p$, approximately 480,000ν or 60 volts, from the spectrum of Mg III. The effective charge which enters the v correction through must lie between 7 and 11, and about 9 seems a reasonable choice for it. This leads to 1/3 as the value of the ratio above. On LS coupling the shift in the $3d$ doublet separation is

$$\delta E=(4/3)\epsilon(F_0G_1/E_0^2)(1+\tfrac{1}{3})\backsimeq 0.9\nu,$$

sufficient to invert the levels, although not to the extent of the 1.5ν discrepancy indicated by observation. The jJ result is half this, and the actual Mg II atom must lie somewhere between. Further contributions toward inversion may be expected from transitions of a core electron to other p orbits. The direct integrals for transitions to $4p$ and $5p$ were calculated, and found to be 0.9 and 0.56 volt electrons, respectively. The corresponding exchange integrals are small, so that the computations cannot be rigorous. If they diminish in the same ratio as the F_0's the combined inverting tendency of these configurations is about 0.4 times that of the first excited core level. We shall see, moreover, that all the inverting effects would be somewhat larger if more accurate radial wave functions were used. We are thus led to believe that the observed inversion of the $3d$ doublet may be wholly accounted for by the effect treated in this paper.

Conclusions

The effect of excited core states on the optical doublet separation is toward inversion if F_0 and G_1 are of opposite sign. A general argument for the signs of these radial integrals can be made for the elements of Table I. For the nearest perturbing state, $(2p)^5\ (3p)\ (3d)$, F_0 and G_1 are opposite in sign. Only one wave function, that of $3p$, has a node. In the direct integral the function is weighted by $2p$, which has its maximum far in; for the exchange integral the important region is that of greater r, because of the overlapping with $3d$. The node will always fall between these two weighted regions. While the largest contribution may be expected from this configuration similar effects arise from transitions to other p levels, the magnitude of whose cumulative shifting tendency it is difficult to estimate. More nodes occur in the np wave functions, $(n>3)$, but the principal contribution to G_1 will come between the first two nodes, and that to

[12] C. G. Darwin, Proc. Roy. Soc. **A118**, 673 (1928).

F_0 before the first one, so that the difference in sign persists. In a non-Coulomb central field, such as Hartree's, all the nodes are farther in than those of hydrogen-like functions, making $|-G_1|$ greater. It seems not likely that the accompanying diminution in F_0 would entirely compensate this increase, so that the numerical answer should be larger than that calculated for the $2p \rightarrow 3p$ transition in Mg II.

For actual inversion there must be, in addition to the tendency toward inversion due to different signs of F_0 and G_1, an enormously larger spin orbit interaction energy for the x-ray levels than for the optical ones. This condition is satisfied for the first few elements of Table I.

In the inversion of $4d$ the argument is analogous. The overlapping for $np \cdot 4d$ is in general farther out and opposite in sign to that of $2p \cdot np$, but the shift, even where the condition on the separation ratio is satisfied, should be less than that for $3d$. This is in accord with the observations in Al III. The $5f$ term of Cs I is analogous to the $4d$ of Al III.

Thus it appears that both the tendency toward inversion and the inversion itself can be roughly predicted from a consideration of the quantum numbers associated with the states capable of perturbing the doublet, and the ratio of the optical and x-ray doublet separations.

The writer is deeply indebted to Professor J. R. Oppenheimer, with whom this investigation was carried out, and to the Physics Department of the University of California for a Whiting Fellowship during the past year.

An Application of Probabilities to the Counting of Alpha-Particles

NORMAN I. ADAMS, JR., *Sloane Physics Laboratory, Yale University*

(Received August 1, 1933)

The Poisson law of probability is directly applicable to radioactive emissions only in certain simple cases. In general, when a radioactive series such as the thorium series is present the probability function is complex. It can be found readily, however, if the interval of time for which probabilities are calculated is chosen so as to be either very short or very long compared with the mean life of each radioactive substance involved. The probability function for α-particles from the thorium series is determined on the basis of an interval of five minutes and is illustrated graphically in a special case.

WHEN events are distributed individually and collectively at random, the probability of any number of events occurring within a chosen interval is given by the Poisson law $p(n)=\epsilon^n e^{-\epsilon}/n!$.[1] Here n is the number of events whose probability is required, ϵ is the mean or expected number for the given interval and $e=2.71828$, as usual. The rays emitted during the disintegration of a radioactive substance or of a mixture of effectively independent radioactive substances constitute a set of events distributed individually and collectively at random in time, at least in the case where the amount of radioactive material does not vary appreciably over a period of time sufficiently great to contain a large number of the basic intervals for which the probability of events is desired. Experimental verification of the Poisson law as applied to simple radioactive disintegrations has been obtained in the case of α-particles by Rutherford and Geiger[2] and in the case of β-particles by Kovarik.[3]

Unfortunately, in many cases of radioactive disintegration the events are not distributed individually and collectively at random. Such a case has arisen in experiments now being conducted by Kovarik and the writer to make an accurate determination of the disintegration constant of thorium. Here α-particles are counted by the same method as in the recent new determination of the disintegration constant of uranium.[4] Since the α-particles counted do not come from thorium alone but from the entire thorium series containing six α-particle emitters, each dependent on the preceding, the events are not individually at random and the Poisson law does not apply.

The general derivation of the probability law for the case just quoted appears to be very difficult. We can, however, deduce the form of the probability function if a simple restriction is imposed. Let us suppose that the interval of time for which the probability of n α-particles must be found is either very short or very long compared with the mean life of each of the six α-particle emitters in the thorium series. We assume that the thorium and its following products are in radioactive equilibrium, so that the amount of each substance present is effectively constant, the mean life of thorium being so great. Evidently the number of α-particles coming from any product x, say, whose mean life is long compared to the chosen interval, is a small fraction of the number of atoms of x present or produced during the interval and the distribution of these α-particles in time is in accord with the Poisson law. On the other hand, the number of α-particles coming from a product y whose mean life is short compared to the interval is equal simply to the number of atoms of y produced during the interval from the preceding substance in the radioactive series. Thus, if y follows x the

[1] For an explanation of the criterion "individually and collectively at random" and a complete discussion of the Poisson law the reader is referred to Fry, *Probability and Its Engineering Uses*, Chapter VIII.

[2] Rutherford and Geiger, Phil. Mag. [6] **20**, 698–707 (1910).

[3] Kovarik, Phys. Rev. **13**, 272–280 (1919).

[4] Kovarik and Adams, Phys. Rev. **40**, 718–726 (1932).

α-particles are associated in groups of two, the distribution of the groups in time following the Poisson law. Similarly, if another product z of short life follows y in turn, the α-particles are associated in groups of three and so on.

The substances in the thorium series which give rise to α-particles are shown in Table I. As five minutes is a convenient period for which to record counts experimentally, let us use this length of time as the basic interval in calculating probabilities. Examination of the table shows

TABLE I.

Substance	*Mean life*
Thorium	$1.8(10)^{10}$ yr.
Radiothorium	2.74 yr.
Thorium X	5.25 day
Thoron	78.6 sec.
Thorium A	0.21 sec.
Thorium C	87.4 min.

that thorium, radiothorium and thorium C emit α-particles distributed individually and collectively at random, while thorium X, thoron and thorium A give rise to α-particles in groups of three similarly distributed. Thus, if ϵ is the mean rate of emission for the entire thorium series, the probability functions for the α-particles coming from the "singles" class and from the "triples" class are, respectively,

$$p_s(n_s)=\frac{(\epsilon/2)^{n_s}e^{-\epsilon/2}}{n_s!}, \quad p_t(n_t)=\tfrac{1}{3}\frac{(\epsilon/6)^{n_t/3}e^{-\epsilon/6}}{(n_t/3)!},$$

where $n_s=0, 1, 2, 3$, etc., and $n_t=0, 3, 6, 9$, etc. The factor $\frac{1}{3}$ in the second expression is introduced to normalize the coordinates in the usual manner.

It is now a simple matter to find the probability function for any number of α-particles in the chosen interval for the entire series. Consider, for example, five. This number may be composed of one triple and two singles, or of five singles, the total probability function for which is

$$p_t(3)\cdot p_s(2)+p_t(0)\cdot p_s(5).$$

Similarly, the probability function for six α-particles is

$$p_t(6)\cdot p_s(0)+p_t(3)\cdot p_s(3)+p_t(0)\cdot p_s(6),$$

and that for seven is

$$p_t(6)\cdot p_s(1)+p_t(3)\cdot p_s(4)+p_t(0)\cdot p_s(7).$$

Evidently the general form of the probability function depends on whether the number of α-particles is one less than, equal to or one greater than an integral multiple of three. If we denote by ν a number of α-particles which is an integral multiple of three, we have, for the three cases just mentioned,

$$p_{-1}(\nu-1)=\tfrac{1}{3}e^{-2\epsilon/3}\left[\frac{(\epsilon/6)^{\nu/3-1}(\epsilon/2)^2}{(\nu/3-1)!2!}+\frac{(\epsilon/6)^{\nu/3-2}(\epsilon/2)^5}{(\nu/3-2)!5!}+\cdots+\frac{(\epsilon/6)^1(\epsilon/2)^{\nu-4}}{1!(\nu-4)!}+\frac{(\epsilon/6)^0(\epsilon/2)^{\nu-1}}{0!(\nu-1)!}\right]$$

$$p_0(\nu)=\tfrac{1}{3}e^{-2\epsilon/3}\left[\frac{(\epsilon/6)^{\nu/3}(\epsilon/2)^0}{(\nu/3)!0!}+\frac{(\epsilon/6)^{\nu/3-1}(\epsilon/2)^3}{(\nu/3-1)!3!}+\frac{(\epsilon/6)^{\nu/3-2}(\epsilon/2)^6}{(\nu/3-2)!6!}+\cdots+\frac{(\epsilon/6)^1(\epsilon/2)^{\nu-3}}{1!(\nu-3)!}+\frac{(\epsilon/6)^0(\epsilon/2)^{\nu}}{0!\nu!}\right]$$

$$p_{+1}(\nu+1)=\tfrac{1}{3}e^{-2\epsilon/3}\left[\frac{(\epsilon/6)^{\nu/3}(\epsilon/2)^1}{(\nu/3)!1!}+\frac{(\epsilon/6)^{\nu/3-1}(\epsilon/2)^4}{(\nu/3-1)!4!}+\frac{(\epsilon/6)^{\nu/3-2}(\epsilon/2)^7}{(\nu/3-2)!7!}+\cdots+\frac{(\epsilon/6)^1(\epsilon/2)^{\nu-2}}{1!(\nu-2)!}+\frac{(\epsilon/6)^0(\epsilon/2)^{\nu+1}}{0!(\nu+1)!}\right].$$

We may use these expressions separately if we choose, but it is simpler to employ the composite function $P(\nu)=p_{-1}(\nu-1)+p_0(\nu)+p_{+1}(\nu+1)$

which applies to the coordinate interval $\nu-1$ to $\nu+1$, inclusive. After some manipulation we find

$$P(\nu)=\tfrac{1}{3}e^{-2\epsilon/3}\sum_{x=0}^{\nu/3}\frac{(\epsilon/6)^{\nu/3-x}(\epsilon/2)^{3x}}{(\nu/3-x)\,!(3x)\,!}\times\left(\frac{3x}{\epsilon/2}+1+\frac{\epsilon/2}{3x+1}\right)$$

$$=\tfrac{1}{3}(\epsilon/6)^{\nu/3}e^{-2\epsilon/3}\sum_{x=0}^{\nu/3}\frac{(3^{\frac{1}{2}}\epsilon/2)^{2x}}{(\nu/3-x)\,!(3x)\,!}\times\left(\frac{3x}{\epsilon/2}+1+\frac{\epsilon/2}{3x+1}\right).$$

Since the coordinates have been normalized, the actual probability of a number of α-particles within the coordinate interval $\nu-1$ to $\nu+1$ inclusive is $3P(\nu)$ and the probability for an extended interval ν_1-1 to ν_2+1, say, is $3\sum_{\nu_1}^{\nu_2}P(\nu)$. When ϵ is large we may replace $P(\nu)$ by a continuous function $P(n)$ and express the probability as the integral $\int_{n_1}^{n_2}P(n)dn$ in the usual way.

The probability curve $P(n)$ for $\epsilon=210$ is shown in Fig. 1. For the sake of comparison the curve $p(n)=\epsilon^n e^{-\epsilon}/n!$ is indicated by the broken line. This curve applies to any case where α-particles are produced by a single substance or by a mixture of effectively independent substances, such as the uranium series. It is evident that the standard deviation σ for $P(n)$ is considerably greater than for $p(n)$. In fact, in the first case the value of σ, obtained from the curve, is approximately 21, while in the second case it is known to be $210^{\frac{1}{2}}=14.5$. This difference is easily detected experimentally.

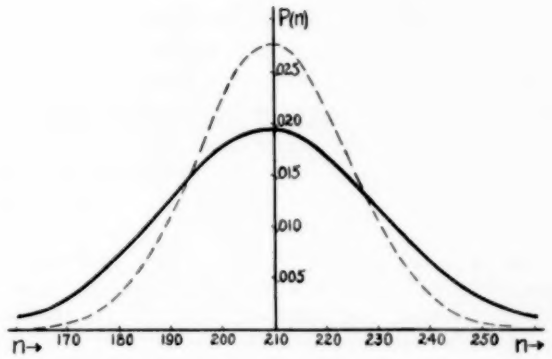

FIG. 1.

The Exponential Law of Radioactive Disintegration

ARTHUR E. RUARK, *University of Pittsburgh*

(Received June 22, 1933)

The decay law, $N=N_0e^{-\lambda t}$, is based on the assumption that the probability w of an atom disintegrating in unit time is constant. The question arises whether this assumption is necessary. It might happen that atoms of different ages have different decay probabilities; and w might depend on age in such a way that exponential decay curves would result. A theorem of Wolfke, however, can be interpreted in such a manner as to show that w cannot depend on the age of the atom. This result is generalized. Consider a series whose members A, B, etc., have decay probabilities w_A, w_B, etc. If all members decay exponentially, if all w's are smooth and continuous functions of their variables and if each w is, at most, a function of the age of the atom, the ages of its ancestors and the ages of its descendants; then the w's are constant; and so in this more general case, the assumption of constant decay probability which underlies the wave mechanical theory of disintegration is necessary as well as sufficient.

I. The Physical Meaning of the Decay Constant

SCHWEIDLER derived the radioactive decay law,

$$N=N_0e^{-\lambda t}, \tag{1}$$

by assuming that in a preparation of N atoms the number which disintegrate in time dt is $N\lambda dt$, where λ is independent of the time. The quantum theory of disintegration may be said to explain this assumption. The wave-mechanical picture of nuclei as potential barriers and the customary statistical interpretation lead to the statement that the probability of decay in unit time is constant. Wolfke[1] has pointed out that the experimental facts admit an alternative interpretation. It is conceivable that an individual atom, born at time zero, may possess a mechanism whose operation will cause it to decay between t and $t+dt$. Wolfke shows that if this is true, the exponential law of disintegration requires that a fraction $\lambda e^{-\lambda t}dt$ of the atoms born at time zero shall decay in the interval dt. According to this picture, chance is involved in the assignment of lives to the atoms at the time of birth but after that the behavior of each atom is determinate until it decays, when chance must enter again to fix the life of the daughter atom and so on. This alternation between determinate and indeterminate behavior seems unsatisfactory.

[1] Wolfke, Phys. Zeits. **30**, 899 (1929).

The discussion by Wolfke leads to the more general question whether radioactive atoms show aging effects. In dealing with such a fundamental point it is well to rely as much as possible on experiment rather than intuition. Let us examine the meaning of λ, considered as an empirical constant, on the basis of decay experiments. In any preparation the atoms which decompose in a time-element dt are of various ages and it is conceivable that atoms of different ages may transform at different rates, in such a way that the composite decay curve is exponential. If we write $w(t-a)dt$ for the fraction of the atoms born at time a and still present at time t which will decay between t and $t+dt$, the experimental value of λ appropriate to the time t is the *mean value* of w for atoms of all ages, decaying in that interval. Thus time-constancy of λ does not prove that w is constant, although, of course, if w were a function of age, we should expect that λ would depend on the mode of preparing the specimen, so that variations of λ, due to this cause, would have been discovered. However, careful research[2] has failed to reveal such variations. Therefore the question of interest is, what forms of w are consistent with a constant value of λ for all preparations? This question may be answered

[2] Rutherford, Wiener Berichte, **120**, 303 (1911); Poole, Phil. Mag. [6] **27**, 714 (1914); Curie, Le Radium **7**, 33 (1910); J. de Physique **10**, 328 (1929); Behounek, J. de Physique **4**, 77 (1923).

partially by reinterpreting the results of Wolfke. We define $p(t-a)dt$ as the fraction of the atoms born between a and $a+da$ which decompose between t and $t+dt$. Whereas Wolfke considers that the life of each atom is well determined as soon as it is born, we make no such assumption. It is immaterial which atoms will decompose in dt; all we wish to know is $p(t-a)$. Assuming that the exponential law is obeyed by the whole preparation, Wolfke's equations show that $p(t-a)=\lambda e^{-\lambda(t-a)}$ and that w is constant. All this is on the assumption that p is at most a function of $t-a$. Apparently no experiments have been performed to show whether the decay constant of an aggregation of radioactive atoms depends on the lives of their ancestors and unborn descendants. The possibility of dependence on the lives of the immediate parents could be tested by using a preparation containing *RaD*, *E* and *F*. *RaE* is removed and for a short interval, I_1, the preparation is allowed to grow another crop of *RaE*. This is quickly removed and is allowed to produce *RaF*, which is removed. A small additional crop of *RaF* is permitted to accumulate in the *RaE* preparation, and is removed during a short interval I_2. This crop of *RaF* consists of atoms having parents which were born in the interval I_1 and which disintegrated in the interval I_2. Investigation of a series of such preparations would show whether λ for *RaF* is a function of the ages of the parent atoms; but this is unnecessary, for we shall now prove by analysis of ordinary half-life experiments that the probability of disintegration per unit time is constant.

II. Generalization of Wolfke's Theorem

The general proof is complicated so we shall present the special case of a series having two unstable members, A and B, and a stable end-product, C. Of the A-atoms born in the interval da, an arbitrary number $f(a)da$ will be included in our preparation. Collection is begun at time a_1 and ceases at time a_2. Of the A-atoms born at time a, a certain fraction $p(a, b, c)db\ dc$ will disintegrate in the interval b to $b+db$, while their daughter B-atoms will give rise to C-atoms in the interval c to $c+dc$. It is assumed that p is a smooth and continuous function of its variables, since otherwise our analysis would fail.

By hypothesis, p depends only on the lives of the A- and B-atoms, so it is of the form $p(b-a, c-b)$. The number of A-atoms in the preparation at time t is

$$N_A(t)=\int_{a=a_1}^{a=a_2}\int_{b=t}^{b=\infty}\int_{c=b}^{c=\infty} f(a)p(b-a, c-b)dc\ db\ da, \quad (2)$$

for this is simply the number whose death occurs after time t.

Let us now form a preparation of B-atoms. The number of A-atoms decaying in the interval db is

$$\int_{a=a_1}^{a=a_2}\int_{c=b}^{c=\infty} f(a)p(b-a, c-b)dc\ da\cdot db,$$

and of these we incorporate the *fraction* $g(b)$ in our B-preparation. The number surviving at time t is

$$\int_{a_1}^{a_2}\int_{t}^{\infty} f(a)g(b)p(b-a, c-b)dc\ da\cdot db,$$

and so if accumulation proceeds from b_1 to b_2, we have

$$N_B(t)=\int_{a_1}^{a_2}\int_{b_1}^{b_2}\int_{t}^{\infty} f(a)g(b)p(b-a, c-b)dc\ db\ da. \quad (3)$$

If $N_B(t)=N_B(0)e^{-\lambda_B t}$ for all such preparations, then

$$\int_{a_1}^{a_2}\int_{b_1}^{b_2}\int_{t}^{\infty} f(a)g(b)p(b-a, c-b)dc\ db\ da$$
$$=e^{-\lambda_B t}\int_{a_1}^{a_2}\int_{b_1}^{b_2}\int_{0}^{\infty} f(a)g(b)p(b-a, c-b)dc\ db\ da. \quad (4)$$

Since $f(a)$ and $g(b)$ are arbitrary,

$$\int_{t}^{\infty} p(b-a, c-b)dc=e^{-\lambda_B t}\int_{0}^{\infty} p(b-a, c-b)dc. \quad (5)$$

This equation represents all we can learn about p by studying B-preparations. Differentiating with respect to t, using (5) and differentiating again, we get a differential equation whose solution is

$$p(b-a, t-b) = F(b-a)e^{-\lambda_B(t-b)}, \quad (6)$$

where $F(b-a)$ is an arbitrary function. Now suppose that $N_A(t) = N_A(0)e^{-\lambda_A t}$, for all A-preparations. An argument similar to that above gives us F, and using the fact that

$$\int_a^\infty \int_b^\infty p(b-a, c-b)dc\, db = 1, \quad (7)$$

we get

$$p(b-a, c-b) = \lambda_A e^{-\lambda_A(b-a)}\lambda_B e^{-\lambda_B(c-b)}. \quad (8)$$

It follows in an elementary way that $w_A = \lambda_A$ and $w_B = \lambda_B$, which are the results desired.

I wish to thank Dr. Morris Muskat for helpful discussion.

Calculation of Characteristic Values for Periodic Potentials

HAROLD D. KOENIG, *University of Michigan*

(Received June 24, 1933)

Section II reviews the general properties of the solutions of differential equations with periodic coefficients, the so-called Hill and Mathieu equations. In Section III asymptotic formulae for the eigenvalues of the Mathieu equation in the oscillatory region (Eq. (9)) are obtained by applying the Schrödinger perturbation theory to the problem of the physical pendulum. Section IV applies the W. K. B. method to the Hill equations. Implicit equations for the eigenvalues are obtained (§9, Eq. (28), (30) §10). They are valid for $E < V_{max}$. In the introduction (Section I) a group of physical problems are mentioned, to which the results may be applied.

I. INTRODUCTION

IN a number of physical problems differential equations with periodic coefficients occur. These include, for instance, the problems of the vibrations of the elliptic membrane (Mathieu's original problem), the diffraction of light around an elliptic cylinder,[1] the variations of the orbit of the moon due to the sun's attraction (Hill's original problem), quantum mechanics of electrons in a crystal,[2] quantum mechanics of the physical pendulum,[3] the rotation of molecules in a crystal,[4] the torsional vibrations of the CH_2 or CH_3 group in the ethylene or ethane molecule.[5]

Unfortunately our knowledge of the Mathieu functions and of the corresponding eigenvalue problem is still rather incomplete, especially on the numerical side, although valuable work in this direction has been done recently by Ince and Goldstein.[6] Some advances can be made, in my opinion, by starting from the physical problems and by the use of the approximation methods suggested by them. So we shall apply in Section III the Schrödinger perturbation theory to the problem of the physical pendulum from the "oscillator" side and obtain certain asymptotic series for the eigenvalues and the Mathieu functions themselves. In Section IV we shall apply the well-known W. K. B. method to a slightly more general problem and obtain asymptotic expressions also for certain Mathieu functions of fractional order.

In Section II we will first give a more qualitative discussion of the properties of the Hill equation, of which the Mathieu equation is a special case. For all details and further developments, especially on the mathematical side, I refer to Whittaker and Watson,[7] Ince[8] and to the recent monograph of M. J. O. Strutt.[9]

II. GENERAL THEOREMS ON THE HILL EQUATION

§1. The Floquet theorem

We will write the Hill equation in the form:

$$d^2y/dx^2+(\lambda-gF(x))y=0, \qquad (1)$$

in which λ and g are constants; $F(x)=F(x+\pi)$ and $F(x)$ is so normalized that:

$$\int_0^\pi F(x)dx=0 \quad |F(x)|\leqq 1. \qquad (2)$$

The Mathieu equation is the special case corresponding to $F(x)=\cos 2x$. The Floquet theorem[10] states that the general solution of (1) is of the form:

$$y=C_1e^{\sigma_1 x}u_1(x)+C_2e^{\sigma_2 x}u_2(x) \qquad (3a)$$

[1] See P. Epstein, Enc. der Math. Wiss. Vol. **5**, p. 507.

[2] F. Bloch, Zeits. f. Physik **52**, 555 (1929). Ph. Morse, Phys. Rev. **35**, 1310 (1930).

[3] E. U. Condon, Phys. Rev. **31**, 891 (1928).

[4] L. Pauling, Phys. Rev. **31**, 430 (1930).

[5] H. Nielsen, Phys. Rev. **40**, 445 (1932).

[6] Ince, Proc. Roy. Soc. Edinburgh **46**, 20, 316 (1926); **47**, 294 (1927). J. London Math. Soc. **2**, 46 (1927). Goldstein, Trans. Camb. Phil. Soc. **23**, 303 (1927).

[7] Whittaker and Watson, *Modern Analysis*, Chapter 19.

[8] Ince, *Differential Equations*.

[9] M. J. O. Strutt, *Lamé sche, Mathieusche und verwandte Funktionen in Physik und Technik*, Springer, Berlin, 1932.

[10] It is analogous to the Bloch theorem in the theory of metals.

or of the form:

$$y=e^{\sigma x}[C_1u_1(x)+C_2\{xu_1(x)+u_2(x)\}]. \quad (3b)$$

In here u_1 and u_2 are periodic in x with the period π; $\pi\sigma_1$ and $\pi\sigma_2$ in (3a) are the logarithms of the roots of a quadratic equation:[11]

$$s^2-2bs+1=0. \quad (4)$$

From this it follows that $\sigma_1=-\sigma_2$ and σ_1, σ_2 are either both real or conjugate complex. Therefore σ_1 and σ_2 can only be either both real or both pure imaginary. Eq. (3b) corresponds to the case that the quadratic Eq. (4) has two equal roots, of which $\pi\sigma$ is then the log. Because the double root of (4) can be only ±1, σ must be either zero or $\pm i$.

§2. Stable and unstable solutions

The σ_1 and σ_2 in (3a) are certain complicated functions of λ and g, the determination of which is the main problem in the theory.

The solutions where the σ are real are called "unstable" solutions because they become infinite with $\pm x$. So if, e.g., y represents the displacement of a body from its orbit and x the time (as in Hill's problem), in such a solution the body would go farther and farther away from its orbit. The solutions where the σ are pure imaginary are called "stable" solutions. They remain oscillatory in infinity.

Because $\sigma=f(\lambda, g)$ we can draw curves in a λ, g diagram on which σ is a constant. One can prove that an infinite set of curves arises for each value of σ. The σ imaginary curves fill regions which we will call the stable regions. The σ real curves fill the rest of the diagram; they give the unstable regions (see Fig. 1). The solutions of type (3b), contain one stable and one unstable solution. They correspond to the curves which separate the stable and unstable regions. Each stable region is bounded by a curve corresponding to $\sigma=0$ and one corresponding to $\sigma=\pm i$. In the case of the Mathieu equation the stable solutions corresponding to these double root values of σ are the Mathieu functions of even ($\sigma=0$) and odd ($\sigma=\pm i$) order. The corresponding solutions of the Hill equation might be called the Hill functions.

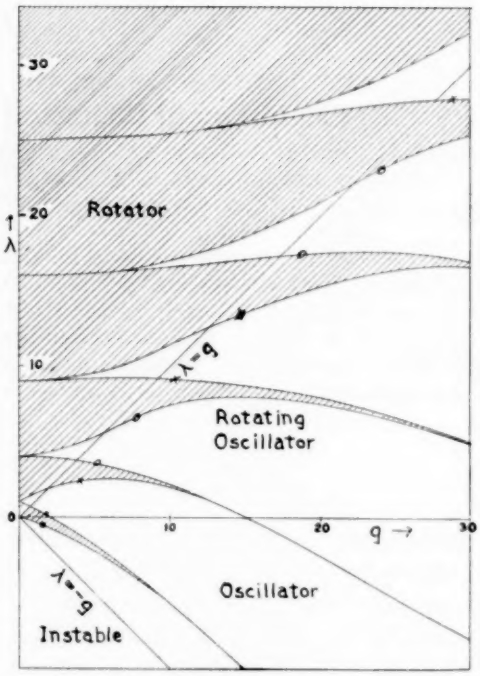

FIG. 1. Plot of regions of stable and unstable solution for $y''+(\lambda+g\cos 2x)y=0$. Regions of stable solution are shaded. Points used to plot curves taken from Strutt's monograph, page 24.

§3. The extreme cases

In Fig. 1 we have four distinct regions: $\lambda<-g$, no stable solutions; $-g<\lambda<0$, almost all points correspond to unstable solutions; $0<\lambda<g$, regions of unstable solutions and regions of stable solutions both present with regions of unstable solution covering greater area; $\lambda>g$, greater part of area covered by regions of stable solutions.

The region $\lambda>g$ is called the rotator side since in a quantum mechanical problem it is the case when the total energy which corresponds to λ is always greater than the potential energy, the maximum value of which is g.[12] The region

[11] The principal values of the log have to be taken. The coefficient b is real. For a proof of these statements see Note 1.

[12] In the quantum theory of metals this region corresponds to the case of nearly free electrons. It seems paradoxical that there are still unstable or "forbidden" regions, although they are narrow. It becomes clear, when one observes that there the de Broglie wave-length fulfills the Bragg total reflection condition.[13]

[13] See further L. Brillouin, *Die Quantenstatistik*, etc., Berlin, Springer, 1931.

$-g<\lambda<0$ is called the oscillator side since, in a quantum mechanical problem, it corresponds to the case when the system oscillates about a potential minimum.[14]

The transition region $0<\lambda<g$ may be called the rotating oscillator region. In here the very broad stable bands of the rotator side go over into the extremely narrow stable regions of the oscillator side.

§4. The proper solutions

The proper solutions are those stable solutions having a preassigned period in x. Since u_1 and u_2 have the period π, the solutions having a period $\nu\pi$ where ν is an integer, are those for which $\sigma=2ri/\nu$ where $|r|$ is any integer $\leqq\nu/2$ or zero.

The problem of finding these proper solutions and the corresponding values of λ (the eigenvalues) as function of g usually arises in quantum mechanics where the potential $V(\theta)$ has a period $2\pi/\nu$ in an angle θ. Then θ and $\theta+2\pi$ correspond to the same position so $\psi(\theta)=\psi(\theta+2\pi)$ if ψ is to be single valued. Then after we transform to x so that $V(x)=V(x+\pi)$ we must have:

$$\psi(x)=\psi(x+\nu\pi).$$

In the following chapters we will only be concerned with these eigenvalue problems. We will distinguish between one, two, three, etc., minima problems according to the value of $\nu(=1, 2, 3,$ etc.). The general character of the eigenvalues in these different cases can be easily seen from the Floquet theorem. Take first $\nu=1$; then r can be only zero and we get, because $\sigma=0$ and we only want the stable solution, the Mathieu or Hill functions of even order. Because the other solution in (3*b*) must be discarded as being unstable, it is clear that the corresponding eigenvalues are not degenerated.[15] They are given by the curves marked with a circle in Fig. 1. For $\nu=2$, $r=0$ or ±1; we get, according to the definition in §2, both the Mathieu or Hill functions of even and odd order; the eigenvalues are again not degenerated. They are represented by the lines marked with either a circle or a cross. The case $\nu=3$ gives something new (see Fig. 2). The value $r=0$ gives again the even order Mathieu functions with non-degenerate eigenvalues; $r=+1$ and $r=-1$ correspond to the two distinct solutions of Eq. (3*a*) with $\sigma_1=2i/3$, $\sigma_2=-2i/3$. The eigenvalues are therefore clearly doubly degenerate. For $\nu=4$ (see Fig. 3), we get the even and odd order Mathieu functions ($r=0$, $r=\pm2$) and a doubly degenerate eigenvalue corresponding to $r=\pm1$.

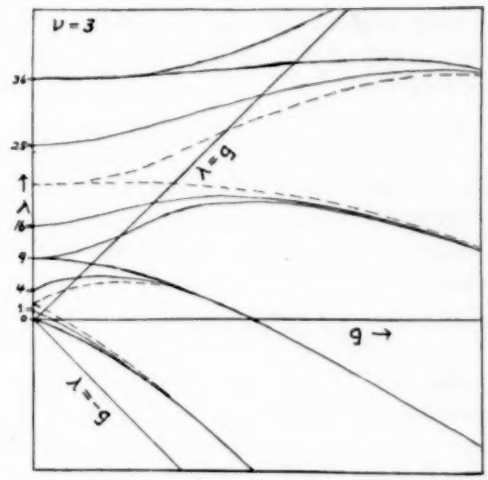

FIG. 2. Eigenvalue curves for a $\nu=3$ problem: $y''+(\lambda+g\cos 2x)y=0$; $y(x)=y(x+3\pi)$. Curves marked = represent eigenvalues degenerate for all values of g. Dotted curves represent the $\sigma=\pm i$ curves and are not eigenvalue curves for this problem.

And so we can go on. In general it is easy to draw qualitatively the eigenvalues as function of g or to connect the eigenvalues at the oscillator

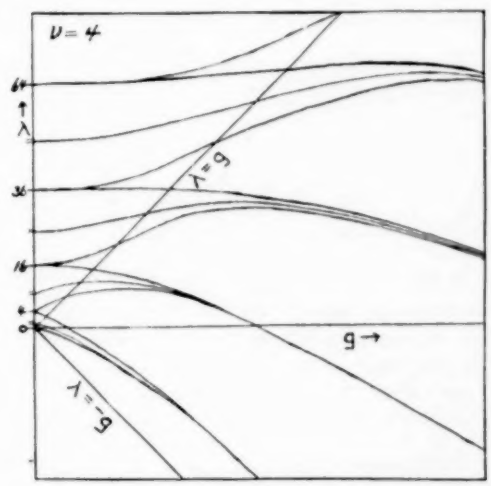

FIG. 3. Eigenvalue curves for a $\nu=4$ problem. Same as in Fig. 2 in all other respects.

[14] In the theory of metals this region corresponds to the case of nearly bound electrons.

[15] Except for certain discrete values of g, where the eigenvalue curves may cross. See Note I.

side with those at the rotator side. In the ν-minima problem for $g=0$, the eigenvalues are given by:

$$\lambda(0)=[n+\tfrac{1}{2}-(-1)^n\tfrac{1}{2}+(-1)^n|i\sigma|]^2 \quad (5a)$$

when σ is again $2ir/\nu$; they are then all doubly degenerate except the lowest. On the extreme oscillator side ($g\to+\infty$), one finds easily (see Section III):

$$\lambda(\infty)+g=4(n+\tfrac{1}{2})g^{\frac{1}{2}}. \quad (5b)$$

The eigenvalues here are ν-fold degenerate. To connect the eigenvalues for one extreme of g to those at the other extreme we need the *oscillation theorem*.[16] This theorem states that the eigenvalues are ordered in such a manner that if λ_m corresponds to a proper solution having m nodes in the interval $0\leq x<\nu\pi$ then $\lambda_m>\lambda_n$ if $m>n$. It is easy to see that the number of nodes m corresponds to the integer n of (5a) and (5b) by:

$$m=\nu[n+\tfrac{1}{2}-(-1)^n\tfrac{1}{2}+(-1)^n|i\sigma|].$$

So the ν lowest levels on the rotator side must join to the lowest ν-fold degenerate level of the oscillator side; the second group of ν rotator levels joins the next oscillator level, etc. This enables us to draw the connecting lines, if one still remembers that all the levels are in the whole range of g doubly degenerated except those corresponding to the even and odd order Hill functions. The curves corresponding to these cannot be drawn without further analysis because, as is remarked in Note I, those with the same n may cross a finite number of times.[17]

III. Perturbation Theory Attack

§5. The quantum theory of the physical pendulum

The Schrödinger equation for a pendulum of length r and having a bob of mass m oscillating in the gravitational field of the earth is:[18]

$$d^2\psi/d\theta^2+(8\pi^2mr^2/h^2)(E-2mgr\sin^2\tfrac{1}{2}\theta)\psi=0, \quad (6)$$

where θ is the angle between the vertical and the string of the pendulum. We introduce the new variables given below and expand the $\sin^2\frac{1}{2}\theta$ term in a power series.

$$x=\tfrac{1}{2}r\theta; \qquad k=4\pi mg^{\frac{1}{2}}/r; \qquad \alpha=32\pi^2mr^2E/h^2; \qquad \mu^2=1/r. \quad (7)$$

The equation now takes a form allowing the Schrödinger perturbation theory to be applied quite readily.

$$d^2\psi/dx^2+[\alpha-2k^2\sum_{i=0}^{\infty}(-\mu)^i(2x)^{2i+2}/(2i+2)!]\psi=0. \quad (8)$$

The perturbation parameter is μ. The zero order equation is then the well-known equation for the harmonic oscillator, with the eigenvalues $\alpha_n{}^0=4k(n+\frac{1}{2})$ and the eigenfunctions:

$$\psi_n{}^0=(2k/\pi)^{1/4}2^{-n/2}(n!)^{-\frac{1}{2}}e^{-kx^2}H_n(x(2k)^{\frac{1}{2}}),$$

where H_n is the nth order Hermite polynomial. Without any trouble one can carry out the perturbation calculation to the second order in the eigenfunction and to the third order in α.[19] The

[16] Ince, *Ordinary Differential* equation, p. 246. This question of connection was considered by Nielsen (reference 5) where one finds a figure in the case $\nu=6$.

[17] For an example where they cross once, see Strutt, reference 9, Fig. 3. In the case of the Mathieu functions (Fig. 2) they don't cross at all.

[18] A more likely problem is a dipole oscillating in a plane in a homogeneous electric field.

[19] The matrix elements involved in the perturbation formulae can all be obtained with the help of the integrals:

$$\int_{-\infty}^{+\infty}x^{2p}e^{-x^2}H_n(x)H_m(x)dx=\sum_{j=0}^{p-(m+n)/2}\binom{2p}{2j}\binom{2p-2j}{p-j+(m+n)/2}\frac{2^{(m+n)/2+j-p}}{((m+n)/2+j-p)!}\Gamma(j+\tfrac{1}{2}),$$

where $m+n$ must be even. If $m+n$ is odd the integral vanishes.

results are given below:

$$\alpha_n = \sum_0^\infty \alpha_n{}^j \mu^j$$

$$\alpha_n{}^0 = 4(n+\tfrac{1}{2})k,$$

$$\alpha_n{}' = -\tfrac{1}{4}(2n^2+n+1),$$

$$\alpha_n{}^2 = -\frac{1}{4k}\frac{1}{4!}(6n^3+9n^2+9n+3),$$

$$\alpha_n{}^3 = -\frac{3}{4k^2}\left(\frac{1}{4!}\right)^3 \frac{1}{5!}(3600n^5+68611n^4+276241n^3+304691n^2+281690n+61480).$$

The coefficients in the development of the perturbed eigenfunctions in terms of $\psi_n{}^0$, i.e., the coefficients $d_{nm}{}^j$ in:

$$\psi_n = \sum_{j=0}^\infty \mu^j \psi_n{}^j; \qquad \psi_n{}^j = \sum_{m=0}^\infty d_{nm}{}^j \psi_m{}^0$$

have also been calculated, at least for $j=1$ and 2. Because they take up much space and because they will not be used later, we will not reproduce them here. The writer will be glad, though, to communicate the results by letter to anybody who is interested in them.

§6. Discussion

For small values of μ or large values of k the above formulae are very convenient for the numerical calculation of the eigenvalues. For the first three eigenvalues we have:

$$\alpha_0/k = 2-0.25\rho-0.0312^5\rho^2-0.0278^+\rho^3-\cdots,$$

$$\alpha_1/k = 6-1.25\rho-0.2813^-\rho^2-0.4602^-\rho^3-\cdots, \quad (9)$$

$$\alpha_2/k = 10-2.75\rho-1.0938^-\rho^2-2.3761^+\rho^3-\cdots,$$

where $\rho=\mu/k$. To compare these results with the exact calculations of Goldstein we must first transform (8) to the standard form

$$d^2\psi/dx^2+(4a+16q\cos 2x)\psi=0, \qquad (10)$$

so that

$$4a\rho^2 = 4+\alpha\rho/k, \qquad (11a)$$

$$8q = 1/\rho^2. \qquad (11b)$$

For the comparison see Table I. The first column gives q, which determines ρ. From (9) one then calculates α_n/k, which, substituted in (11a), gives our value of a tabulated in column 2. The third column gives the exact values of a according to Goldstein and his symbols for the eigenfunctions, the even order Mathieu functions. We see that if q is large enough the error is very small.

TABLE I.

q	$1/\rho$	Our $-a$	Goldstein $-a$	Function
2	4	6.065	6.065	$n=0$
3	4.898	9.615	9.615	Ce_0
2	4	2.3373	2.3326	$n=1$
3	4.898	4.9593	4.9791	
4	5.656	7.8450	7.8385	Se_2
5	6.325	10.839	10.838	
5	6.325	5.183	5.110	$n=2$
10	8.942	18.371	18.481	
20	12.65	49.087	49.382	Ce_2
40	17.94	115.854	116.202	
100	28.28	329.972	330.137	

One must not expect that taking the higher order perturbations into account will always improve the result. It is fairly certain that (9) are not convergent but asymptotic developments of the eigenvalues in the extreme oscillator side. Even should the series for α_n and ψ_n converge, one cannot be sure that they would converge to the required solution because one does not take the periodicity condition into account. For this reason one must expect that the series for $\psi_n(x)$ represents the even order Mathieu function fairly well only for $-\pi<x\mu^{\frac{1}{2}}<+\pi$. For values of x outside this region we may continue the solution periodically. Furthermore one sees from Fig. 1 that on the extreme oscillator side the

stable regions are extremely narrow so that one may expect that the series (9) will also represent the eigenvalues of all other stable solutions to within their inherent error. In Section IV we will calculate these extremely small splittings.

IV. The W.K.B. Solution

§7. Introduction

We will treat in this chapter the ν-minima problem with the well-known W.K.B. method. The physical problem which it may represent is, e.g., the quantum theory of a wheel (symbolizing a molecule or a radical like CH_2) of 2ν spokes of equal length. The wheel is rotating about a fixed axis and the ends of neighboring spokes carry opposite but equal charges. The wheel is placed in an inhomogeneous electric field (symbolizing the crystal or interatomic forces). The Schrödinger equation would be:

$$d^2\psi/d\theta^2+(8\pi^2I/h^2)(E-V(\theta))\psi=0 \tag{12}$$

where $V(\theta)=V(\theta+2\pi/\nu)$ and we will suppose that $V(\theta)$ has in each period $2\pi/\nu$ one maximum and one minimum and is even around each of them. We measure θ from one of these minima and take θ increasing counterclockwise. We choose the zero energy so that

$$\int_0^{2\pi} V(\theta)d\theta=0.$$

To apply the W.K.B. method we must distinguish between the classical and non-classical regions. The 2ν roots of $E-V(\theta)=0$ are:

$$\theta_i=-a+2(i-1)\pi/\nu, \qquad \theta_i'=+a+2(i-1)\pi/\nu, \tag{13}$$

where a is the first positive root. The region between θ_i and θ_i' will be called the ith classical region $(E-V>0)$ and the region $\theta_i'<\theta<\theta_{i+1}$, the ith non-classical region $(E-V<0)$.

In each classical region the solution of (12) will be oscillatory and be given by:

$$\psi_i=C_ip^{-\frac{1}{2}}\cos\left((2\pi/h)\int_{b_i}^{\theta}pd\theta+\delta_i\right), \tag{14}$$

where b_i abbreviates $2(i-1)\pi/\nu$ and p is the angular momentum $[2I(E-V)]^{\frac{1}{2}}$. In each non-classical region the solution of (12) will consist of a decreasing and an increasing exponential:

$$\psi_i'=A_i\bar{p}^{-\frac{1}{2}}\exp\left((2\pi/h)\int_{b_i'}^{\theta}\bar{p}d\theta\right)+B_i\bar{p}^{-\frac{1}{2}}\exp\left(-(2\pi/h)\int_{b_i'}^{\theta}\bar{p}d\theta\right), \tag{15}$$

where

$$b_i'=2(i-\tfrac{1}{2})\pi/\nu, \qquad \bar{p}=[2I(V-E)]^{\frac{1}{2}}.$$

§8. Application of the connection formulae and of the periodicity condition

The relations between the constants A_i, B_i, C_i and δ_i are determined by the connection formulae of Kramers.[20] Applying these to extend the solution in the ith non-classical region to the ith classical

[20] H. A. Kramers, Zeits. f. Physik **39**, 828 (1926); H. A. Kramers and G. P. Ittmann, Zeits. f. Physik **58**, 217 (1929); A. Zwaan, Diss. Utrecht (1929). These formulae are collected in a paper by L. A. Young and G. E. Uhlenbeck, Phys. Rev. **36**, 1154 (1930). For the application of the method to the two identical minima problem see D. M. Dennison and G. E. Uhlenbeck, Phys. Rev. **41**, 313 (1932) and to the problem of two unequal minima, Ta-You Wu, Phys. Rev. in press. From the standpoint of these papers I treat the case of an infinite number of identical minima, where one requires periodic solutions. This problem has also been considered by M. J. O. Strutt (Math. Ann. **101**, 559 (1929) using an analogous method with incorrect connection formulae.

region and requiring the result to be identical with (14) we obtain:

$$A_i = C_i\beta \cos(\gamma/2+\delta_i+\pi/4), \qquad B_i = (C_i/2\beta)\sin(\gamma/2+\delta_i+\pi/4), \tag{16}$$

where:

$$\beta = \exp\left((2\pi/h)\int_{b_i'}^{\theta_{i+1}} \bar{p}d\theta\right) = \exp\left((\pi/h)\int_{\theta_i'}^{\theta_2} \bar{p}d\theta\right), \tag{17}$$

$$\gamma = (2\pi/h)\int_{\theta_i}^{\theta_i'} pd\theta = (2\pi/h)\int_{\theta_1}^{\theta_i'} pd\theta. \tag{18}$$

We extend the solution in the ith non-classical region to the succeeding $(i+1)$th classical region in the same manner and obtain:

$$A_i = (C_{i+1}/2\beta)\sin(\gamma/2-\delta_{i+1}+\pi/4), \qquad B_i = \beta C_{i+1}\cos(\gamma/2-\delta_{i+1}+\pi/4). \tag{19}$$

Eqs. (16) and (19) immediately lead to a recurrence relation between the phases δ_i:

$$2\beta^2 \cot(\gamma/2+\delta_i+\pi/4) = (1/2\beta^2)\,\mathrm{tg}(\gamma/2-\delta_{i+1}+\pi/4) \tag{20}$$

and to a set of linear homogeneous equations for the amplitudes C_i [21]

$$C_i\beta\cos(\gamma/2+\delta_i+\pi/4) = (C_{i+1}/2\beta)\sin(\gamma/2-\delta_{i+1}+\pi/4). \tag{21}$$

Since ψ must have the period 2π, we must require:

$$\delta_i = \delta_{i+\nu}, \qquad C_i = C_{i+\nu}. \tag{22}$$

Therefore (21) are ν homogeneous linear equations in the ν unknowns C_i. In order that the solution be not identical zero, the determinant of the coefficients must vanish giving:

$$\beta^\nu \prod_{k=1}^{\nu} \cos(\gamma/2+\delta_k+\pi/4) = (2\beta)^{-\nu} \prod_{k=1}^{\nu} \sin(\gamma/2-\delta_k+\pi/4). \tag{23}$$

At least one of the C_i will now be arbitrary, which is just what one needs to normalize the solution. From (20) and (23) the simpler form follows:

$$\prod_{k=1}^{\nu} \cos(\gamma+2\delta_k) = \prod_{k=i}^{\nu} \cos(\gamma-2\delta_k). \tag{24}$$

Because of (22) Eqs. (20) and (24) become $\nu+1$ equations for the ν δ_i and γ, which may be solved for γ in terms of β and integers (the quantum numbers) only. Since, if $V(\theta)$ is given, γ and β depend on E only, this will give an implicit equation for the eigenvalues of E.

§9. Solution in special cases

This solution of (20) and (24) for small values of ν is given below. Introducing the abbreviations:

$$\varphi_1 = 2\tan^{-1}(1/2\beta^2), \qquad \varphi_2 = 2\tan^{-1}\left[2\beta^2/1+4\beta^4+(1+4\beta^4+16\beta^8)^{\frac{1}{2}}\right]$$

we obtain:

$\nu=1$: $\gamma = (n+\frac{1}{2})\pi-(-1)^n\varphi_1$; $\quad 4\delta_1 = \pi-(-1)^n\pi$, (a)

$\nu=2$: $\gamma = (n+\frac{1}{2})\pi\pm\varphi_1$; $\quad 4\delta_1 = -4\delta_2 = \pi-(-1)^n\pi$, (b)

$\nu=3$: $\gamma = (n+\frac{1}{2})\pi-(-1)^n\varphi_1$; $\quad 4\delta_1 = 4\delta_2 = 4\delta_3 = \pi-(-1)^n\pi$, (a)

$\gamma = (n+\frac{1}{2})\pi+(-1)^n\varphi_2$; $\quad 4\delta_1 = \pi\mp(-1)^n\pi$, $\delta_2 = -\delta_3 = \pm\frac{1}{2}(-1)^n\varphi_2$, (c)

[21] They arise from equating the first relations (16) and (19). Equating the second relations will give the same set of linear equations because of (20).

$\nu=4$: $\gamma=(n+\frac{1}{2})\pi\pm\varphi_1$; $4\delta_1=-4\delta_2=4\delta_3=-4\delta_4=\pi-(-1)^n\pi$, (b)

$\gamma=(n+\frac{1}{2})\pi$; $\delta_1=\delta_3=0,\ \pi/2$; $\delta_2=\delta_4=\delta_1+\pi/2$, (c)

$\nu=6$: $\gamma=(n+\frac{1}{2})\pi\pm\varphi_1$; $4\delta_1=-4\delta_2=+4\delta_3=-4\delta_4=4\delta_5=-4\delta_6=\pi-(-1)^n\pi$, (b)

$\gamma=(n+\frac{1}{2})\pi+(-1)^n\varphi_2$; $4\delta_1=4\delta_4=\pi\mp(-1)^n\pi$; $\delta_2=-\delta_3=\delta_5=-\delta_6=\pm(-1)^n\frac{1}{2}\varphi_2$, (c)

$\gamma=(n+\frac{1}{2})\pi-(-1)^n\varphi_2$; $4\delta_1=4\delta_4=\pi\pm(-1)^n\pi$; $\delta_2=-\delta_3=\delta_5=-\delta_6=\mp(-1)^n\frac{1}{2}\varphi_2$. (c)

The equations marked (*a*) correspond to the even order Hill functions, those marked (*b*) to the Hill functions of both orders, those marked (*c*) to the doubly degenerate solutions (see Figs. 2 and 3, Section II).

TABLE II. *Splitting of first three eigenvalues for* $\nu=4$, $V(\theta)=-g\cos 4\theta$.

n	q	a'_1	a'_2	a'_3	n	q	a'_1	a'_2	a'_3
0	1	10.49	10.75	11.01	2	3	78.64	80.93	83.05
	2	15.26	15.27	15.28		5	112.03	112.65	113.27
	3	17.79	17.80	17.81		8	146.48	146.52	146.56
1	2	42.19	43.63	44.97	3	5	143.47	147.48	152.25
	3	51.26	52.15	53.04		8	194.43	194.96	195.49
	5	72.17	72.17	72.17		12.5	251.72	251.76	251.80

Table II shows the splitting of the first three eigenvalues in the case $\nu=4$, $V(\theta)=-g\cos 4\theta$. We set:

$$16q=8\pi^2Ig/h^2 \quad \text{and} \quad a'=8\pi^2I(E+g)/h^2$$

to approach the standard form (10). The a' is connected with the a of (10) by:

$$a=a'-4q.$$

The middle column gives the doubly degenerate eigenvalues (see Fig. 3).

§10. The general solution

We wish to correlate our W.K.B. solution with the Floquet theorem. To obtain the same notation as in Section II we introduce the variable $x=\nu\theta/2$, so that $V(x)=V(x+\pi)$ and $\psi(x)=\psi(x+\nu\pi)$. As in the proof of the Floquet theorem (see Note I) we will start with a fundamental set of W.K.B. solutions $y_1(x)$ and $y_2(x)$. For y_1 we choose the solution for which the phase δ_1 in the first classical region is zero and which is then extended over the whole region without regard for the periodicity condition. For y_2 we choose the analogous solution with $\delta_1=\pi/2$. With the help of the connection formulae (20) and (21) we can write the characteristic equation analogous to (4) immediately:

$$s^2-2bs+c=0, \tag{25}$$

where now

$$2b=-(1/2\beta^2)(1+4\beta^4)\sin(\gamma+\pi/2), \tag{26}$$

$$c=[1+32\beta^8/[(1+16\beta^8)^2+64\beta^4\csc^2(\gamma+\pi/2)]]^{\frac{1}{2}}. \tag{27}$$

One sees that, in contrast to the case where one starts with two exact solutions, the coefficient c is now not unity. However, since β is always >1, c is always nearly one ($1<c<1.04$). The difference is clearly due to our approximations. In the following we will take $c=1$. Calling the log of the roots of (25) again $\pi\sigma_1$ and $\pi\sigma_2$ we have then $\sigma_1=-\sigma_2=\sigma$ and from (26) follows:

$$\sin(\gamma+\pi/2)=-4\beta^2/(4\beta^4+1)\cos i\sigma\pi=\operatorname{sech}D\cos i\sigma\pi, \tag{28}$$

where

$$D=\log 2\beta^2=\frac{\pi\nu}{h}\int_{x_1'}^{x_2}\bar{p}dx+\log 2. \tag{29}$$

For the proper solutions we must take $\sigma = 2ri/\nu$, $|r| \leq \nu/2$ or zero and then (28) is an implicit equation for E.[22] Comparing these results with the exact solution in the case of the Mathieu equation one finds that (28) gives too wide stable regions if E is near $V_{\max}$. We can still improve the result (28) in the following manner. From (28) follows

$$\gamma = (n+\tfrac{1}{2})\pi - (-1)^n \sin^{-1}(\operatorname{sech} D \cos i\sigma\pi).$$

Now if β is large, sech D is very small and we may put the $\sin^{-1}$ equal to its argument. So

$$\gamma = (n+\tfrac{1}{2})\pi - (-1)^n \operatorname{sech} D \cos i\sigma\pi. \tag{30}$$

If we now use (30) for all values of D, we get considerable better results for E near $V_{\max}$, i.e., $D \geqq \log 2$. Furthermore, (30) exhibits for E near $V_{\max}$ the so-called quarter quantization of Kramers and Ittmann (reference 16), which must be expected.[23]

The author wishes to acknowledge his indebtedness to Professor Otto Laporte of the University of Michigan who suggested the problem and to Professor G. E. Uhlenbeck whose advice was of great value in carrying the work to a successful conclusion.

Note I.

Because most books do not contain the complete proof of the Floquet theorem we will give it here.

Let $y_1(x)$, $y_2(x)$ be a set of fundamental solutions of (1). Then because (1) is invariant under the transformation $x' = x+\pi$, $y_1(x+\pi)$ and $y_2(x+\pi)$ will also be solutions of (1). We must have therefore:[24]

$$\begin{aligned} y_1(x+\pi) &= d_{11}y_1(x) + d_{12}y_2(x), \\ y_2(x+\pi) &= d_{21}y_1(x) + d_{22}y_2(x). \end{aligned} \tag{α}$$

We wish now to find a solution $y = c_1y_1 + c_2y_2$ so that $y(x+\pi) = sy(x)$. Using (α) we find that c_1, c_2 must fulfill the equations:

$$\begin{aligned} c_1(s-d_{11}) + c_2d_{12} &= 0, \\ c_1d_{21} + c_2(s-d_{22}) &= 0. \end{aligned} \tag{β}$$

The necessary and sufficient condition that (β) has at least one solution is:

$$\begin{vmatrix} s-d_{11} & d_{12} \\ d_{21} & s-d_{22} \end{vmatrix} = 0.$$

One proves easily that:

$$d_{11}d_{22} - d_{12}d_{21} = \Delta(\pi)/\Delta(0) = 1,$$

when $\Delta(x) = y_1y_2' - y_2y_1'$ is the Wronskian, which is a constant as a consequence of (1). We get therefore for s the quadratic equation (Eq. (4) of Section II)

$$s^2 - (d_{11}+d_{22})s + 1 = 0. \tag{γ}$$

There are two main cases:

a. (γ) has two single roots. We can then find two of the required solutions $y(x)$ and this leads to (3a).

b. (γ) has one double root, which must be ± 1. Supposing d_{12} and d_{21} not both zero, we can then find only one set of c_i, i.e., one required solution $\bar{y}(x)$. To find the second solution substitute $y = x\bar{y} + z$. We find for z:

$$z'' + (\lambda - gF(x))z = -2d\bar{y}/dx. \tag{δ}$$

$\bar{y}$ has the period $\pi(s=+1)$ or $2\pi(s=-1)$. The homogeneous part of (δ) has $\bar{y}$ as the only periodic solution. We will be able to find a solution of (δ) with period π or 2π if and only if $\bar{y}$ is orthogonal to the right-hand side, which is obvious. So we are led to (3b).

There remains the possibility that d_{12} and d_{21} are both zero. Then the c_i are arbitrary and all solutions are periodic with period π or 2π. We get again (3a) but with $\sigma_1 = \sigma_2 = 0$ or $\pm i$, so that both solutions are stable. One can prove that this can only occur for discrete values of g. They are the points where the eigenvalue curves for the Hill functions may cross (see §4).

---

[22] Strutt (reference 16) obtains by his method the equation which would result if one omits the log 2 in the definition of D. That this cannot be correct follows immediately from the fact that then for $E = V_{\max}$ all solutions would be stable, contrary to the known results (see Fig. 1; $E = V_{\max}$ corresponds to $\lambda = g$).

[23] Quarter quantization is to be expected for the limits of the stable regions if E is near $V_{\max}$. Then $\sigma = 0, \pm i$, and sech $D \leqq 0.8 \leqq \frac{1}{4}\pi$ so that (30) goes over in: $\gamma = (n+\frac{1}{2})\pi \pm \frac{1}{4}\pi$.

[24] The y_1, y_2 may be chosen real and then the d_{ij} will also be real.

The Energy Levels of the Rare-Gas Configurations*

GEORGE H. SHORTLEY, *Palmer Physical Laboratory, Princeton University*

(Received August 4, 1933)

The secular equations expressing the electrostatic and spin-orbit interactions of the configurations p^5p and p^5d are found to be very conveniently handled if one neglects the interaction between levels which have different levels of the ionic doublet as parents, an approximation significant for all but the lowest p^5p's of neon and argon. The 10 levels of p^5p and the 12 of p^5d are each expressed in terms of six parameters, one of which corresponds directly to the ionic doublet splitting. It is found that the higher members of the p^5p series in neon and argon, the lowest configurations of this type in krypton and xenon, and all eight members of the neon p^5d series agree with these formulas to within the magnitude of the above-mentioned neglected interaction (which becomes relatively very small for the higher series members) in all cases where two configurations do not obviously strongly perturb each other. Because of the generally very weak interaction between configurations in these spectra, better agreement between theory and observed data is found than has been the case for any other atoms. This calculation gives the eigenstates for these configurations exact specification in the *jj*-coupling scheme.

THE structure of the rare-gas spectra is recalled by Fig. 1, which is a plot of the energy levels of neon I, the most completely analyzed of these spectra, as given by Bacher and Goudsmit. All known levels of the rare gases are included in the systems $n'p^5nl$ where $n'=2, 3, \cdots$ for neon, argon, $\cdots$. This makes these spectra remarkably clean, almost as clean as one-electron doublet spectra. As seen in Fig. 1, the configurations of each series rapidly divide, with increasing n, into two groups of levels. The upper of these groups approaches the $^2P_{1/2}$ limit of the ion, the lower the $^2P_{3/2}$ limit. For p^5s the upper and lower groups each consist of two levels, and for neon this configuration is completely known up to $2p^511s$. For p^5p the upper group consists of four levels and the lower of six; this configuration is completely known in neon up to $2p^57p$. For $l>1$, the upper group consists of four levels and the lower of eight; the $2p^5nd$ of neon are completely analyzed up to $n=10$, while only two levels of the lowest p^5f are found.

The configuration p^5s has been considered in detail by Laporte and Inglis and by Condon and Shortley,[1] who used the formulas[2] derived by Houston for the configuration sp. We shall here consider the configurations p^5p and p^5d.

The configuration $n'p^5np$

The configuration p^5p contains 1 level with $J=3$, 3 with $J=2$, 4 with $J=1$, and 2 with $J=0$. Hence the diagonalization of the Hamiltonian for this configuration involves the solution of a linear, a quadratic, a cubic, and a quartic equation. These equations contain as parameters six radial integrals. Given the values of these parameters, the solution of these equations is rather complicated; to obtain the values of these parameters from the observed energies and then check the self-consistency of the equations, as we propose to do, is much more complicated. A simplification valid in many cases can, however, be made. Just as our consideration of one configuration at a time is an approximation in which we neglect the interaction between configurations, so we may use an approximation in which we also neglect the interaction between the groups of levels of the same configuration which

* Presented at the Washington Meeting of the American Physical Society, April 28, 1933.

[1] Laporte and Inglis, Phys. Rev. **35**, 1337 (1930); Condon and Shortley, Phys. Rev. **35**, 1342 (1930).

[2] That these formulas are applicable with change of sign of the spin-orbit parameter and hence of Houston's X is readily shown from previous results [Shortley, Phys. Rev. **40**, 185 (1932)]. That X was found to be negative in these comparisons then shows that the electrostatic integral $G_0(sp)$ is positive, as is perhaps to be expected [cf. Bacher, Phys. Rev. **43**, 264 (1933)].

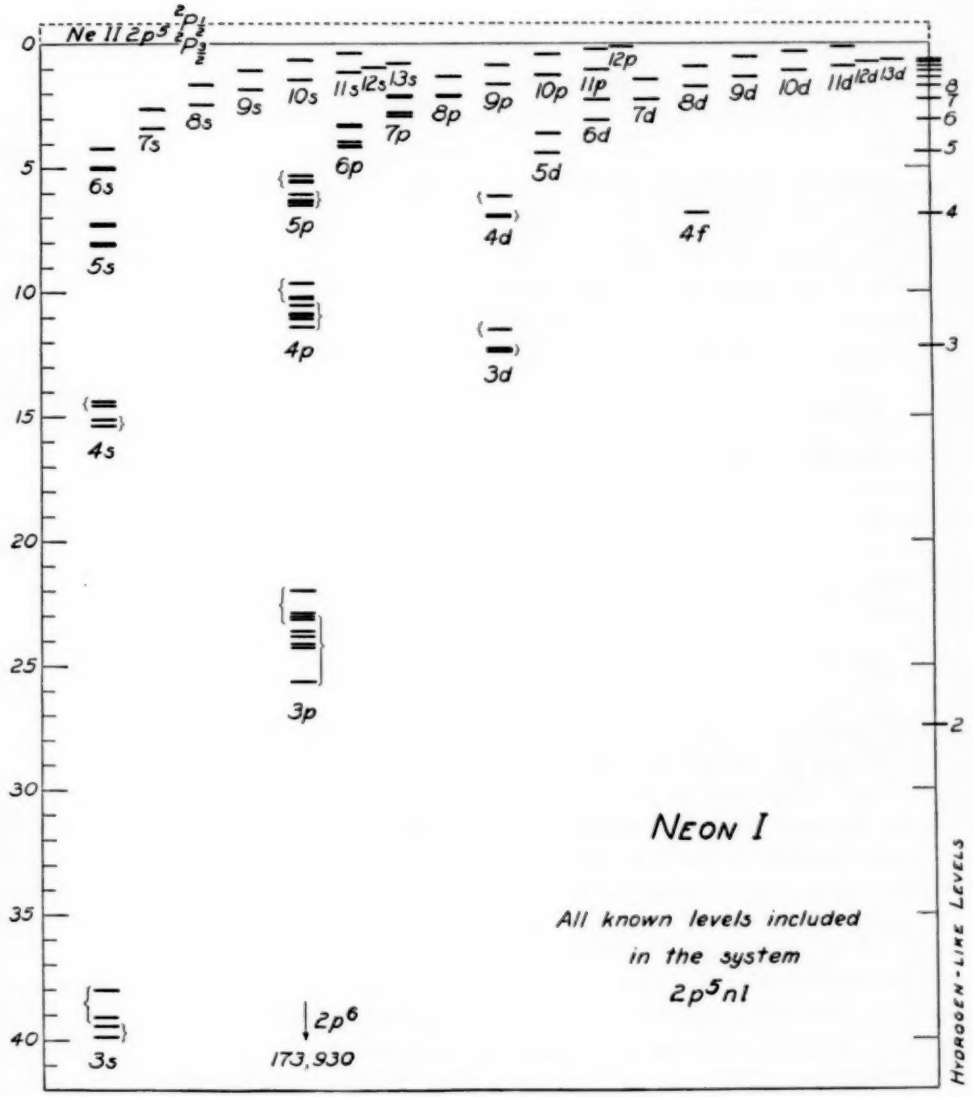

FIG. 1. Scale in thousands of cm^{-1}. Each line represents in general a group of observed levels not "resolved" on this scale.

have different levels of the ionic doublet as parents. This latter approximation is expected (cf. Fig. 1) to be increasingly good as we go up the series of configurations.

Now the quantum number which distinguishes levels belonging to one parent from those belonging to the other is the j value of the p^5 group, which is also the j value of the missing electron.[3] Hence in order to split the secular equation according to parentage, it is necessary to obtain the matrix of the Hamiltonian in the jj-coupling scheme.

The matrix of spin-orbit interaction is diagonal in jj coupling, the diagonal element having the

[3] Cf. §2 of Shortley, Phys. Rev. **43**, 451 (1933).

value

$$(A\,|\,V^1\,|\,A)=\sum_i \zeta_{nl}\,l^i\cdot\tfrac{1}{2}\{j^i(j^i+1)-l^i(l^i+1)-s^i(s^i+1)\}, \quad (1)$$

where the summation is taken over all electrons in the configuration.[4] This element is independent of the J and M_J values of the state A. The matrix for $n'p^5np$ is the same as that for $n'pnp$ with reversed sign of $\zeta'=\zeta_{n'p}$. The values of the elements are

$$\begin{array}{lll} & n'p^5np & \\ a & (\tfrac{3}{2},\tfrac{3}{2}): & -\tfrac{1}{2}\zeta'+\tfrac{1}{2}\zeta \\ b & (\tfrac{3}{2},\tfrac{1}{2}): & -\tfrac{1}{2}\zeta'-\zeta \\ c & (\tfrac{1}{2},\tfrac{3}{2}): & \zeta'+\tfrac{1}{2}\zeta \\ d & (\tfrac{1}{2},\tfrac{1}{2}): & \zeta'-\zeta. \end{array} \quad (2)$$

In the parentheses are given the j values first of the p^5 core and then of the added p electron. The letters a, b, c, d are introduced as a convenient abbreviation for the four possible combinations of j values. States labeled by a and b belong to the lower doublet level, states labeled by c and d to the higher doublet level of the ion.

The matrix of electrostatic interaction is diagonal in LS coupling; the diagonal elements are given on page 193 of reference 4. With the transformation of reference 3 this matrix is found in jj coupling to have the value

$-F_0+$

	3a
3a	$-F_2$

	2a	2b	2c
2a	$3F_2+4G_2$	$-2F_2+4G_2$	$2F_2-4G_2$
2b	$-2F_2+4G_2$	$4G_2$	$-F_2-4G_2$
2c	$2F_2-4G_2$	$-F_2-4G_2$	$4G_2$

	1a	1b	1c	1d
1a	$-F_2$	$2\cdot5^{\frac{1}{2}}F_2$	$-2\cdot5^{\frac{1}{2}}F_2$	$10^{\frac{1}{2}}F_2$
1b	$2\cdot5^{\frac{1}{2}}F_2$	0	$5F_2$	0
1c	$-2\cdot5^{\frac{1}{2}}F_2$	$5F_2$	0	0
1d	$10^{\frac{1}{2}}F_2$	0	0	0

	0a	0d
0a	$-5F_2+4G_0$	$-5\cdot2^{\frac{1}{2}}F_2+2\cdot2^{\frac{1}{2}}G_0$
0d	$-5\cdot2^{\frac{1}{2}}F_2+2\cdot2^{\frac{1}{2}}G_0$	$2G_0$

. . . . . (3)

In the notation here used the J value is given as an arabic numeral, followed by a letter which specifies the electronic j values according to the scheme (2). The matrices are independent of the value of M_J.

Adding the spin-orbit interaction (2) and splitting these matrices according to the parent j values as indicated by the broken lines, we obtain the following equations for the energy levels:

Upper levels

$$\begin{array}{lll} (2c) = -F_0+ & \zeta'+\tfrac{1}{2}\zeta & +4G_2 \\ (1c) = -F_0+ & \zeta'+\tfrac{1}{2}\zeta & \\ (1d) = -F_0+ & \zeta'-\zeta & \\ (0d) = -F_0+ & \zeta'-\zeta & +2G_0 \end{array} \quad (4)$$

[4] Notation as in §5 of Shortley, Phys. Rev. **40**, 185 (1932).

Lower levels

$$
\begin{aligned}
(3a) &= -F_0 - \tfrac{1}{2}\zeta' + \tfrac{1}{2}\zeta - \quad F_2 \\
\left.\begin{matrix} 2a' \\ 2b' \end{matrix}\right\} &= -F_0 - \tfrac{1}{2}\zeta' - \tfrac{1}{4}\zeta + \tfrac{3}{2}F_2 \qquad +4G_2 \pm [(\tfrac{3}{4}\zeta + \tfrac{3}{2}F_2)^2 + (2F_2 - 4G_2)^2]^{\frac{1}{2}} \\
\left.\begin{matrix} 1a' \\ 1b' \end{matrix}\right\} &= -F_0 - \tfrac{1}{2}\zeta' - \tfrac{1}{4}\zeta - \tfrac{1}{2}F_2 \qquad \pm [(\tfrac{3}{4}\zeta - \tfrac{1}{2}F_2)^2 + 20F_2^2]^{\frac{1}{2}} \\
(0a) &= -F_0 - \tfrac{1}{2}\zeta' + \tfrac{1}{2}\zeta - 5F_2 \qquad +4G_0.
\end{aligned}
\tag{4 cont.}
$$

The six unprimed levels of this group belong in our approximation rigorously to the quantum numbers assigned to them. The eigenstates for the primed levels are linear combinations of those for the corresponding unprimed levels. We arbitrarily denote the higher of the two levels by a' and the lower by b' since the level a would lie above the level b if the electrostatic interaction vanished.

Now the value of one of the parameters, ζ', should in all cases in which our approximation is good be obtainable from the splitting of the parent doublet, which is just $\frac{3}{2}\zeta'$. But this splitting is known from the spectra of the ions only to an accuracy of one wave number. Hence we prefer to determine this parameter, along with the rest, from the data for each configuration, and then to check it against the doublet splitting of the ion later.

The six linear expressions in (4) should determine the six parameters. From the values of the parameters we could then predict absolute positions of the other four levels. However, in order to make the values of the parameters less sensitive to the small perturbations which must exist both between the two parts of one configuration and between neighboring configurations, we prefer to fit by least squares the eight quantities obtained by adding to the above six levels the means of $2a'$ and $2b'$ and of $1a'$ and $1b'$. *This leaves the separations* $2a'-2b'$ *and* $1a'-1b'$ *to be absolutely predicted.*

The results of such a calculation are shown in Fig. 2 for neon, Fig. 3 for argon, and Fig. 4 for krypton and xenon. In these figures the empirical value for $1b'$ has been taken as the zero for each configuration; a break in the wave-number scale indicates the separation between the two groups of levels.

The first question one asks concerns the validity of the neglect of interaction between the two groups of levels. If the parameters we have obtained are approximately correct, the magnitude of this interaction may be found by using the interaction elements of the matrices (3) according to the second-order perturbation theory. In this way the *largest* interaction was found to have approximately the value represented by the length of the short black bar drawn underneath each configuration. This gives an idea of the agreement to be expected in the comparison.

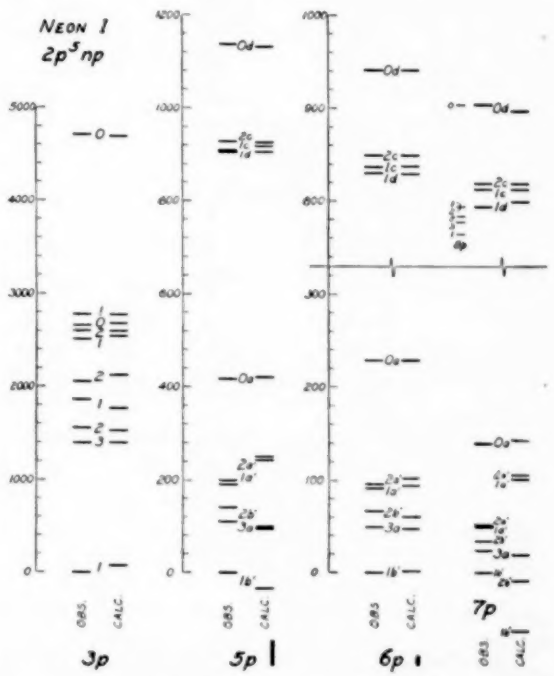

FIG. 2. (The lengths of the black bars represent the maximum interaction between the two groups of levels in each configuration.)

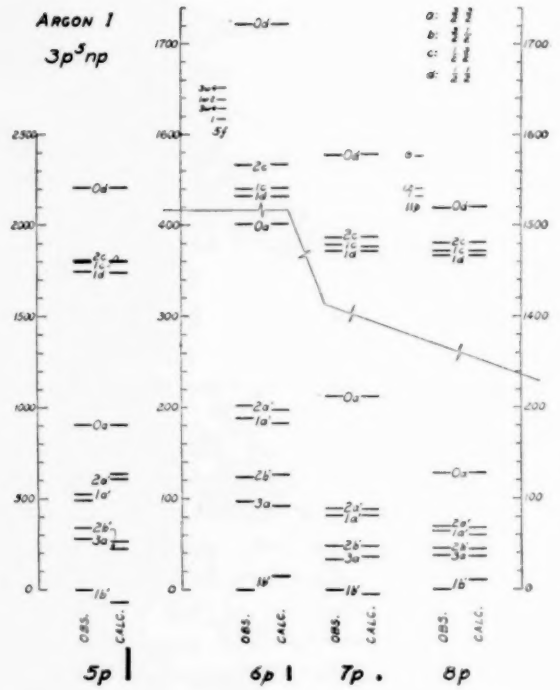

FIG. 3. (The lengths of the black bars represent the maximum interaction between the two groups of levels in each configuration.)

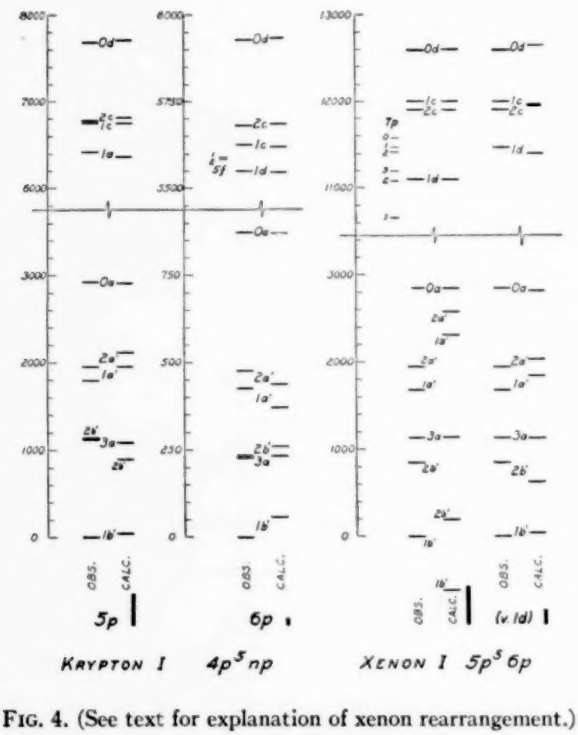

FIG. 4. (See text for explanation of xenon rearrangement.)

Having obtained the values of the parameters, one can readily find the coefficients in the expansion

$$\psi(Ja')=\psi(Ja)(Ja|Ja')+\psi(Jb)(Jb|Ja'),$$
$$\psi(Jb')=\psi(Ja)(Ja|Jb')+\psi(Jb)(Jb|Jb'). \quad (5)$$

Since $|(a|a')|^2=|(b|b')|^2$, $|(a|b')|^2=|(b|a')|^2$, and $|(a|a')|^2+|(b|a')|^2=1$; one may call $|(Ja|Ja')|^2$ the purity of the levels Ja' and Jb'. It is, so far as this work is concerned, purely accidental that the electrostatic interaction between $1c$ and $1d$ vanishes identically and hence that these levels are to our approximation 100 percent pure. To the same approximation the separation between these two levels represents just the doublet splitting of the np electron in the central field due to the core.

NEON I (CF. FIG. 2)

The $2p^53p$ is taken from the work of Inglis and Ginsburg,[5] who solved the complete secular equation in LS coupling using the levels of $J=0$, 2, 3, and the mean of the four levels with $J=1$ to obtain the parameters, leaving otherwise the $J=1$ levels to be absolutely predicted.

The $2p^55p$ is the first of the series to which our approximation is at all applicable. These levels agree to within the rather large maximum interaction between the groups.

For $2p^56p$, the interaction is much smaller and the agreement correspondingly better.

TABLE I. *Neon I* $2p^5np$.

	$3p$	$5p$	$6p$	$7p$
F_0	−1737	−385.8	−314.7	−291.9
F_2	157.7	31.0	10.4	18.3
G_0	750.5	112.6	55.8	49.0
G_2	44.8	1.9	3.0	−1.7
ζ'	403	528.6	520.2	521.0
ζ	40	8.1	5.4	13.2
$(2a\|2a')$		0.921	0.977	
$(2b\|2a')$		−0.390	−0.208	
$(1a\|1a')$		0.683	0.697	
$(1b\|1a')$		0.730	0.716	
% Purity $2a'b'$		84.8	95.5	
% Purity $1a'b'$		46.6	48.6	

[5] Inglis and Ginsburg, Phys. Rev. **43**, 194 (1933). With regard to this configuration see also St. Rozental, Zeits. f. Physik **83**, 534 (1933).

$2p^5 7p$ is found to agree not at all; the reason is that the lower $8p$ group exactly overlaps the upper $7p$ and is therefore expected to interact strongly with it.

The values of the parameters and the coefficients in (5) are given by Table I. The significance to be attached to these values must be judged by comparison with Fig. 2. The value of ζ' is to be compared with the value 521 obtained from the parent doublet splitting of 782 cm^{-1}.

Argon I (cf. Fig. 3)

The p^5p configurations of argon remain rather well separated from each other up to $3p^5 8p$, the last of the series which is completely known. $8p\,0a$ falls about 200 cm^{-1} below $7p\ 1d$ and the lower group of $11p$ falls close to the upper group of $8p$ as indicated in the figure. There is definite evidence of perturbation on $8p$. The $5f$ group overlapping $6p$ does not have a pronounced effect.

Table II. *Argon I* $3p^5np$.

	$5p$	$6p$	$7p$	$8p$
F_0	−805.8	−585.6	−521.4	−515.7
F_2	75.7	18.7	9.8	5.5
G_0	235.6	95.5	53.6	28.3
G_2	2.0	6.4	2.5	2.5
ζ'	977.2	952.3	953.5	953.3
ζ	44.1	7.1	3.6	5.0
$(2a\|2a')$	0.927	0.986	0.968	0.999
$(2b\|2a')$	−0.378	−0.168	−0.254	−0.045
$(1a\|1a')$	0.702	0.690	0.690	0.723
$(1b\|1a')$	0.712	0.724	0.725	0.692
% Purity $2a'b'$	85.9	97.2	93.7	99.8
% Purity $1a'b'$	49.3	47.6	47.6	52.3

The constants are given in Table II. The value of ζ' is to be compared with the 954 obtained from the ionic doublet splitting of 1431 cm^{-1}.

Krypton I and Xenon I (cf. Fig. 4)

Even the lowest p^5p's of krypton and xenon are amenable to treatment with our approximation. For krypton the $2p^5 5p$ and $6p$ are completely known. The $2p^5 5p$ agrees to within the error of the approximation. The $6p$ shows definite evidence of outside perturbation which is undoubtedly mainly due to the lower group of $7p$ which lies at only 6200 on the $6p$ scale, rather than to the $5f$ levels plotted.

In xenon only the $5p^5 6p$ is complete. This in the first plot agrees very poorly with the calculations. It is definitely perturbed by the lower $7p$ group which overlaps as indicated. Although one cannot make a rigorous assignment of these overlapping levels to configurations one suspects on comparing this figure with the others that the highest $J=1$ of $7p$ might belong more exactly to $6p$ than the $1d$ assigned to it. If one makes this rearrangement one obtains the plot on the right which shows a decidedly better agreement.

The constants for these spectra have the values given in Table III. ζ' for krypton is to be compared with the 3581 obtained from the ion. The doublet splitting for the xenon ion is not known.

Table III.

	Krypton I $4p^5np$		*Xenon I* $5p^56p$	
	$5p$	$6p$	Given	Rearranged
F_0	−2984	−2028.4	−4764	−4682
F_2	213	34.8	321	198
G_0	671	194.1	748	622
G_2	20	16.3	−25	−2
ζ'	3632	3567.6	7028	7094
ζ	246	49.0	599	374
$(2a\|2a')$	0.955	0.999		0.954
$(2b\|2a')$	−0.297	−0.022		−0.299
$(1a\|1a')$	0.736	0.750		0.775
$(1b\|1a')$	0.678	0.662		0.632
% Purity $2a'b'$	91.2	99.9		91.0
% Purity $1a'b'$	54.2	56.2		60.1

The configuration $n'p^5nd$

The diagonal elements of spin-orbit interaction for p^5d in jj coupling are

$$\begin{array}{lll} & n'p^5nd & \\ a & (3/2, 5/2): & -\tfrac{1}{2}\zeta_p + \zeta_d \\ b & (3/2, 3/2): & -\tfrac{1}{2}\zeta_p - \tfrac{3}{2}\zeta_d \\ c & (1/2, 5/2): & \zeta_p + \zeta_d \\ d & (1/2, 3/2): & \zeta_p - \tfrac{3}{2}\zeta_d, \end{array} \qquad (6)$$

where we have introduced a notation a, b, c, d similar to that used for p^5p. Here the parameter ζ_p, which is the same as the former ζ', accomplishes the splitting of the configuration into two

groups, states characterized by a and b lying in the upper group, those characterized by c and d in the lower.

The electrostatic energies in LS coupling have the values

$$\begin{aligned} {}^3F &= -F_0 - 2F_2 & {}^1F &= -F_0 - 2F_2 + 90G_3 & {}^3D &= -F_0 + 7F_2 \\ {}^1D &= -F_0 + 7F_2 & {}^3P &= -F_0 - 7F_2 & {}^1P &= -F_0 - 7F_2 + 20G_1. \end{aligned} \tag{7}$$

Transforming to jj coupling gives the electrostatic matrices

$-F_0+$

	$4a$
$4a$	$-2F_2$

	$3a$	$3b$	$3c$
$3a$	$2\frac{2}{5}F_2+24G_3$	$-\frac{4}{5}\cdot 6\frac{1}{2}F_2+12\cdot 6\frac{1}{2}G_3$	$8\frac{1}{5}\cdot 5\frac{1}{2}F_2-12\cdot 5\frac{1}{2}G_3$
$3b$	$-\frac{4}{5}\cdot 6\frac{1}{2}F_2+12\cdot 6\frac{1}{2}G_3$	$-7\frac{1}{5}F_2+36G_3$	$-\frac{1}{5}\cdot 30\frac{1}{2}F_2-6\cdot 30\frac{1}{2}G_3$
$3c$	$8\frac{1}{5}\cdot 5\frac{1}{2}F_2-12\cdot 5\frac{1}{2}G_3$	$-\frac{1}{5}\cdot 30\frac{1}{2}F_2-6\cdot 30\frac{1}{2}G_3$	$30G_3$

	$2a$	$2b$	$2c$	$2d$
$2a$	$\frac{4}{5}F_2$	$\frac{2}{5}\cdot 21\frac{1}{2}F_2$	$-8\frac{4}{5}\cdot 14\frac{1}{2}F_2$	$\frac{3}{5}\cdot 21\frac{1}{2}F_2$
$2b$	$\frac{3}{5}\cdot 21\frac{1}{2}F_2$	$2\frac{1}{5}F_2$	$\frac{7}{5}\cdot 6\frac{1}{2}F_2$	$1\frac{4}{5}F_2$
$2c$	$-8\frac{4}{5}\cdot 14\frac{1}{2}F_2$	$\frac{7}{5}\cdot 6\frac{1}{2}F_2$	0	0
$2d$	$\frac{3}{5}\cdot 21\frac{1}{2}F_2$	$1\frac{4}{5}F_2$	0	0

	$1a$	$1b$	$1d$
$1a$	$-2\frac{8}{5}F_2+12G_1$	$1\frac{4}{5}F_2+4G_1$	$-\frac{7}{5}\cdot 5\frac{1}{2}F_2+4\cdot 5\frac{1}{2}G_1$
$1b$	$1\frac{4}{5}F_2+4G_1$	$-\frac{7}{5}F_2+\frac{4}{3}G_1$	$-1\frac{4}{5}\cdot 5\frac{1}{2}F_2+\frac{4}{3}\cdot 5\frac{1}{2}G_1$
$1d$	$-\frac{7}{5}\cdot 5\frac{1}{2}F_2+4\cdot 5\frac{1}{2}G_1$	$-1\frac{4}{5}\cdot 5\frac{1}{2}F_2+\frac{4}{3}\cdot 5\frac{1}{2}G_1$	$2\frac{0}{3}G_1$

	$0b$
$0b$	$-7F_2$

(8)

Just as in the case of p^5p we find if we neglect the interaction between levels belonging to different parents the following formulas to express the twelve levels in terms of six parameters:

$$\begin{aligned} (3c) &= -F_0 + \zeta_p + \zeta_d + 30G_3 \\ (2c) &= -F_0 + \zeta_p + \zeta_d \\ (2d) &= -F_0 + \zeta_p - \tfrac{3}{2}\zeta_d \\ (1d) &= -F_0 + \zeta_p - \tfrac{3}{2}\zeta_d + 2\tfrac{0}{3}G_1 \\ (4a) &= -F_0 - \tfrac{1}{2}\zeta_p + \zeta_d - 2F_2 \end{aligned} \tag{9}$$

$$\left.\begin{matrix}3a'\\3b'\end{matrix}\right\} = -F_0-\tfrac{1}{2}\zeta_p-\tfrac{1}{45}\zeta_d+\tfrac{3}{2}F_2+30G_3 \pm[(\tfrac{29}{10}F_2-6G_3+\tfrac{5}{45}\zeta_d)^2+96(3G_3-\tfrac{1}{5}F_2)^2]^{\frac{1}{2}}$$

$$\left.\begin{matrix}2a'\\2b'\end{matrix}\right\} = -F_0-\tfrac{1}{2}\zeta_p-\tfrac{1}{45}\zeta_d+\tfrac{5}{2}F_2 \qquad \pm[(\tfrac{5}{45}\zeta_d-\tfrac{17}{10}F_2)^2+\tfrac{84}{25}F_2^2]^{\frac{1}{2}} \qquad (9)\ cont.$$

$$\left.\begin{matrix}1a'\\1b'\end{matrix}\right\} = -F_0-\tfrac{1}{2}\zeta_p-\tfrac{1}{45}\zeta_d-\tfrac{7}{2}F_2+\tfrac{209}{3}G_1\pm[(\tfrac{5}{45}\zeta_d-\tfrac{21}{10}F_2+\tfrac{19}{3}G_1)^2+(4G_1+\tfrac{14}{5}F_2)^2]^{\frac{1}{2}}$$

$$(0b) = -F_0-\tfrac{1}{2}\zeta_p-\tfrac{3}{25}\zeta_d-7\ F_2.$$

We take the six levels given by linear expressions and the means of $3a'$, $3b'$; $2a'$, $2b'$; and $1a'$, $1b'$; fitting the six parameters to these nine quantities by least squares. *This leaves the $3a'$-$3b'$, $2a'$-$2b'$, $1a'$-$1b'$ separations to be absolutely predicted.*

From Fig. 1 we see that our approximation should be applicable to all the p^5d's of neon I. Since these are known completely from $3d$ through $10d$ we obtain the long series of configurations plotted in Fig. 5. These all agree within the accuracy of the calculation[6] except $6d$ and $7d$, which are clearly perturbed. The most of this perturbation is due to the fact that the upper group of $6d$ lies only 26 cm^{-1} below the lower of

[6] The extreme coarseness of the wave-number scale for the right half of the plot is to be noted.

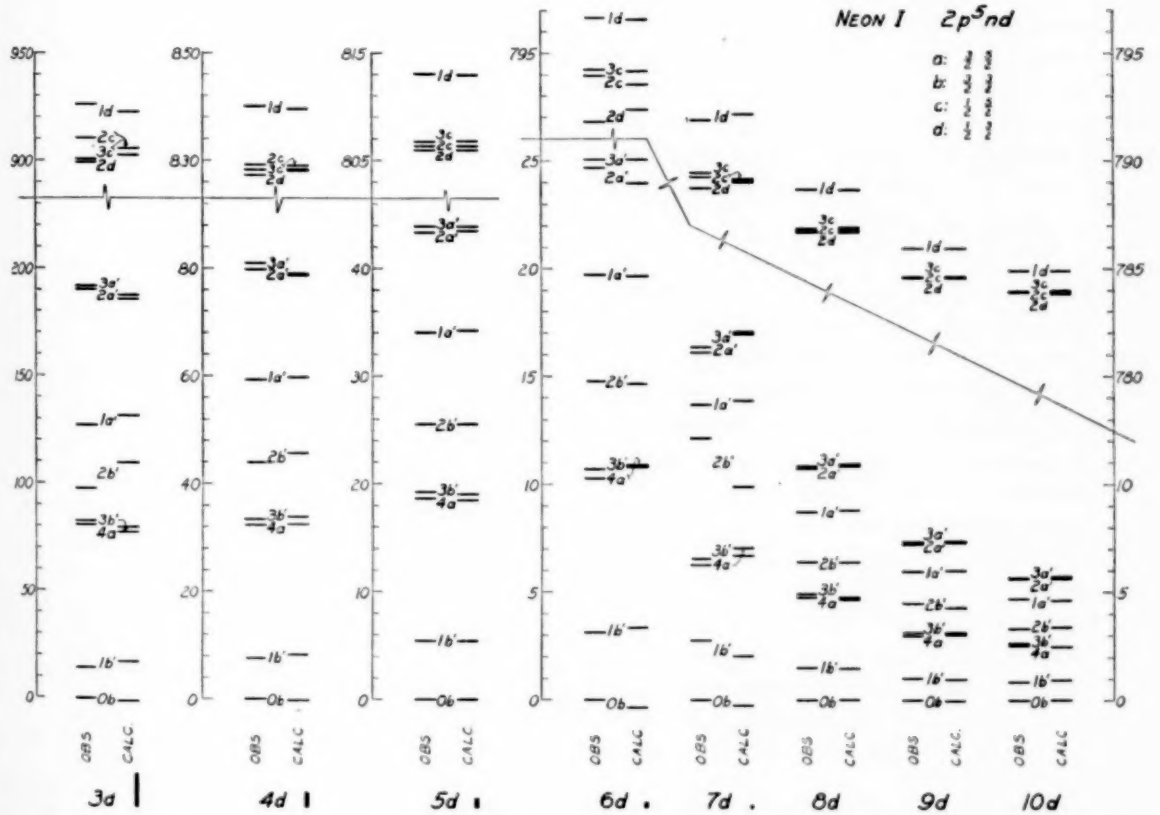

FIG. 5. Except for $6d$ and $7d$, which perturb each other, the agreement is within the accuracy, indicated by the lengths of the black bars, of the neglect of interaction between levels belonging to different parents; in the cases $8d$, $9d$, $10d$, where the maximum discrepancy is only 0.20 cm^{-1}, this agreement is within the accuracy of the calculation.

TABLE IV. *Neon I* $2p^5nd$.

	3*d*	4*d*	5*d*	6*d*	7*d*	8*d*	9*d*	10*d*
F_0	−374.23	−306.59	−285.78	−273.97	−269.61	−266.52	−264.38	−263.55
F_2	15.507	6.595	3.620	2.008	1.433	0.900	0.615	0.467
G_1	2.98	1.70	1.04	0.64	0.47	0.29	0.20	0.16
G_3	0.002	0.026	0.016	0.020	−0.004	0.004	0.001	0.002
ζ_p	530.11	521.62	520.40	519.10	519.49	520.24	520.20	520.35
ζ_d	1.178	0.002	0.141	0.476	0.064	0.043	0.000	0.044
$(3a \mid 3a')$	0.957	0.959	0.961	0.970	0.955	0.962	0.96	0.96
$(3b \mid 3a')$	−0.285	−0.281	−0.276	−0.241	−0.297	−0.276	−0.29	−0.27
$(2a \mid 2a')$	0.413	0.399	0.406	0.444	0.41	0.41	0.40	0.41
$(2b \mid 2a')$	0.911	0.917	0.914	0.898	0.91	0.92	0.91	0.91
$(1a \mid 1a')$	0.615	0.638	0.659	0.697	0.682	0.677	0.678	0.67
$(1b \mid 1a')$	0.789	0.770	0.751	0.718	0.733	0.736	0.735	0.74
% Purity $3a'b'$	91.6	92.0	92.4	94.1	91.2	92.5	92	92
% Purity $2a'b'$	17.1	15.9	16.5	19.7	17	16	16	17
% Purity $1a'b'$	37.8	40.7	43.4	48.6	46.5	45.8	46.0	45

7*d*. That there is further perturbation on the *upper group* of 7*d* is shown by the abnormally large 2*c*-2*d* separation, which should be just the 7*d* electron doublet splitting. This further perturbation may be attributed to the fact that the lower part of 9*d* lies 100 cm^{-1} above the upper of 7*d* and perhaps to the $2p^5 10s$ which lies about 20 cm^{-1} above 7*d*.

The constants used in these calculations are given by Table IV. The value of ζ_p is to be compared with the 521 obtained from the ionic doublet splitting. We should from the values here given predict a doublet splitting of 780.4 ± 0.2 cm^{-1} in comparison with the observed 782 cm^{-1}.

Thus the present theory accounts very satisfactorily for the observed structure of these rare-gas configurations. The perturbations which occur seem to be small except when two configurations of the same series overlap. Since there can be no spin-orbit perturbation corresponding to the interaction which splits the configuration into two groups, in estimating the mutual perturbation of two configurations we should compare the distance of the nearest levels not to the overall configuration size but to the much smaller spread of each group of levels. This requires that two configurations lie very close in order appreciably to affect each other.

In those cases in which our approximations are valid we have obtained the actual eigenfunctions for each level in terms of the *jj*-coupling scheme.[7] From these eigenfunctions we shall calculate the Zeeman effect, Stark effect, and line strengths for these configurations.

[7] The phases in this scheme are chosen in the following definite way (cf. reference 3). By use of Wigner's formula (*Gruppentheorie*, p. 206) for the addition of l and $\bar{l}$ to obtain L, l^i and s^i are added to obtain j^i, l^e and s^e to obtain j^e, and j^i and j^e to obtain J, each addition being made with the correlation to l and $\bar{l}$ in the order specified. Here i refers to the p^5 core, e to the added p or d electron.

The Half-Life of Actinouranium and the Problem of Geologic Time[1]

FORREST WESTERN AND ARTHUR E. RUARK, *University of Pittsburgh*

(Received June 22, 1933)

The actinium series arises from an isotope U^{235}, or from two such isotopes U^{239} and U^{235}, genetically connected. From work of Hahn and Meitner, the first possibility is almost certainly right. Assuming as a working hypothesis that U^{235} is the only long-lived uranium isotope, equations are developed for determining its decay constant λ_4 from data concerning radioactive minerals and substances. These equations also give the decay constant λ_1 of U^{238} and mineral ages. The results depend on the value of the actinium "branching" ratio, which lies between 0.03 and 0.04. Computations are carried out using both of these extreme values. Four minerals are discussed but only two, Karlshus bröggerite and Wilberforce uraninite, yield reliable results. The mean values from these are:

Branching ratio:	0.03	0.04
λ_4 in yr.$^{-1}$	2.28×10^{-9}	1.79×10^{-9}
λ_1 in yr.$^{-1}$	0.1514×10^{-9}	0.1509×10^{-9}

Branching ratio:	00.3	00.4
Half life of U^{235}, yr.	3.10×10^{8}	3.96×10^{8}
Half life of U^{238}, yr.	4.58×10^{9}	4.60×10^{9}

The best value for the half-life of U^{238} is $(4.58\pm0.09)\ 10^9$ yr. If U^{239} exists and has a half-life long compared with that of U^{235}, the values for λ_4 would apply to U^{239}. The ages, insensitive to the value of the branching ratio, are: Karlshus bröggerite, 0.81×10^9 yr.; Wilberforce uraninite, 1.04×10^9 yr. Since quantitative study of chemical alteration may throw light on the process and prove helpful in determining decay constants and mineral ages, equations are developed to show the effect of uniform leaching. Rates of removal or addition of Pb, U and Th are assumed different, but each of them is supposed constant in time. The resulting equations are applied to Katanga pitchblende, to illustrate the method.

I. The Present Status of the Actinouranium Hypothesis

IT is generally accepted that the actinium series contains at least one member which is an isotope of uranium. Actinium has always been found in uranium minerals when search for it has been made. Further, the ratio of actinium to uranium is not far from constant and its deviation from constancy may be reasonably explained as a result of alteration of these minerals. Hahn and Meitner[2] found that protoactinium slowly accumulates in pure uranium compounds. Their observations show that UY is derived from uranium; the problem which remains is to determine the details of their relationship.

The earlier view that the actinium series originates by branching of the uranium series was discredited by Aston's[3] mass-spectrograph studies of common and radiogenic leads in which he showed that some uranium leads contain amounts of Pb^{207} too large to come from any source other than the actinium series.

This means we must adopt the hypothesis of Piccard,[4] that the actinium series contains one or more uranium isotopes, genetically independent of U^{238} and U^{234}. Piccard supported a scheme of disintegration involving two so-called actinouranium isotopes, related through intermediate β-rayers in the same way as the isotopes U^{238} and U^{234} (Fig. 1). Similar schemes involving two genetically connected isotopes, U^{239} and U^{235}, have been suggested by several workers but have never been supported by strong evidence. Hahn[5] has made extensive experiments to detect β-radiations which would be expected to occur in the hypothetical sequence of disintegrations connecting U^{239} and U^{235}. He found no evidence of such radiations. It is fair to conclude from his

[1] Preliminary notes: Phys. Rev. **42**, 903 (1932); **43**, 205 (1933) and **43**, 781 (1933).

[2] Hahn and Meitner, Berichte deutschen Chem. Ges. **54**, 69 (1923).

[3] Aston, Nature **120**, 224 (1927); **123**, 313 (1929); **129**, 649 (1932); Proc. Roy. Soc. **A140**, 535 (1933).

[4] Piccard, Arch. Science Phys. et Nat. **44**, 161 (1917). See also T. R. Wilkins, Nature **117**, 719 (1926); and Phys. Rev. **29**, 352 (1928).

[5] Hahn, Zeits. anorg. Chem. **147**, 16 (1925).

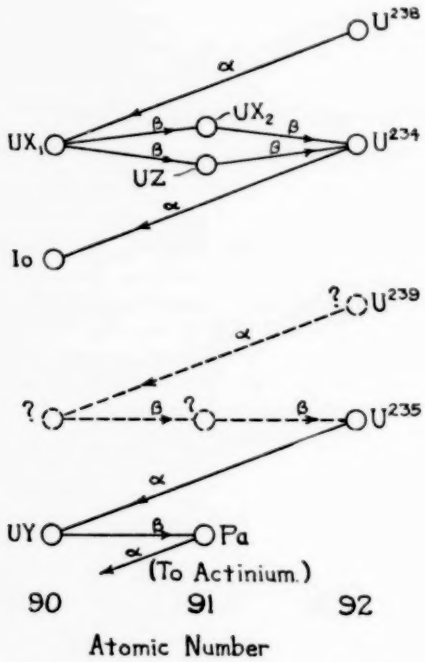

FIG. 1. Connection of the uranium and actinium series.

results that (1) either U^{239} does not exist; or (2) if it does exist, and if its immediate products are β-rayers, isotopic with UX_1 and UX_2, these products must be so short-lived as to escape detection in spite of careful search.

In the light of our knowledge of the half-lives of UX_1, UX_2, and UZ, the first-mentioned possibility appears much more probable than the second. If it is correct, then U^{235} is the parent of the actinium series. Let us assume, as a working hypothesis, that this is true. Then from existing data, it is possible to obtain an approximate value of the decay constant of U^{235} and thereby improve our knowledge of that of U^{238}; the ages of certain minerals can also be obtained.[6] This done, we may consider how the results would be modified in the improbable event that both U^{239} and U^{235} exist. Decay constants of both isotopes cannot be rigorously determined at present because there are more unknowns than equations, but *if* one of the isotopes has a much longer half-life than the other, the previous analysis will furnish a good approximation to the decay constant of the more stable isotope. There are indications that *if* both isotopes exist, U^{239} will have a much longer life than U^{235}. Fajans[7] has pointed out that for isotopic α-rayers the half-life increases with atomic weight, RaF being the sole exception.

We shall often speak, for convenience, as though the existence of a single actinouranium isotope, U^{235}, were an established fact. The reader is asked, therefore, to bear the above remarks in mind.

II. Notation; Discussion of the Actinium Branching Ratio

The subscripts 1, 2, 3 and 4 refer to the uranium isotopes U^{238}, U^{234}, the hypothetical U^{239} and U^{235}, respectively, while the subscripts Pa, Ac, Th, and Pb refer to the elements of which they are the symbols. Our notation is:

N_1, N_2, etc.—numbers of atoms of the respective isotopes of U, per gram of U now present.
N—the sum of N_1, N_2, N_3 and N_4.
N'_{206}, N'_{207}, N'_{208}—numbers of atoms of the respective isotopes of Pb, per gram of U now present.
N_{206}, N_{207}, N_{208}—numbers of atoms of these isotopes produced by radioactive disintegration.
N_{Pb}, N_{Th}, N_L—numbers of atoms of the respective elements, and of common lead, per gram of U now present.
λ_1, λ_2, etc., λ_{Pa}, λ_{Ac}, λ_{Th}—decay constants of uranium isotopes, etc.
f_{206}, f_{207}, f_{208}—fractions of N_{Pb} (total lead) constituted by Pb^{206}, etc.
a_{206}, a_{207}, a_{208}—fractions of N_L (common lead) constituted by Pb^{206}, etc.
U/Pb, U/Th—ratio of mass of U to mass of Pb, etc.
W_1, W_2, etc.—atomic weights on the chemical scale, $O=16$.

The actinium branching ratio, R, is defined by

$$R \equiv \lambda_{Ac} N_{Ac}/E, \tag{1}$$

where E represents one-half the number of α particles emitted per second by all the isotopes in one gram of uranium. Kovarik and Adams[8] found that $E=12{,}385$ α-particles/sec. per gram of U, with an uncertainty of 1 percent. The use of the ratio

$$B \equiv \frac{\lambda_4 N_4}{\lambda_1 N_1} \equiv \frac{\lambda_{Ac} N_{Ac}}{\lambda_1 N_1} \equiv \frac{\lambda_{Pa} N_{Pa}}{\lambda_1 N_1}, \tag{2}$$

[6] The calculations are based on the orthodox radioactive families (Fig. 1).

[7] Fajans, Le Radium **10**, 171 (1913); *Radioelements and Isotopes*, p. 31, McGraw-Hill Book Co., N. Y., 1931.

[8] Kovarik and Adams, Phys. Rev. **40**, 718 (1932).

rather than R, simplifies many equations, so we shall adopt it. The available values show a considerable spread and we can only state[9] that with high probability B lies between 0.03 and 0.04. Calculations will be made using both these limiting values.

III. Equations for Determining Half-Lives of Uranium Isotopes, and Mineral Ages

On the working hypothesis adopted here, that the actinium series contains only one long-lived uranium isotope, we have just enough data to calculate its decay constant and the ages of certain minerals. The relations involved are as follows.

Since the intermediate members of the uranium and thorium series are so short-lived as to be present in negligible amounts, we may write

$$N_{206}=N_1(e^{\lambda_1 t}-1); \quad (3) \qquad N_{208}=N_{\mathrm{Th}}(e^{\lambda_{\mathrm{Th}} t}-1). \quad (4)$$

If the actinium series originates in U^{235},[10]

$$N_{207}=N_4(e^{\lambda_4 t}-1). \tag{5}$$

Also,

$$\lambda_2 N_2=\lambda_1 N_1; \quad (6) \qquad \lambda_4 N_4=B\lambda_1 N_1. \quad (7)$$

The observed quantities of the lead isotopes consist of original and radiogenic lead, as indicated by the equation,

$$N'_{206}=a_{206}N_L+N_{206}, \tag{8}$$

and two similar relations, (9) and (10), giving N'_{207} and N'_{208}. From the definition of Avogadro's number,

$$N_1W_1+N_2W_2+N_4W_4=6.064\ 10^{23}, \tag{11}$$

and from the experiments of Kovarik and Adams,

$$\lambda_1N_1+\lambda_2N_2+\lambda_4N_4=2(3.9083\times 10^{11}) \text{ per year.} \tag{12}$$

These equations contain ten unknowns: N_1, N_2, N_4, λ_1, λ_4, N_{206}, N_{207}, N_{208}, N_L, and t.[11] It is easy to eliminate all unknowns except λ_1, λ_4 and t. With times in years, and decay constants in yr.$^{-1}$, the result is,

$$\lambda_1=\frac{3.9083\ 10^{11}}{6.064\ 10^{23}(1+B/2)}\,W_1\left(1+\frac{W_4}{W_1}B\frac{\lambda_1}{\lambda_4}\right); \tag{13}$$

$$(e^{\lambda_1 t}-1)-B\frac{a_{206}\lambda_1}{a_{207}\lambda_4}(e^{\lambda_4 t}-1)=\frac{N_{\mathrm{Pb}}}{N}\left(f_{206}-\frac{a_{206}}{a_{207}}\cdot f_{207}\right)\left(1+B\frac{\lambda_1}{\lambda_4}\right); \tag{14}$$

$$(e^{\lambda_4 t}-1)-\frac{f_{206}}{f_{208}}\frac{W_{\mathrm{U}}}{W_{\mathrm{Th}}}\frac{\mathrm{Th}}{\mathrm{U}}\left(1+B\frac{\lambda_1}{\lambda_4}\right)(e^{\lambda_{\mathrm{Th}} t}-1)=\frac{N_{\mathrm{Pb}}}{N}\left(f_{206}-\frac{a_{206}}{a_{208}}\cdot f_{208}\right)\left(1+B\frac{\lambda_1}{\lambda_4}\right). \tag{15}$$

---

[9] Western and Ruark, Phys. Rev. **42**, 903 (1932); **43**, 205 (1933).

[10] If the series originates in U^{239} and if U^{235} is short-lived compared to U^{239}, we would write

$$N_{207}=N_3(e^{\lambda_3 t}-1);$$

and Eqs. (9) and (10) would contain additional terms.

[11] Walling found the half-life of U^{234} to be 342,500 years [Zeits. f. physik. Chemie **B10**, 467 (1930)]. Collie [Proc. Roy. Soc. **A131**, 541 (1931)], concluded that this half-life is not less than 10^6 years, but it seems unlikely that it is much more than 10^6 years. The mass of U^{234} in uranium can be neglected in comparison with the masses of U^{238} and U^{235}, although its activity, of course, cannot be neglected. For our purpose, it is unnecessary to know λ_2 exactly. The value of λ_{Th} was redetermined by Kirsch, who finds the half-life to be $1.8\ 10^{10}$ yr. [Phys. Zeits. **31**, 1718 (1930); also Kirsch and Lane, Proc. A. A. A. S. **66**, 357 (1931)].

In (14) and (15) we use the very close approximation, $N/N_1 = 1 + B\lambda_1/\lambda_4$, obtained by neglecting N_2 as compared with N_1 and N_4. It is convenient to write $T = 10^{-9}t$, $L_1 = 10^9\lambda_1/2.3026$, etc., so that T is the mineral age in billions of years, and to rewrite the equations in a form adapted to solution by approximations. Inserting the values of coefficients of a general nature and replacing exponentials by powers of 10, we have[12]

$$L_1 = [1/(1+B/2)]0.06663(1+0.9874B(L_1/L_4)); \tag{16}$$

$$10^{L_1T}-1 = (N_{Pb}/N)(f_{206}-0.5600f_{208})(1+B(L_1/L_4))+0.5746(Th/U)(10^{\cdot 01672T}-1)(1+B(L_1/L_4)); \tag{17}$$

$$\frac{L_4T}{10^{L_4T}-1} = \frac{1.374BL_1T}{(10^{L_1T}-1)-(N_{Pb}/N)(f_{206}-1.374f_{207})(1+B(L_1/L_4))}. \tag{18}$$

IV. Application of Equations to Mineral Data

Table I gives the best values now obtainable for the isotopic and atomic weights of lead, uranium, and thorium.[13] The uncertainty of these figures is 0.03 atomic weight units, with the exception of that for common lead, where the uncertainty is 0.007 unit. Table II shows relevant portions of Aston's[14] mass analyses of leads, and Table III gives analyses of three of the minerals from which these leads were derived. The analysis of Katanga pitchblende is not available.

Table I. *Isotopic and atomic weights.*

Element or isotope	Atomic weight Chemical scale
Lead, 206	205.98
207	206.98
208	207.98
Ordinary lead, chemically	207.22
Thorium, calculated	232.03
Uranium, 234	234.04
235	235.04
238	238.04
239?	239.05
Uranium, natural mixture[15]	238.04

[12] To effect a solution, one neglects at first the terms containing B. By using a rough value of T in the thorium term, an approximate value for $10^{L_1T}-1$ is obtained from (17); this and the corresponding value of L_1T are substituted in (18), which gives L_4T. L_1/L_4 is computed and is used in (16) to obtain a fair value of L_1. T is calculated from L_1T and the process is repeated. The convergence is good for uranium minerals and little would be saved by using approximate equations. A graph of $x/(10^x-1)$ facilitates the work.

[13] Western and Ruark, J. Chem. Phys. **1**, 717 (1933).

[14] Proc. Roy. Soc. **A140**, 535 (1933).

[15] Calculated on the hypothesis that U^{235} is the only actinouranium isotope by using an approximate value of the half-life of this isotope.

Of the minerals described, the thorite is not satisfactory for determining uranium decay constants because of the susceptibility of thorium

Table II. *Isotopic constitution of ordinary and radiogenic leads.*

Ordinary lead	Norwegian bröggerite	Katanga pitch-blende	Wilber-force uraninite	Norwegian thorite
Chemical atomic weight:				
207.22	206.14[a]	206.048[b]	206.195[c]	207.90[d]
Percentage 206:				
27.75	86.8	93.3	85.9	4.6
Percentage 207:				
20.20	9.3	6.7	8.3	1.3
Percentage 208:				
49.55	3.9	(0.02)	5.8	94.1
Other isotopes:				
2.5	0	0	0	0

[a] Raade, Norway. Calculated from isotope-percentages, and isotopic weights of Table I.

[b] Hönigschmid and Birckenbach, Ber. **56**, 1837 (1923); von Grosse and Kurbatow, quoted by Aston, Proc. Roy. Soc. **A140**, 535 (1933).

[c] Baxter and Bliss, J. Am. Chem. Soc. **52**, 4851 (1930).

[d] Fajans, Sitz. Heidelb. Akad. Wiss. **3** (1918); Hönigschmid, Phys. Zeits. **19**, 437 (1918); Zeits. f. Elektrochemie **25**, 91 (1919).

Table III. *Mineral analyses.*

	Norwegian bröggerite[a]	Wilberforce uraninite[b]	Norwegian thorite[c]
Percentage U	61.16	53.52	0.45
Percentage Th	4.38	10.37	30.10
Percentage Pb	8.02	9.26	0.35
Th/U	0.0716	0.194	66.1
Pb/U	0.131	0.173	0.78

[a] Fenner and Piggot, Nature **123**, 793 (1929).

[b] Wells, reported by Baxter and Bliss, reference c to Table II.

[c] Fajans, Zeits. f. Elektrochemie **24**, 163 (1918); Phys. Zeits. **19**, 438 (1918).

minerals to leaching and because of the small amounts of Pb^{206} and Pb^{207} in the mineral. Decay constants computed from this mineral are listed in Table IV as a matter of record but are devoid of significance. The data on the uraninite and the bröggerite appear fairly trustworthy. It is well known that alteration of a uranium mineral increases the lead-ratio,[16] $Pb/(U+kTh)$. The uraninite, described in detail by Kirsch and Lane,[17] has a lead-ratio slightly higher than that of some samples from the same vicinity but the difference is not great enough to affect our calculations materially. Fenner and Piggot[18] described the bröggerite as being without evidence of alteration. Comparison of its analysis with Gleditsch's[19] analyses of five samples from the same mine shows that, while its uranium content is in agreement with the lowest value of uranium from these, both the thorium content and the lead content are only about ninety percent of the lowest values found for these quantities in the Gleditsch samples. The low thorium content may indicate alteration. If so, calculations based on the Gleditsch samples show that the maximum effect of leaching on the values calculated for λ_4 and t from the Fenner-Piggot sample would be to raise the one, and lower the other about five percent. λ_1 is insensitive to such alteration. We assume, accordingly, that the mineral is unaltered and base our computations on the Fenner-Piggot analysis.

TABLE IV. *Calculated decay constants and mineral ages.*

Thorite	Bröggerite		Uraninite	
$B=0.03$	$B=0.03$	$B=0.04$	$B=0.03$	$B=0.04$
	Age (yrs.$\times10^{-9}$)			
0.34	0.805	0.809	1.036	1.041
	λ_1 (per yr.$\times10^{9}$)			
0.1512	0.1514	0.1508	0.1515	0.1510
	Half-life of U^{238} (yrs.$\times10^{-9}$)			
4.58	4.578	4.595	4.574	4.590
	λ_4 (per yr.$\times10^{9}$)			
12 ± 1	2.62	2.07	1.94	1.51
	Half-life of U^{235} (yrs.$\times10^{-9}$)			
0.056	0.264	0.334	0.357	0.459

Values calculated from the three minerals discussed above are given in Table IV. The agreement between the results from the bröggerite and uraninite is satisfactory. It is unfortunate that the required data are not available for more good uranium minerals, to indicate whether this agreement is genuine.[20]

Kirsch and Lane[17] have shown that the age of the Wilberforce uraninite is $(1.03\pm0.10)10^9$ years.

V. The Effect of Leaching on Radioactive Age Determinations

In recent years techniques have been developed for judging whether or not a mineral specimen is essentially unaltered.[21] The principal aims of such work have been the selection of unaltered specimens, the establishment of reliable lead-ratios and the attempt to understand why leaching increases the lead-uranium ratio in uranium minerals, while it decreases the lead-thorium ratio in thorium minerals.[22]

It is desirable to begin a quantitative study of leaching which, as our knowledge increases, may throw additional light on the process and prove an aid in determining the ages of certain minerals.

---

[16] Here $k=\lambda_{Th}W_{208}W_U/\lambda_U W_{206}W_{Th}$. By using Kirsch's value of λ_{Th}, $k=0.26$.

[17] Kirsch and Lane, Proc. A. A. A. S. **66**, 357 (1931).

[18] Fenner and Piggot, Nature **123**, 793 (1929).

[19] Gleditsch, Ark. Mat. Og Naturv. Kristiania **36** (1), 184 (1919); Norske Videns. Akad. Oslo **I**, Mat. Nat. Kl. No. 3 (1925).

[20] The kolm of Grüllhögen, Sweden has attracted much attention. The atomic weight of the lead is 206.013. Aston (Proc. Roy. Soc. **A140**, 535 (1933)) obtained a single mass-spectrum which showed Pb^{206} and Pb^{207} but he states that this spectrum was unsuitable for photometry. Previously several writers calculated the composition of the lead on the assumption that it contains only Pb^{206} and Pb^{207}. The results depend markedly on the values used for the isotopic weights. By using the weights in Table I, such a calculation gives 96.7 percent and 3.3 percent, respectively, for these two isotopes. However, these values are so sensitive to the isotopic weights that with the limits of error placed on the latter, the value computed for λ_4 can vary from about 0.015×10^{-9} yr.$^{-1}$ to 3.6×10^{-9} yr.$^{-1}$. Without a more complete mass analysis, the kolm cannot give information on the decay constant of actinouranium. The mineral age is 0.42×10^9 yr., with an uncertainty of 4 percent.

[21] Kirsch, *Geologie und Radioaktivität*, pp. 132–180. Work of Ellsworth, Todd, Davis, and Hecht and Körner is described by Holmes on pp. 324–8 and 365–6 of *The Age of the Earth*, Bulletin 80 of the National Research Council, Washington, D. C. (1931).

[22] Holmes, Phil. Mag. **1**, 1055 (1926).

It is possible to improve our understanding of the effects of alteration by considering three hypothetical cases:

(1) *Initial alteration.* In this case practically no radiogenic lead is present when leaching occurs so the effect of alteration is the same as that of a decrease in the initial concentrations of U and Th.

(2) *Recent alteration.* Here the composition of the lead is almost unaffected. With a knowledge of the value of λ_4, isotopic analysis would make possible a correct age determination by equations (3), (5), (7), (8) and (9), even though the ratios Pb/U and Th/U were untrustworthy. This case may be realized in a rough way by some uraninites; for Ellsworth,[23] discussing uraninites of Villeneuve, says, "The lead ratio fortunately increases only slightly so long as the mineral remains black due to an appreciable UO_2 content, but once the UO_2 is entirely oxidized, uranium is lost much faster than lead, and the lead ratio rises to a large and entirely misleading value."

(3) *Uniform alteration.* It may be that for some minerals, the net effect of alteration is nearly the same as if it had taken place at a uniform rate. The simplicity of this assumption recommends it as a first approximation. If, in a radioactive series, the subscripts p and d refer to the long-lived parent element and the end-product, respectively, and if the intermediate elements can be neglected, uniform leaching is defined by

$$dN_p/dt = -(\lambda_p + k_p)N_p;$$
$$dN_d/dt = \lambda_p N_p - k_d N_d, \qquad (19)$$

where k_p and k_d may be called alteration constants. If we put $k = k_p - k_d$,

$$N_d = [\lambda_p/(\lambda_p + k)]N_p(e^{(\lambda_p + k)t} - 1). \qquad (20)$$

Application of (20) to each of the radioactive series gives three equations containing t, $k_U - k_{Pb}$ and $k_{Th} - k_{Pb}$ as unknowns. Thus t can be obtained directly but in order to use these equations in finding alteration constants, we need the analysis of the mineral, the isotopic composition of the lead it contains and the analysis of an unaltered specimen from the same deposit, if there be such.

As an illustration, the method may be applied to the Katanga pitchblende of Table II, by making some assumptions of uncertain validity. The lead was separated from a composite sample of altered material by Hönigschmid and Birckenbach.[24] They made no mineral analysis, feeling that the lead-ratio would be without significance. However, data on pp. 367–368 of *The Age of the Earth*, show that for three altered specimens designated as *I*, *J* and *K*, the mean ratio of lead to uranium is 0.096, while for several unaltered specimens it is close to 0.080. We write (Pb/U)′ for the latter ratio to distinguish it from the value for the leached specimen. Thorium is practically absent. Assuming these data are appropriate to the material of Hönigschmid and Birckenbach, we can write equations which determine λ_1, λ_4, $k_U - k_{Pb}$ and t. Eq. (13) applies directly. For an unleached thorium-free mineral,

$$\frac{205.98\,N_{206} + 206.98\,N_{207}}{238.04\,N} = \left(\frac{\text{Pb}}{\text{U}}\right)',$$

which may be written

$$e^{\lambda_1 t} - 1 = \frac{238.04}{205.98}\left(1 + B\frac{\lambda_1}{\lambda_4}\right)\left(\frac{\text{Pb}}{\text{U}}\right)' - \frac{206.98}{205.98}B\frac{\lambda_1}{\lambda_4}(e^{\lambda_4 t} - 1). \qquad (21)$$

Further, we have two equations obtained by applying (20) to the uranium and actinium series. The results are: $\lambda_1 = 0.1514 \times 10^{-9}$ per year, $\lambda_4 = 2.8 \times 10^{-9}$ per year, $k_U - k_{Pb} = 0.64 \times 10^{-9}$ per year and $t = 0.55 \times 10^9$ years. Only the value obtained for λ_4 can yield any test of the assumption of uniform alteration. In this case the character of the data is such that, even if λ_4 were accurately known, no definite conclusion could be drawn. It is believed that when λ_4 is more accurately known and further mineral data are available, similar investigations may throw much light on alteration processes.

[23] H. V. Ellsworth, Am. Mineral. **15**, 455 (1930).

[24] Hönigschmid and Birckenbach, Ber. d. D. chem. Gesellschaft, p. 1837 (1923).

VI. Conclusions

In view of our present knowledge, a value of three or four hundred million years for the half-life of the principal actinouranium isotope cannot be far from correct. Further study of the actinium branching ratio and complete data on additional minerals are needed to yield a more accurate value.

The value calculated for the half-life of U^{238} is relatively insensitive to that of actinouranium. Consequently, the uncertainty in the former is no larger than the uncertainty in our knowledge of the rate at which uranium gives off α particles. Judging from the small mean deviation in the counting experiments of Kovarik and Adams, a liberal estimate of all uncertainties allows us to state the half-life of U^{238} as $(4.58_4 \pm 0.09) \times 10^9$ years, assuming that U^{239} does not exist. Kovarik and Adams[8] gave $4.52_4 \times 10^9$ years. This was computed on the branching hypothesis and the value used for the atomic weight of uranium was 238.17, which is too high. Our value should be considered as replacing that of Kovarik and Adams, since we have employed their data on the rate of emission of α particles by uranium, and have taken account of U^{235}. The value of the International Radium-Standards Commission,[25] 4.4×10^9 years, is not comparable with ours. The Commission states that no account was taken of the actinium series, because the half-life of actinouranium was not sufficiently well known.

The U^{235} content of uranium lies between 0.15 and 0.35 percent, provided U^{239} does not exist. The wide variation given is largely due to uncertainty in our knowledge of the branching ratio. On the other hand, if U^{239} exists and is long-lived in comparison to U^{235}, the same figures would apply to the former. A content of U^{239} ten times higher than the larger value given here would not explain the present atomic weight, 238.14, assigned to uranium.

---

[25] Rev. Mod. Phys. **3**, 427 (1930).

Electro-Optical Kerr Effect in Gases

C. W. BRUCE, *University of Virginia*

(Received June 7, 1933)

The Kerr constant B of CO_2 has been measured as a function of density from 0.06 to 0.32 g/cm³ and as a function of temperature from 7.2 to 34.6°C. The results are in agreement with the Langevin-Born theory. The absolute value of B for CO_2 has been measured and is 0.34×10^{-10} per atmosphere for wave-length 4550A and temperature 34.6°C. This is also the theoretical value of B for CO_2. The probable error of the measured value is 2 percent. The absolute value of B for N_2 measured by comparison with CO_2 is 0.057×10^{-10} for the above wave-length and temperature, with a probable error of 3 percent. The corresponding theoretical value for N_2 is 0.050×10^{-10}. The Kerr constant of H_2 is shown to be less than 0.01×10^{-10} which is not in disagreement with the theoretical value of 0.005×10^{-10}.

I. INTRODUCTION

IN 1875 Kerr[1] discovered that if an optically isotropic substance be placed in an electric field it acquires the optical properties of a uniaxial crystal with the optic axis in the direction of the electric field. The law governing this phenomenon, proposed by Kerr, states that if n_1 and n_2 are the refractive indices for the components of the light vector vibrating parallel and perpendicular to the lines of force in the substance, respectively, their phase difference D in radians after passing through the field E, in absolute electrostatic units, is

$$D=2\pi l(n_1-n_2)/\lambda=2\pi BlE^2, \qquad (1)$$

where l is the length of the light path through the field, λ is the wave-length of the light in a vacuum and B is the so-called Kerr constant of the substance.

The theory of the Kerr effect as worked out by Langevin,[2] Born[3] and others connects the Kerr constant with the index of refraction, dielectric constant and the light scattering coefficient (depolarization constant).[4, 5]

Langevin assumes that the molecules are electrically and optically anisotropic and, as a result of the orienting action of the electric field upon the induced doublets in the molecules, the substance as a whole becomes doubly refracting. Born extended the theory to include the permanent moment of the molecule. Raman and Krishnan[6] have further modified the Langevin-Born theory so that it becomes applicable to liquids in which the contribution of the molecules to the field becomes large. The quantum mechanics of the Kerr effect has yielded little more than these classical theories.[7]

From the Langevin-Born theory, for a non-polar gas

$$B\equiv B_mN=\pi N(n^2+2)^2(\epsilon+2)^2\theta/27n\lambda, \qquad (2)$$

$$\theta=(1/45kT)[(a_1-a_2)(b_1-b_2)+(a_2-a_3)(b_2-b_3)+(a_3-a_1)(b_3-b_1)], \qquad (2a)$$

where B_m is the Kerr constant per molecule; N, the number of molecules per unit volume; n, the ordinary index of refraction; ϵ, electrostatic value of dielectric constant; k, Boltzmann's constant; T, absolute temperature; $b_1b_2b_3$, moments induced in the molecule along its three principal axes of optical anisotropy by unit electrical force in the light wave acting along the three axes respectively; and $a_1a_2a_3$, moments induced along the same axes by unit electrostatic force. From (2) and (2a)

$$B\equiv B_mN\propto N(n^2+2)^2(\epsilon+2)^2/n \qquad (3)$$

[1] Kerr, Phil. Mag. (4) **50**, 337 (1875).
[2] Langevin, Le Radium **7**, 249 (1910).
[3] Born, Ann. d. Physik **55**, 177 (1918).
[4] See Beams, Rev. Mod. Phys. **4**, 133 (1932).
[5] See Szivessy, Handbuch d. Physik Vol. XXI, Julius Springer (1929).
[6] Raman and Krishnan, Proc. Roy. Soc. **A117**, 1, 589 (1927).
[7] See Van Vleck, *Electric and Magnetic Susceptibilities*, p. 366, Oxford University Press (1932).

if λ and T are held constant while the density is varied. It is also seen from (2) and (2a) that if N and λ are held constant and T is varied BT = constant, since, for a nonpolar substance, ϵ and n are practically independent of the temperature.

From a result of the theory of light scattering by molecules[8] and an assumption due to Gans[9] it may be shown that for a nonpolar gas at low densities,

$$B=\frac{(n^2-1)(\epsilon-1)}{8\pi Nn\lambda kT}\frac{3\Delta}{6-7\Delta}, \tag{4}$$

where Δ is the light-scattering coefficient (depolarization constant) of the molecule. Formula (4) is sufficiently accurate for this experiment.

The theory for the transmission of plane polarized light through the Kerr cell, which is the same as through a uniaxial crystal, shows that the intensity of the Kerr beam is

$$I=I_0\sin^2(D/2), \tag{5}$$

where I_0 is the intensity of light through the Kerr cell and D is the phase difference in radians between the ordinary and the extraordinary ray. Using the value of D from (5) in (1) gives

$$B=(1/\pi lE^2)\arcsin(I/I_0)^{\frac{1}{2}}, \tag{6}$$

which for most work in gases may be written

$$B=(1/\pi lE^2)(I/I_0)^{\frac{1}{2}}. \tag{7}$$

From (7)

$$B\propto I^{\frac{1}{2}} \tag{8}$$

if I_0E, and l are constant. Eq. (7) is the one by which B is determined from experiment. The error in using (7) instead of (6) in reducing the measures in this experiment is never greater than 0.1 percent.

Three tests may be applied to test the validity of the Langevin-Born theory. These are: (1) a comparison of the experimental value of the Kerr constant as a function of density with the theoretical value as given by Eq. (3), (2) the examination of the constancy of BT when the density and the wave-length of the light are held constant while the temperature is changed and (3) a comparison of the absolute values of B given by Eq. (4) with the values given by experiment using Eq. (7). Needless to say experimental values of n and ϵ are used in Eqs. (3) and (4). These three tests may be taken as the object of this paper.

II. Experimental Arrangement

A modification of the method of Stevenson and Beams[10] is used. The novelty of their method consists in placing the polarizer and analyzer inside the Kerr cell containing the gas under high pressure. This method eliminates the effect of strains in the windows of the Kerr cell and allows higher field strength to be used. On account of difficulty with the nicol prisms under high pressure they were replaced by a double image polarizer and analyzer. Fig. 1 shows the optical system of the final arrangement. C_1 is a photronic

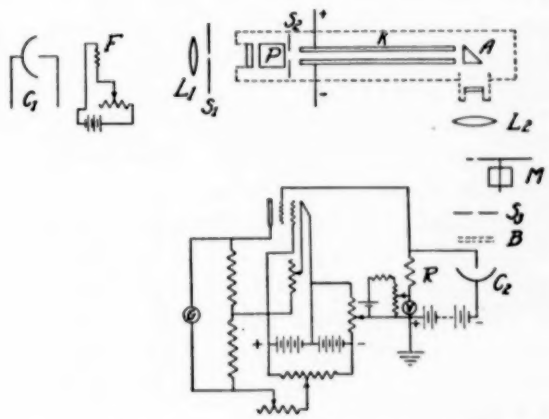

Fig. 1. Optical system and circuit of d.c. amplifier.

cell used to correct for small variations in the light source F. The light from F is collimated by L_1. The stop S_1 limits the size of the beam of light entering the polarizer P which is a calcite crystal, set so that the plane of polarization of the light makes an angle of 45° with the field between the plates K of the Kerr cell. S_2 cuts out the extraordinary ray. The analyzer is a Cotton[11] prism made of crystal quartz. It is set parallel to the polarizer so that with no field on the Kerr cell there is a single beam of light coming from the analyzer, called hereafter the light beam. With the field applied light through the Kerr cell

[8] See Marx, *Handbuch der Radiologie*, p. 781.
[9] Gans, Ann. d. Physik **65**, 97 (1921).
[10] Stevenson and Beams, Phys. Rev. **38**, 133 (1931).
[11] Cotton, Comptes Rendus **193**, 268 (1931).

becomes elliptically polarized so that two beams of light leave the analyzer, the ordinary ray comparable in intensity with the light beam and the extraordinary ray of small intensity, hereafter called the Kerr beam. The lens L_2 brings the light to a focus at S_3, which may be set to cut out the ordinary ray but to allow the Kerr beam to pass through the filter B to the evacuated potassium hydride photoelectric cell C_2, used in conjunction with a d.c. amplifier to measure the light intensity. A rotating sector M driven at a high speed by a motor may be placed in the path of the light beam to cut down its intensity to approximately that of the Kerr beam so that by a slight shift of S_3 it could also be measured to obtain absolute values of the Kerr constant. The plates K are held in position by Bakelite rings and held apart by Bakelite separators 4 mm thick. The plates are 90 cm long and 2.5 cm wide. Electrical connections with the plates are made through ordinary spark plugs, the bases of which are soldered into holes bored in the tube.

Fig. 1 also gives the electrical circuit of the d.c. amplifier. By a separate experiment the deflection of the galvanometer was found to be proportional to the light falling on C_2 in the range used. The resistance R is 10^{10} or 10^{11} ohms depending on the sensitivity required. This entire circuit was placed inside a metal box for shielding. The inside of the box was kept dry by P_2O_5. This circuit is a modification of the one given by DuBridge.[12]

Fig. 2 shows the construction of the analyzer end of the Kerr cell. Copper washers at C and lead foil at L form gas-tight seals. The window W is glass 3 cm thick and 3 cm in diameter. By the worm gear G the analyzer may be set accurately parallel to the polarizer. The barrel of the Kerr cell is a cold-drawn steel tube 3.8 cm inside in diameter with walls 1.25 cm thick.

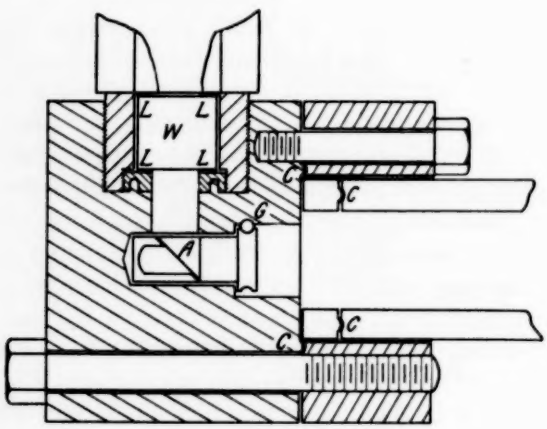

FIG. 2. Construction of end of Kerr cell.

The high voltage applied to the Kerr cell was obtained by rectifying the current from a five kilowatt x-ray transformer. The high voltage circuit is essentially the same as that of Stevenson and Beams.[13] The voltage applied to the plates of the Kerr cell was measured by a Wulf electrostatic voltmeter capable of measuring up to 50,000 volts with an accuracy of 0.5 percent. The period of the quartz fiber of the voltmeter is such that it will detect a 60-cycle ripple in the voltage. Under the conditions of this experiment the ripple was too small to be detected.

The gas pressures were measured to 0.1 atmosphere by a carefully calibrated bourdon spring gauge used in conjunction with a dead weight piston gauge. Amagat's[14] data on CO_2 were used to turn pressures into densities.

The gases used were from commercial cylinders but tests on CO_2 showed it to be better than 99.5 percent pure. The purity of the hydrogen and nitrogen is not known. The gases were dried by allowing them to pass through P_2O_5 before being used.

III. Experimental Procedure and Results

The variation of the Kerr effect with density was determined without the rotating sector and was standardized by setting the analyzer slightly off the parallel position. In this way about 0.2 percent of the light through the Kerr cell goes along with the Kerr beam to the photoelectric cell. This light measured with the field off furnishes a complete check on the line-up of the optical system as well as a check on the sensitivity of the amplifier.

The variation of B with density and the absolute values were measured at a temperature of 34.6°C held constant by placing the cell in an electrically heated water bath, the temperature of which was regulated by a mercury-in-glass

[12] DuBridge, Phys. Rev. **37**, 392 (1931).

[13] Stevenson and Beams, Phys. Rev. **38**, 133 (1931).

[14] Amagat, Comptes Rendus, 663 (1885).

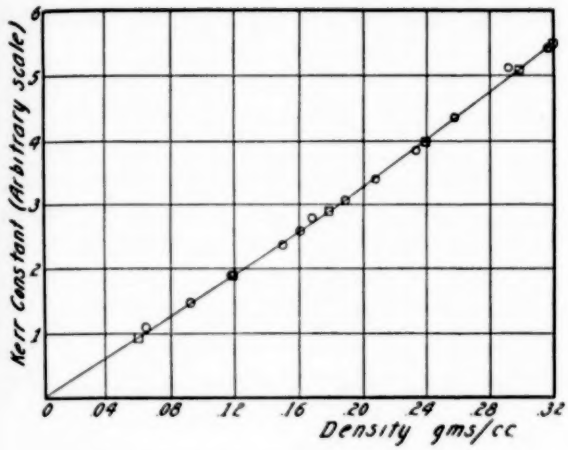

FIG. 3. Variation of Kerr constant with density.

thermostat. It is estimated that the temperature varied less than 0.01°C.

Fig. 3 shows the variation of the Kerr effect with density in CO_2 compared with the variation as computed from Eq. (3). The constant of proportionality in (3) was so chosen as to make the theoretical curve agree with the experimental at one point other than at the origin. The squares represent points computed by Eq. (3). Values for ϵ were taken from the data of Uhlig, Keyes and Kirkwood[15] and n from Phillips[16] measures on the index of refraction for 4358A. The average deviation of the experimental points from the curve drawn from theory is less than 1 percent if one omits the first measure for which the Kerr effect is small.

Fig. 4 shows the variation of the Kerr constant per molecule with density in CO_2. Again the curve drawn is a theoretical one computed from Eq. (3). The Kerr constant per molecule increases with density as predicted by theory.

Table I gives measurements on the variation of the Kerr constant with temperature in CO_2. BT is constant within the limits of error *of the measurements*, estimated to be approximately 0.5 percent.

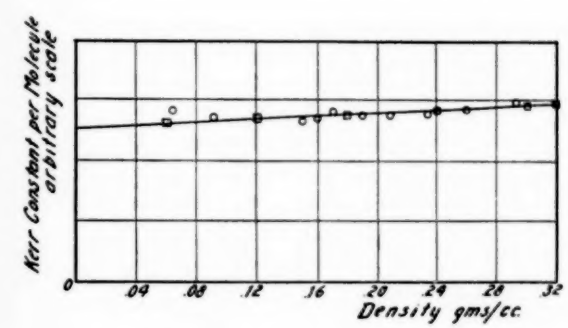

FIG. 4. Variation of Kerr constant per molecule with density.

TABLE I. *Variation of Kerr constant with temperature.*

Temperature (absolute)	307.6	280.2
Density, g/cm³	0.1035	0.1035
(Intensity of Kerr beam)$^{\frac{1}{2}}$	1.36	1.50
T (Intensity of Kerr beam)$^{\frac{1}{2}}$ or BT	418.	420.

The absolute value of B for CO_2 was measured at 34.6°C for a density of 0.1775 g/cm³ and wave-length 4550A. This value of B reduced to a density corresponding to a pressure of one atmosphere is 0.34×10^{-10} and is probably not more than 2 percent in error. The most uncertain quantity is the wave-length of light used. A Zeiss C filter gave a narrow band of wave-lengths, the effective wave-length of which depends on the character of the source and the variation of the sensitivity of the photo-cell with wave-length. With a monochromator an intensity wave-length curve was obtained from which the effective wave-length was determined to be 4550A.

For comparison with the previously measured value of B for CO_2 it is necessary to reduce the above value to wave-length 5890A and 17.5°C. From the data of Phillips[16] on n and from Eq. (4) the reduction gives 0.28×10^{-10}. The theoretical value of B computed by (4) is 0.28×10^{-10}. The experimental value obtained by Szivessy[5] is 0.24×10^{-10}. The agreement here between experiment and theory shows the essential correctness of the theory. From the variation in the values of the light scattering coefficient Δ as determined by different observers[17] it would appear that for non-polar gases the light-scattering coefficient might be determined more accurately from measures of the Kerr constant than from direct measures.

The Kerr constant B was measured for N_2 in terms of that for CO_2 since the value of B for N_2

[15] Uhlig, Keyes and Kirkwood, J. Chem. Phys. **1**, 155 (1933).

[16] Phillips, Proc. Roy. Soc. **A97**, 226 (1920).

[17] Wien-Harms, Handbuch der Exp. Physik, Vol. XIX.

is so small as to make the use of the rotating sector impractical. The Kerr constant for N_2 is one-sixth that of CO_2, or $B(N_2)$ is 0.057×10^{-10} for 4550A and 34.6°C. The probable error of this value is 3 percent. Formula (4) gives $B(N_2)=0.050\times10^{-10}$. This measure was made at a density of 0.0915 g/cm³.

An attempt was made to measure the Kerr constant of H_2. With a pressure of 82 atmospheres and a field of 70,000 volts per cm the effect was too small to be detected. This means that the Kerr constant of H_2 is less than 0.01×10^{-10}, which is what one would expect, the theoretical value given by (4) being 0.005×10^{-10}.

IV. Acknowledgments

In conclusion the author gladly acknowledges his indebtedness to Dr. J. W. Beams under whose direction the work was carried out, to Dr. L. G. Hoxton for his suggestions in the preparation of the manuscript and to the other members of the laboratory staff for the interest which they have shown in the work.

Errata.—Variation of the Principal Magnetic Susceptibilities of Certain Paramagnetic Crystals with Temperature

(Phys. Rev. **41**, 818, 1932)

Dr. K. S. Krishnan of Dacca University, India, has recently pointed out an error in the tabulation of certain values in the above paper. In Table II, page 826, the signs of the numbers in the last two rows should all be positive instead of negative. In Table V, page 830, under the column headed θ, the last four figures should read

79	instead of	−79
−99		−74
102		−102
−74		−99

B. W. Bartlett
Bowdoin College, Brunswick, Maine

LETTERS TO THE EDITOR

Prompt publication of brief reports of important discoveries in physics may be secured by addressing them to this department. Closing dates for this department are, for the first issue of the month, the twentieth of the preceding month; for the second issue, the fifth of the month. The Board of Editors does not hold itself responsible for the opinions expressed by the correspondents.

The Ionization of the Noble Gases by Positive Alkali Ions.—A Correction

Dr. Otto Beeck has recently informed me of an error in his calibration of the McLeod gauge used in the work on the ionization of krypton and xenon by positive alkali ions on which we collaborated;[1, 2] and also in the work on the ionization of neon and argon by myself.[3] He suggests that I publish the corrections in this country. The error was caused by his mistaking a piece of coordinate paper with 20 divisions per inch (used for the scale of the gauge) for one divided in millimeters. Thus an error of nearly 38 percent was made in the pressure readings. The values for the efficiencies of ionization (the number of electrons ejected from the gas per initial positive ion per cm path per mm pressure of mercury at 0°C) in krypton and xenon[1, 2] and those in neon and argon[3] must be corrected.

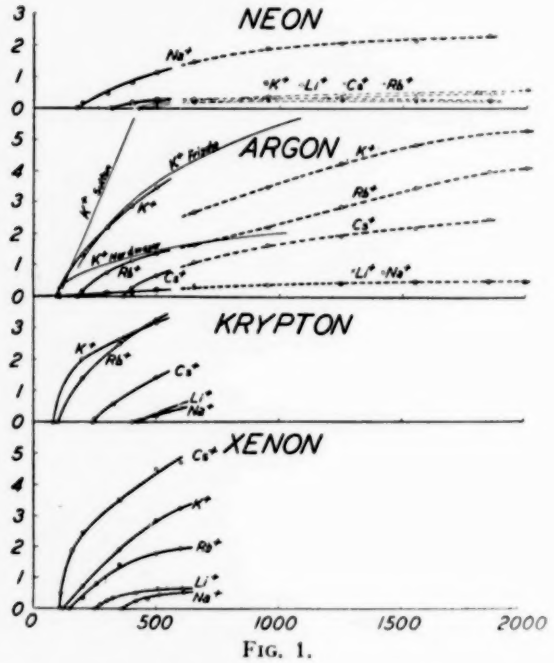

FIG. 1.

The corrected curves (see Fig. 1) for the efficiencies of ionization of the noble gases by the alkali ions are plotted with those of Beeck[4] for neon and argon; and those of Sutton,[5] Frische,[6] and Nordmeyer[7] for K^+ in argon. The unmarked curves in neon and argon are those of Beeck[4] measured in Germany with accelerating potentials of 0–600 volts. The dotted curves are mine[3] (corrected) measured with an apparatus of design different from Beeck's with accelerating potentials of 600–2000 volts. The curves for krypton and xenon are those of Beeck and myself[2] (corrected). The efficiency of ionization is plotted as the ordinate while the accelerating potential in volts is plotted as the abscissa. The noteworthy feature of these comparative curves is the striking fit between the curves of Beeck and those of mine taken in neon and argon with apparatus of different design. The importance in this fit lies in the fact that it indicates that there is no measurable wide-angle scattering of the alkali ions in neon and argon except for the case of K^+ in argon. My apparatus[3] was designed to record all positive ions entering the ionization chamber, while that of Beeck[4] recorded only those striking the collector plate. Any bombarding positive ions scattered outside the cone determined by the entrance slit of the ionization chamber and the collector plate would be lost in Beeck's apparatus. Therefore, if any wide-angle scattering occurred, my values for the efficiencies of ionization would have been lower than the previous ones. This is seen to be the case only with K^+ in argon.

The correction of the pressures does not alter my statement concerning the "probability of ionization"[3] (the chance of an electron being ejected in a collision between a bombarding positive ion and a bombarded gas atom, calculated from the kinetic theory mean free path for the positive ions in the noble gases nearest them in the periodic table). The values of these "probabilities," computed from data taken with the same apparatus[1, 4] with 500 volts as the accelerating potential of the positives, are: Na^+ in neon, 0.025; K^+ in argon, 0.026; Rb^+ in krypton, 0.024*; Cs^+ in xenon, 0.019*.

J. CARLISLE MOUZON

Duke University,
Durham, N. C.,
August 23, 1933.

* Corrected values.

[1] O. Beeck and J. C. Mouzon, Ann. d. Physik **11**, 737 (1931).
[2] O. Beeck and J. C. Mouzon, Phys. Rev. **38**, 967 (1931).
[3] J. C. Mouzon, Phys. Rev. **41**, 605 (1932).
[4] O. Beeck, Ann. d. Physik **6**, 1001 (1930).
[5] R. M. Sutton, Phys. Rev. **33**, 364 (1929).
[6] C. A. Frische, Phys. Rev. **43**, 160 (1933).
[7] M. Nordmeyer, Ann. d. Physik **16**, 717 (1933).

The Possibility of Electric Charge

(1) The difficulty in understanding the existence of corpuscular electric charges has been expressed frequently by the statement that an electron would dissolve within a short time if there were no forces other than electric forces to keep it together. If one puts the question what would be the order of magnitude of the time in which the electron would dissolve in the absence of all non-electric forces, one finds that a continuous distribution of electric charge has no possibility of existence at all. The question what will an accumulation of charge do under its own forces has no answer whatsoever because a continuous charge distribution "doing" anything would contradict either Maxwell's equations or the rules of conservation of energy and momentum and the inertia of energy. Furthermore there is no possibility of inventing any set of mechanical forces that would make it possible for a charge distribution to exist according to these rules, except in symmetrical cases such as a single infinite plane distribution or a single spherical distribution of charge, but barring even the possibility of *two* charged particles. The conclusion to be drawn from this is twofold. Either one gives up the existence of continuous charge altogether and supposes the electron to be a mathematical point, which would contradict the inertia of energy, or one gives up the definition of the charge and flux of charge which is contained in Maxwell's equations: $\rho = \text{div } E$, $\rho v/c = \text{curl } H - \dot{E}/c$.

(2) Maxwell's equations are: $\Delta ivM = P$ and $\Delta ivM^* = 0$, where M is the six-vector of the field, M^* its dual, and P the four-vector of the flux of charge with the components $\rho v/c$ and $i\rho$. An identical transformation leads to the equation

$$-\Delta ivT^e = [P, M] = F,$$

where the tensor T^e is defined by Maxwell's tensions p, Poynting's vector S and the energy density w in the form

$$T^e = \begin{Vmatrix} P_{xx} & P_{xy} & P_{xz} & iS_x/c \\ P_{yx} & P_{yy} & P_{yz} & iS_y/c \\ P_{zx} & P_{zy} & P_{zz} & iS_z/c \\ (i/c)S_x & (i/c)S_y & (i/c)S_z & -w \end{Vmatrix}$$

and $[P, M]$ has the components $\rho(E + [(v/c)H]) =$ Lorentz force and $(i/c)(v \cdot F) =$ rate of work. The conservation rules of momentum and energy require, if $F \neq 0$, that there are non-electric effects with a tensor T^m so that

$$\Delta iv(T^e + T^m) \equiv 0, \qquad \text{or} \qquad -\Delta ivT^e = F = \Delta ivT^m.$$

Since $F \neq 0$ means $P \neq 0$, we would conflict with the conservation rules if we put $T^m = 0$. So a charge does not "dissolve" within a short time under its own electric forces but it cannot exist in any stage of stability or dissolution at all.

(3) The general solution T^m of the equation $\Delta ivT^m = -\Delta ivT^e$ is

$$T^m = T^e + T^h$$

where T^h is any solution of the homogeneous equation $\Delta ivT^h = 0$, belonging to a Maxwell field without charge. (a) The special case $T^m = -T^e$ has no interest since it would mean that the electrodynamic effects are just cancelled by some anti-electrodynamic effects at every point. (b) We try to take T^m as a "mechanical" effect. Mechanical quantities may be defined as *bound* to the substance of the charge and moving with the variable velocity v in such a way that there is no flux of energy S^0 and hence no momentum g^0 with respect to a local system in which the charge rests: $S^0 = c^2 g^0 = 0$. The 10 components P^m, S^m, w^m of T^m in a system in which the charge moves with v can be expressed by the seven rest quantities

$$P_{xx}{}^0 \; P_{xy}{}^0 \; P_{xz}{}^0 \; P_{yy}{}^0 \; P_{yz}{}^0 \; P_{zz}{}^0 \; w^0,$$

by help of three components of v. In a given electromagnetic field the charges and their velocities $v_x\, v_y\, v_z$ are defined in every world point by $P = \Delta ivM$. To bring a given electromagnetic field into agreement with the conservation rules by help of mechanical forces means to satisfy the four equations for T^m

$$\Delta ivT^m = -\Delta ivT^e \qquad \text{(four components)},$$

where the right-hand side is *given* and the 10 components P^m, S^m, w^m of T^m on the left are dependent on the 7 rest-functions p^0 and w^0, which are still free. However, if we really want to consider T^m as *mechanical* forces bound to the substance of the charge we must assume that the rest-tensions P^0 in the charge will be some definite physical functions of the local value of the gradient of v and of higher derivatives of v. Since v is already given by the electrodynamic field, the six $p_{kl}{}^m$ will not be free any more in their local values even if we leave the general form of their dependence on grad v still free. Hence we have only seven less six that is *one* function free to satisfy the four equations $\Delta ivT^m = -\Delta ivT^e$ by help of mechanical forces T^m.

We see, neither can a continuous charge distribution exist by itself nor can it be enabled to exist by help of *mechanical* forces except for the case where the electric forces themselves represent a kind of mechanical system with vanishing flux of energy and barring the slightest motion of the charge in space and time, if there is not perfect plane or spherical symmetry, excluding the case of more than one electric particle.

A. Landé

Ohio State University,
August 27, 1933.

The Emission and Fluorescence Spectra of Sulphur Dioxide

In a paper in this issue, Chow has discussed the emission and absorption spectra of SO_2. In the *Zeitschrift für Physik*[1] which came to our laboratory just after Chow's paper was sent in, Lotmar has presented his results on the fluorescence spectrum in the same region.

Lotmar's fluorescence was excited by the Zn line at 2100A (47,600 cm^{-1}) which falls on the SO_2 absorption band having its violet edge at 47,623 according to Chow. This corresponds to excitation to the B_2 level in Chow's scheme of analysis. Since only part of any band will appear in fluorescence there may be a considerable interval between the center of the fluorescence band which is measured by Lotmar and the violet edge of the same band measured by Chow in emission. Furthermore this interval may vary for different bands, especially for different types of vibrational transition. Consequently a direct comparison of the wave numbers in Chow's list and Lotmar's list has little point. However, comparing the 47,600 value given by Lotmar for the fluorescence band corresponding to the 47,623 (or 47,631 in emission) band of Chow, we may guess that Lotmar's wave numbers should run about 25 cm^{-1} below Chow's.

Making this correction I have compared Lotmar's series with Chow's data in detail and find a fair agreement. Of the three 1370 (ν_3 of Chow, ν_1 of Lotmar) progressions reported by Lotmar (α, β, γ-series) none had been reported completely by Chow, but the first two and fifth and sixth of the α-series and the first two of the γ-series are in his list. The β-series is not.

Of the 1150 (ν_1 of Chow, ν_2 of Lotmar) progressions, the *A*, *B* and *C* series are almost completely represented by bands in Chow's list but by bands usually fitting better elsewhere in his analysis. The *D*, *E*, *F* and *G* series receive no support from Chow's work.

Of the 520 (ν_2 of Chow, ν_3 of Lotmar) progressions, most of the *a*-series has already been recorded by Chow, while the *c*-series has many agreements in spite of four gaps in the list of thirteen bands. The *b*, *d*, *e*, *f* and *g* series receive little or no confirmation but the six members of the *h*-series all appear in Chow's list.

A more significant and more striking comparison is that between the numerical values for the vibrational levels in the normal state as derived from Chow's and from Lotmar's data. They are given in Table I.

TABLE I. *Vibration levels in* SO_2. $\nu_1=1150$; $\nu_2=520$; $\nu_3=1370$.

Level	Chow	Lotmar	Level	Chow	Lotmar
$1\nu_1$	1150	1150	$1\nu_2$	521	520
$2\nu_1$	2300	2300	$2\nu_2$	1043	1040
$3\nu_1$	3450	3450	$3\nu_2$	1553	1560
$4\nu_1$	4600	4600	$4\nu_2$	2069	2075
$5\nu_1$		5750	$5\nu_2$	2578	2590
$6\nu_1$		6900	$6\nu_2$	3086	3110
		etc.	$7\nu_2$	3590	3630
			$8\nu_2$	4093	
				etc.	
$1\nu_3$	1354?	1370	$\nu_1+\nu_2$	1670	1670
$2\nu_3$	2676?	2720	$\nu_1+2\nu_2$	2205	2180
$3\nu_3$	3966?	4060	$\nu_1+\nu_3$	2502	2505
$4\nu_3$		5385			
		etc.			

It is clear that the only serious discrepancy is in the ν_3 progression where Chow's values were admittedly tentative. I think the long progressions of ν_1 and ν_2 with very slow convergence are well established, particularly the ν_2. The ν_3 progression depends almost entirely on Lotmar's work, with some confirmation in the α-series. Perhaps the most interesting agreement is the $\nu_1+\nu_3$ level. This level came out of Chow's analysis purely empirically yet is found to agree perfectly with Lotmar's result and with the infrared value of 2499.[2] As Lotmar points out coupling between these two vibrations is reasonable and I think we may say that we know its amount quite accurately for this first combination.

H. D. SMYTH

Palmer Physical Laboratory,
Princeton, N. J.,
September 15, 1933.

[1] Lotmar, Zeits. f. Physik **83**, 765, 785 (1933).
[2] Dadieu and Kohlrausch, Phys. Zeits. **33**, 167 (1932).

The Isotopes of Hydrogen by the Magneto-Optic Method. The Existence of H^3

In order to test further the presumption that the minima observed in the magneto-optic method as developed by Allison[1] depend upon the isotopes of the positive ions present, we examined water solutions containing approximately 2 and 4 percent of heavy hydrogen (H^2). A solution of HCl in ordinary water gives minima at 15.74 and 15.85 (Allison units); the latter, which is presumably due to H^1, is considerably stronger. These values agree with those reported by Allison in his earlier work in which he concluded the existence of H^2. In the heavy water solution we find the intensity of the 15.74 minimum almost equal to the one at 15.85 and in addition a third minimum at 15.65. The position of this minimum corresponds to that expected of H^3, and its intensity is somewhat less than the 15.74 minimum (H^2) in ordinary water.

We have checked the HCl results with HBr. The minima in the solution in ordinary water are at 12.97 and 13.09 and the new minimum in the heavy water solutions is at 12.84.

The heavy water was supplied to us by Professor G. N. Lewis, and he and Dr. Spedding are carrying out further spectroscopic investigations of the existence of H^3.

WENDELL M. LATIMER
HERBERT A. YOUNG

Department of Chemistry, University of California,
Berkeley, California,
September 25, 1933.

[1] Allison and Murphy, J. A. C. S. **52**, 3796 (1930). Allison, Ind. Eng. Chem. Anal. Ed. **4**, 9 (1932). See Phys. Rev. **37**, 1178 (1931) for halogen acid values.

The Raman Spectrum of Gaseous Carbon Dioxide

In a recent paper[1] it was ventured, that of the six new lines observed by Langseth and Nielsen,[2] probably not more than two are members of the Raman spectrum of gaseous CO_2. This conclusion was based wholly upon the predicted Raman spectrum of the molecule since the corresponding energy levels had not as yet been observed in the infrared.

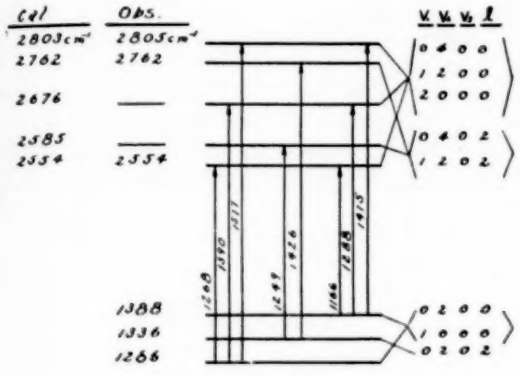

FIG. 1.

More recently[3] Professor E. F. Barker has succeeded in determining the positions of three of the five relevant levels from direct measurements in the infrared. The discovered values are in excellent accord with the calculated ones referred to above.

In the light of these results one may expect to find the Raman lines in question in the immediate neighborhood of the Raman transitions ($\Delta l = 0$) implied by the energy level diagram given in Fig. 1.

ARTHUR ADEL

University of Michigan,
September 25, 1933.

[1] Adel and Dennison, Phys. Rev. **43,** 716 (1933).

[2] Langseth and Nielsen, Zeits. f. physik. Chemie **B19,** 427 (1932).

[3] Barker and Wu, to be published in the near future.

The Allison Magneto-Optic Effect

In an investigation of a transmission line and spark gap system similar to that used by Professor Fred Allison, a few things have been noted which seem of some significance. The trolley arrangement has been slightly modified to form a real two-wire transmission line between the supply condenser and the terminating coil. In order to eliminate the long period oscillatory current from the line, and to obtain the high-frequency oscillations occurring in the spark gap discharge, the line and the condenser spark gap system have been made separate circuits with the line connected directly across the spark gap terminals through two small series capacitances. The capacitance on the low voltage side of the gap is paralleled by a high resistance. In this arrangement the only voltage applied to the line is that appearing across the gap terminals.

A preliminary investigation of the coils at the line terminals reveals the presence of high frequency oscillations ranging from some centimeters to a few meters in wavelength. A change in trolley position produces a marked shift in energy distribution between these high frequency components. This shift or selective effect is apparently from the low frequency to the high frequency side of the band as the line length between gap and coils is increased. These oscillations are due to the capacity between the electrodes of the gap and possibly also to phenomena of the Langmuir-Tonks type. In such a discharge one would naturally expect a broad band of frequencies.

It is futile at present to speculate upon the complete significance of these oscillations, but it is hoped that some correlation between them and the Allison minima can be obtained when more data are available. An investigation is now in progress in which an attempt will be made to calibrate the trolley system in terms of predominating frequencies and determine whether or not there is selective absorption occurring in the cell.

It might be worth while to note that an arrangement similar to the above was tried out by the writer in Professor Allison's laboratory at Auburn this summer. The minima were apparently made considerably sharper, that is more sensitive to trolley shift. Several analyses of unknowns were made with this modification and the isotopes of lead redetermined. The readings were in excellent agreement with those of Bishop, Lawrenz and Dollins.[1] It is perhaps needless to state that for this modification the nicols must be used in the parallel position and the coil fields assisting.

I am much indebted to Professor Frêd Allison for the privilege of using his apparatus and for his courtesy in allowing me to rearrange it in any desired manner. I have also profited a great deal by many discussions with Professor J. W. Beams.

This research is made possible by grants from the National Research Council, the Research Corporation, and the University of Virginia.

L. B. SNODDY

Rouss Physical Laboratory,
University of Virginia,
September 30, 1933.

[1] Bishop, Lawrenz and Dollins, Phys. Rev. **43,** 43 (1933).

Production of Neutrons by High Speed Deutons

In a recent letter to the *Physical Review*[1] we described briefly an apparatus for the acceleration of positive ions and the production of neutrons by bombarding beryllium with helium ions of from 600,000 to 975,000 electron-volts energy. Since then we have bombarded targets of lithium chloride and beryllium with deutons of energies up to 900,000 electron-volts, and have obtained in both cases yields of neutrons several hundred times as great as the yield previously obtained by bombarding beryllium with helium ions.

The same apparatus was used for accelerating the ions and for detecting the neutrons as was described in the previous letter. A sensitive electroscope, the inside walls of which were coated with paraffin, was entirely enclosed in a lead cylinder of 5 cm wall thickness to shield it from x-rays. The neutrons supposedly penetrate the 5 cm of lead and eject recoil hydrogen particles from the paraffin on the inner walls of the electroscope. It is the ionization due to these recoil particles that gives a measure of the intensity of neutrons passing through the chamber. The lead cylinder with the electroscope inside was placed in such a position that the center of the electroscope was 13 cm from the center of the target, and in a direction from it perpendicular to the incident ion beam.

In making the measurements of neutrons produced by deuton bombardment, it was necessary to make several comparison measurements in order to establish the fact that in each case the observed effect was due to neutrons rather than to γ-rays, and that the disintegration was produced by the deutons rather than protons. The hydrogen used to produce the deutons contained only 5 percent of the heavy isotope, so even in the so-called deuton measurements, the greater part of the ions was protons. Each target bombarded with deutons was later bombarded with 100 percent protons for comparison. No effect was observed with protons, except a slight one in the case of lithium, which is discussed below, and it was therefore concluded that the large effects were produced by deutons. Measurements were also made with deutons, with the paraffin removed from the electroscope. With both lithium and beryllium the rate of discharge without paraffin was less than half that with paraffin, indicating that the greater part of the ionization observed was due to recoil particles ejected from the paraffin by neutrons, rather than to γ-rays. The sensitivity of the electroscope to 600,000 volt x-rays filtered through 5 cm of lead was measured and found to be slightly greater without paraffin than with paraffin.

Curves of the efficiency of production of neutrons from lithium chloride and from beryllium as a function of voltage are shown in Fig. 1. The total ion current during all the measurements was 10 microamperes. The background, indicated by a straight line, is the rate of discharge of the electroscope due to x-rays plus its natural leak, and is the same in all cases in which no neutrons or γ-rays are produced. It has been determined by bombarding a brass target with helium ions, a beryllium target with protons, and a brass target with protons.

The lithium chloride target, bombarded with 10 microamperes of protons at 800,000 volts gave a small effect, about twice the background, which was decreased to less than half that when the paraffin was removed from the electroscope, indicating that the radiation was neutrons. It is possible that this is a double process in which the α-particles produced by proton bombardment in turn disintegrate lithium with the production of neutrons. It has

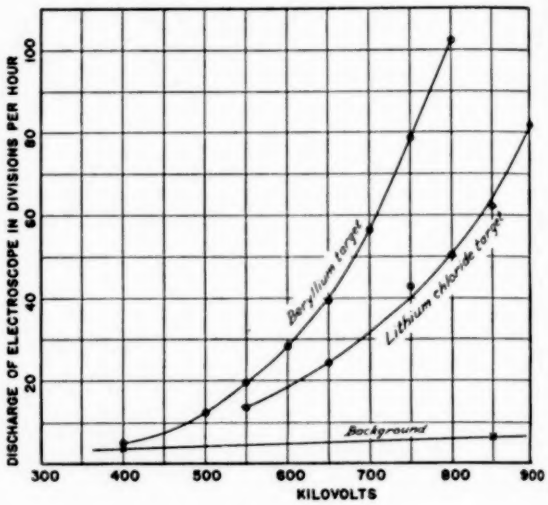

FIG. 1.

already been shown by Curie and Joliot[2] that α-particles of long range are capable of producing neutrons from lithium, and the effect here observed seems to be of the right order of magnitude to be accounted for in that way. However, the effect is to be investigated further.

The simplest hypotheses as to the nature of the two disintegrations with deutons are:

$$Be^9+H^2\rightarrow B^{10}+n^1,$$

$$Li^7+H^2\rightarrow 2He^4+n^1.$$

Assuming tentatively that the mass of the neutron is 1.0065, and taking as values of the other atomic masses referred to O^{16}

Li^7 7.0146	B^{10} 10.0137	H^2 2.0136
Be^9 9.0155	He^4 4.0022	

we find that in the case of the disintegration of beryllium the neutron comes off with a kinetic energy of about 9×10^6 electron-volts. In the case of lithium, the kinetic energy of the neutron plus that of the two α-particles comes out to be about 16×10^6 electron-volts. It is probable that these calculations will be greatly modified by subsequent experimental data, but they serve as a rough approximation

[1] Crane, Lauritsen and Soltan, Phys. Rev. **44**, 514 (1933).
[2] Curie and Joliot, J. de Physique **4**, 278 (1933).

to show that the neutrons produced by this method have a rather high kinetic energy.

It is of interest to make a comparison of the intensity of neutrons produced by bombarding beryllium or lithium with deutons with that obtained by bombarding beryllium with α-particles from a strong polonium source. One division in our electroscope corresponds to about 70 recoil hydrogen particles. At our maximum deuton current (30 microamperes) and at 900,000 volts, about 1000 recoil particles per minute would be obtained, which is of the order of one hundred times the intensity obtained by means of the strongest polonium α-particle sources now in use. It is therefore possible, by the use of deutons, to obtain an efficiency in the artificial production of neutrons which is comparable with the efficiency of production of α-particles by proton bombardment.

We are greatly indebted to Professor G. N. Lewis, who kindly furnished the heavy hydrogen used in these experiments.

H. R. Crane
C. C. Lauritsen
A. Soltan

Kellogg Radiation Laboratory,
California Institute of Technology,
September 30, 1933.